2022 ATE accelerator school

가속기의 활용 I, 연 X-선

Gwangju Institute of Science and Technology
Department of Physics and Photon Science
Prof. Bongjin Simon Mun

포항가속기 연구소, 과학관 1층 대강당

2022.08.08~2022.08.12

Acknowledgements

The presentation on synchrotron radiation section are prepared based on the lecture notes of Dr. Zhi Liu at Advanced Light Source, USA.

The presentation on XPS was prepared based on the lecture notes of Prof. Charles S. Fadley at University of California Davis and Lawrence Berkeley National Laboratory, USA.

B.S. Mun deeply appreciate their permissions of using valuable resources for this summer school. For further information, please visit the following websites.

1. "http://www.physics.ucdavis.edu/fadleygroup/"
2. "http://ast.coe.berkeley.edu/srms/" (Prof. David Attwood's Class on SR & Videos on YouTube)
3. "http://www.er.doe.gov/bes/synchrotron_techniques/"

4.Video on SR: "http://wlap.physics.lsa.umich.edu/cern/lectures/academ/2000/wilson/09/real/f002.htm"

Synchrotron Radiation

Synchrotron radiation occurs when a charge particle moving at *relativistic speeds* follows a *curved trajectory*. (either in a circular motion, like a bending magnet, or a sinusoidal motion, such as a wiggler and an undulator).

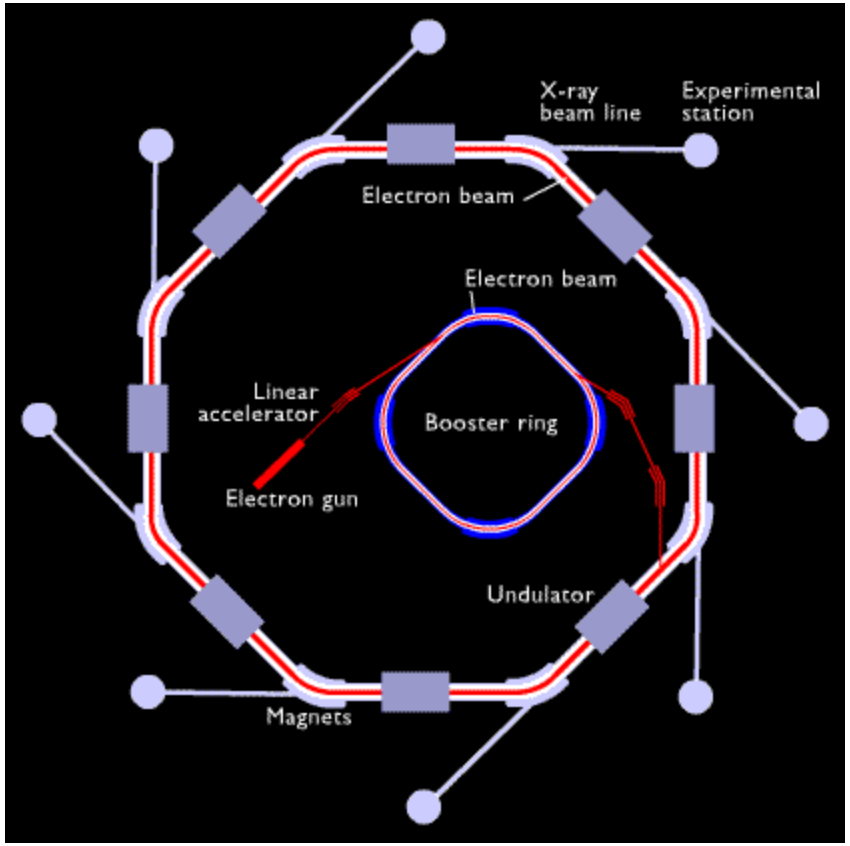

www-ssrl.slac.stanford.edu/~txrf/images/i1442.gif

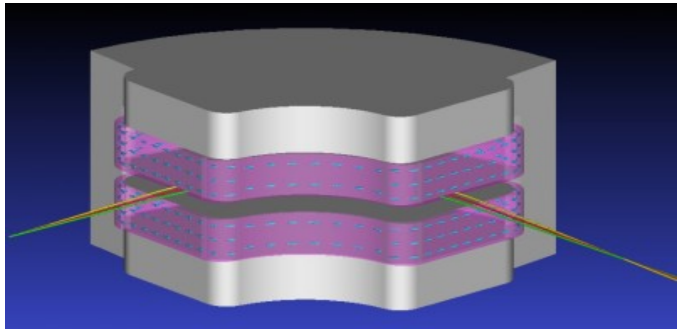

Bending magnet

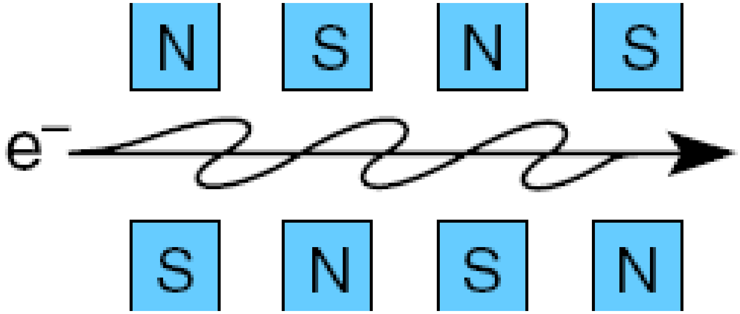

Wiggler/Undulator

Synchrotron Radiation

Synchrotron radiation occurs when a charge moving at relativistic speeds follows a curved trajectory.

1. EM simulation of a bending magnet

electrons

electric field

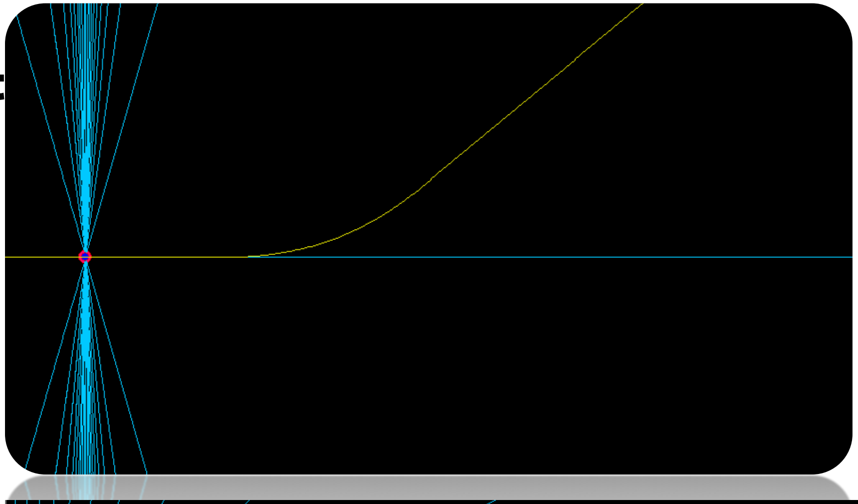

2. EM simulation of a wiggler

electrons

electric field

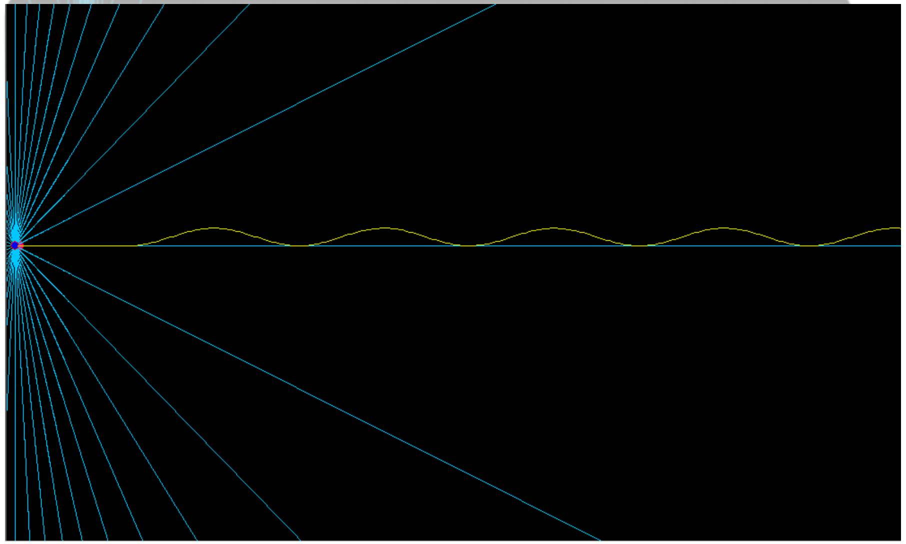

Synchrotron Radiation and Dipole Radiation

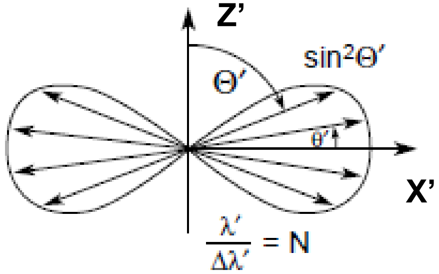

$$\begin{cases} t' &= \gamma\left(t - vx/c^2\right) \\ x' &= \gamma\left(x - vt\right) \\ y' &= y \\ z' &= z \end{cases}$$

Lorentz transformation →

$$\gamma = \frac{1}{\sqrt{1-\frac{v^2}{c^2}}}$$

~ 4000 for 2GeV electrons

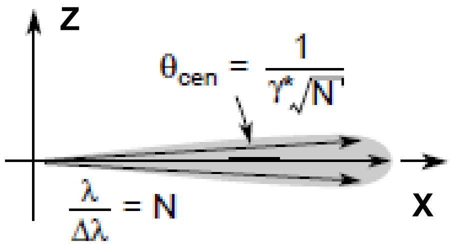

Dipole Radiation at relativistic speed → Undulator Radiation

Bending Magnet SR Characteristics

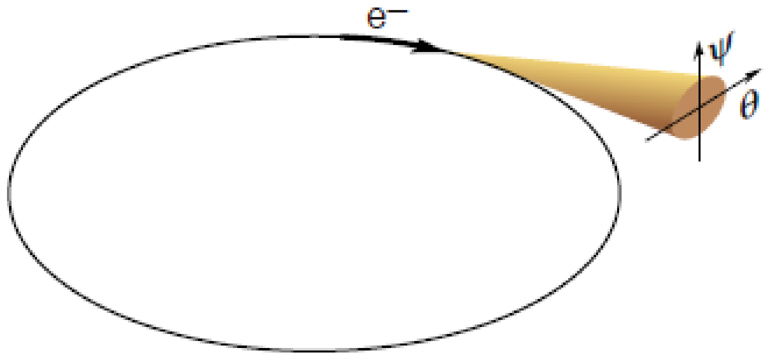

$$E_c = \hbar\omega_c = \frac{3e\hbar B\gamma^2}{2m} \quad (5.7a)$$

$$\boxed{E_c(\text{keV}) = 0.6650\,E_e^2(\text{GeV})\,B(\text{T})} \quad (5.7b)$$

$$\frac{d^2F_B}{d\theta\, d\omega/\omega} = 2.46\times 10^{13}\, E_e(\text{GeV})\, I(\text{A})\, G_1(E/E_c)\,\frac{\text{photons/s}}{\text{mrad}\cdot(0.1\%\text{BW})} \quad (5.8)$$

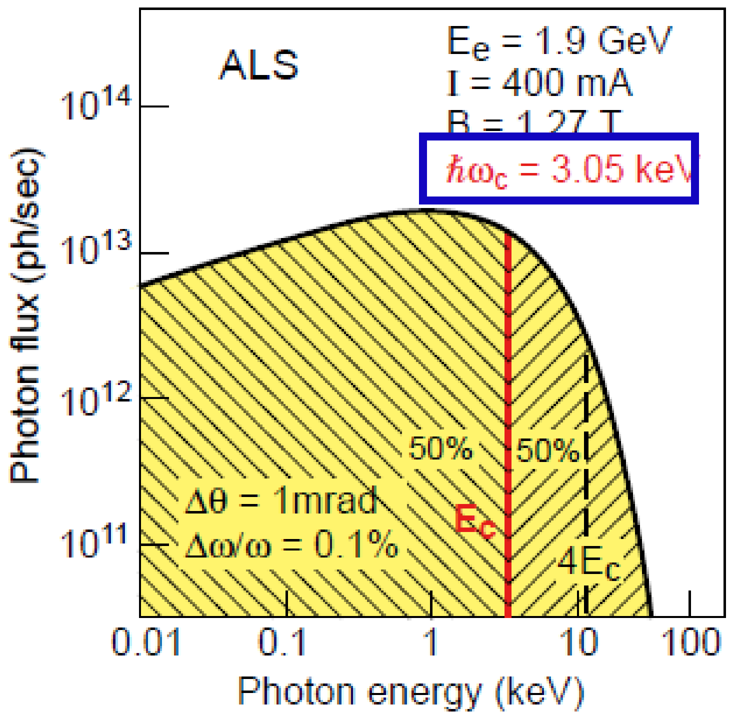

Advantages:
- covers broad spectral range
- least expensive
- most accessable

Disadvantages:
- limited coverage of hard x-rays
- not as bright as undulator

E_c (critical photon energy) is that for which half the radiated power is in higher photon energy and half in lower photon energy.

Synchrotron Radiation: A High Brightness Tunable X-ray Source

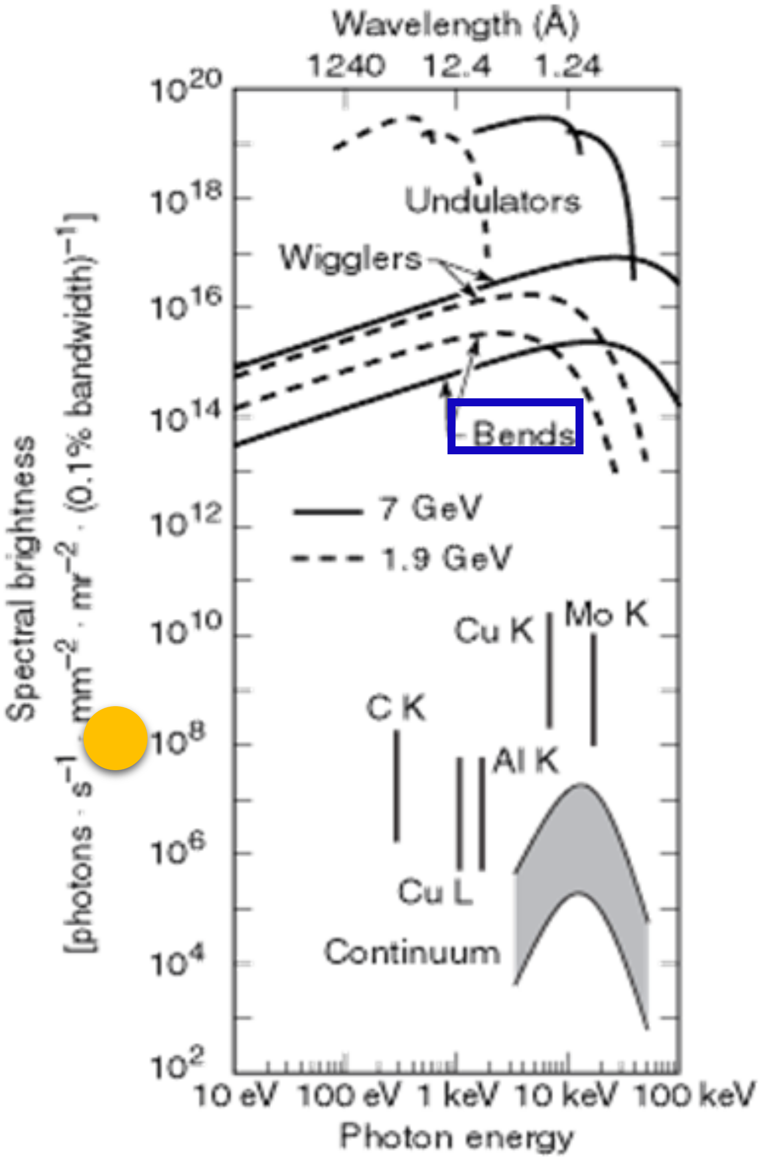

Spectral brightness for several SR sources:

•Several orders of magnitude brighter than the conventional x-ray tube. Trillion times brighter than hospital x-ray.

•A broad emission, tunable.

Equation to remember:

$$E_c(keV) = 0.665 \times E_e^{\,2}(GeV) \times B(T)$$

Power of SR from a Banding Magnet

Another equation to remember:

Power of SR: $$P \propto \frac{E_e^{\,4}}{E_0^{\,4} \times r^2}$$

It is difficult to accelerate electrons. High energy physicists hate this term.

This is why we are using electrons. High energy physicists hate this too.

Higher the energy, Larger the ring

1.9 GeV, γ = 3720, 197 m circumference

ALS, US, 1.9GeV, 197m

ESRF, France, 6 GeV, 884m

SPring-8, Japan, 8GeV, 1.44km

Beamlines are used to Transport Photons to the Sample, and Take a Desired Spectral Slice

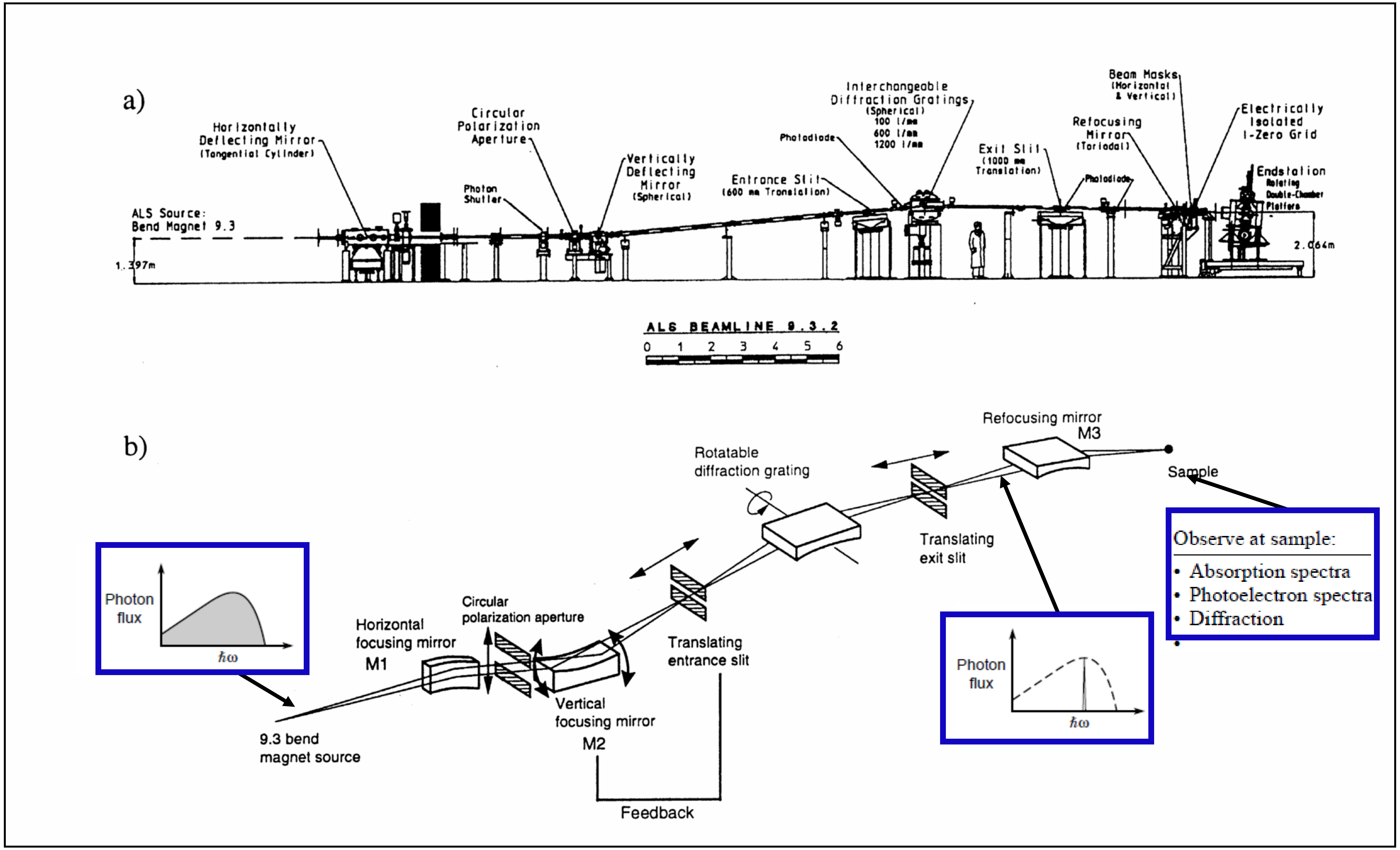

Generation of X-ray in old days

Producing x-rays:
the good
old-fashioned way

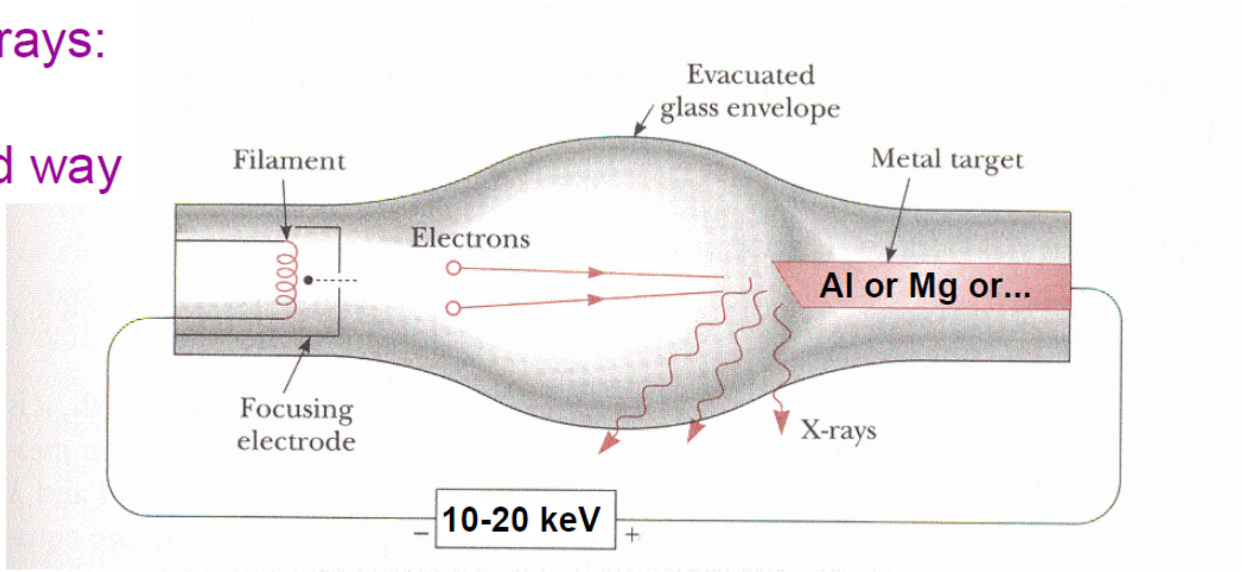

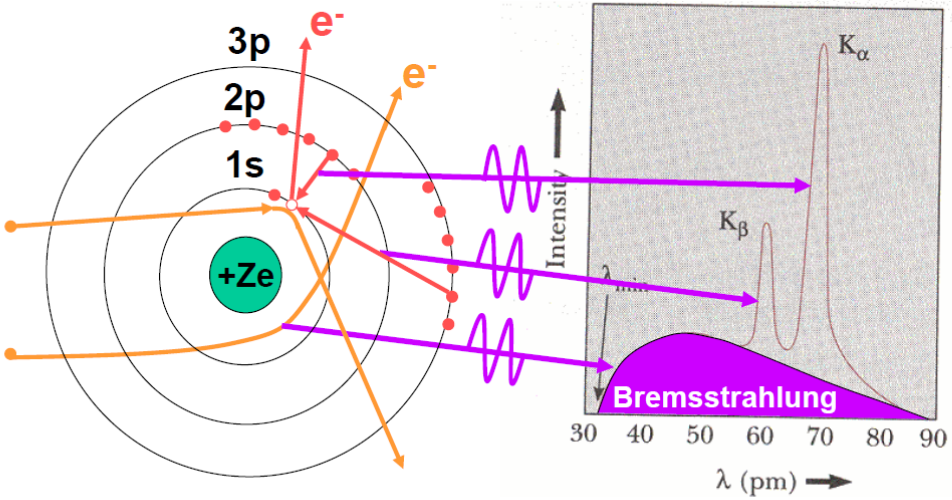

X-Ray energies
from the "X-Ray
Data Booklet"

Table 1-2. Photon energies, in electron volts, of principal K-, L-, and M-shell emission lines.

Element	$K\alpha_1$	$K\alpha_2$	$K\beta_1$	$L\alpha_1$	$L\alpha_2$	$L\beta_1$	$L\beta_2$	$L\gamma_1$	$M\alpha_1$
3 Li	54.3								
4 Be	108.5								
5 B	183.3								
6 C	277								
7 N	392.4								
8 O	524.9								
9 F	676.8								
10 Ne	848.6	848.6							
11 Na	1,040.98	1,040.98	1,071.1						
12 Mg	1,253.60	1,253.60	1,302.2						
13 Al	1,486.70	1,486.27	1,557.45						
14 Si	1,739.98	1,739.38	1,835.94						
15 P	2,013.7	2,012.7	2,139.1						
16 S	2,307.84	2,306.64	2,464.04						
17 Cl	2,622.39	2,620.78	2,815.6						
18 Ar	2,957.70	2,955.63	3,190.5						
19 K	3,313.8	3,311.1	3,589.6						
20 Ca	3,691.68	3,688.09	4,012.7	341.3	341.3	344.9			
21 Sc	4,090.6	4,086.1	4,460.5	395.4	395.4	399.6			

Popular laboratory sources
for photoelectron spectroscopy

What are the advantages of using SR over Conventional X-ray source?

1. Energy Tunability
2. High Brightness & Flux of Photon
3. High Energy Resolution
4. Ultrafast Light Source & Coherence in X-ray regime

Science with Light Sources

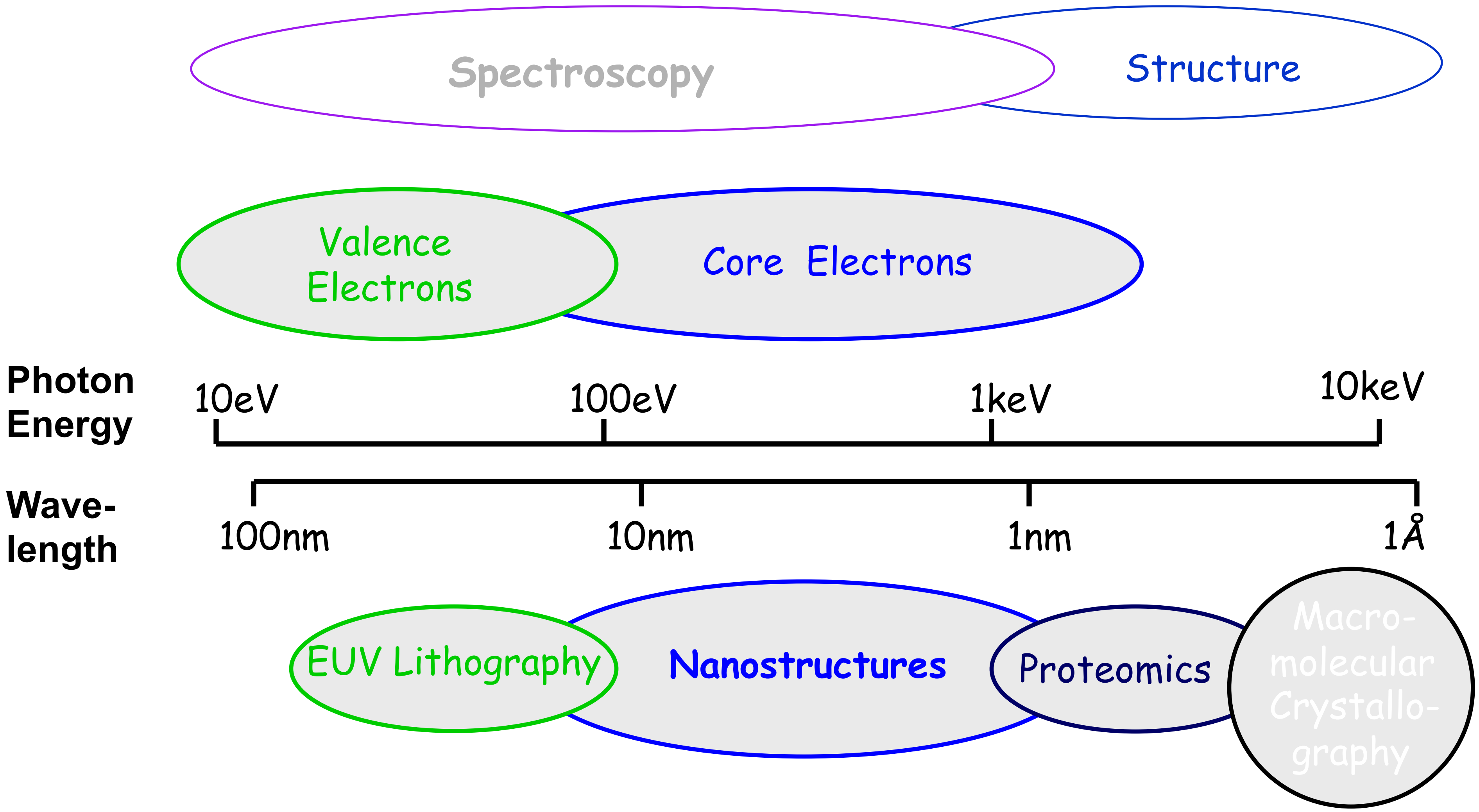

Science with Light Sources

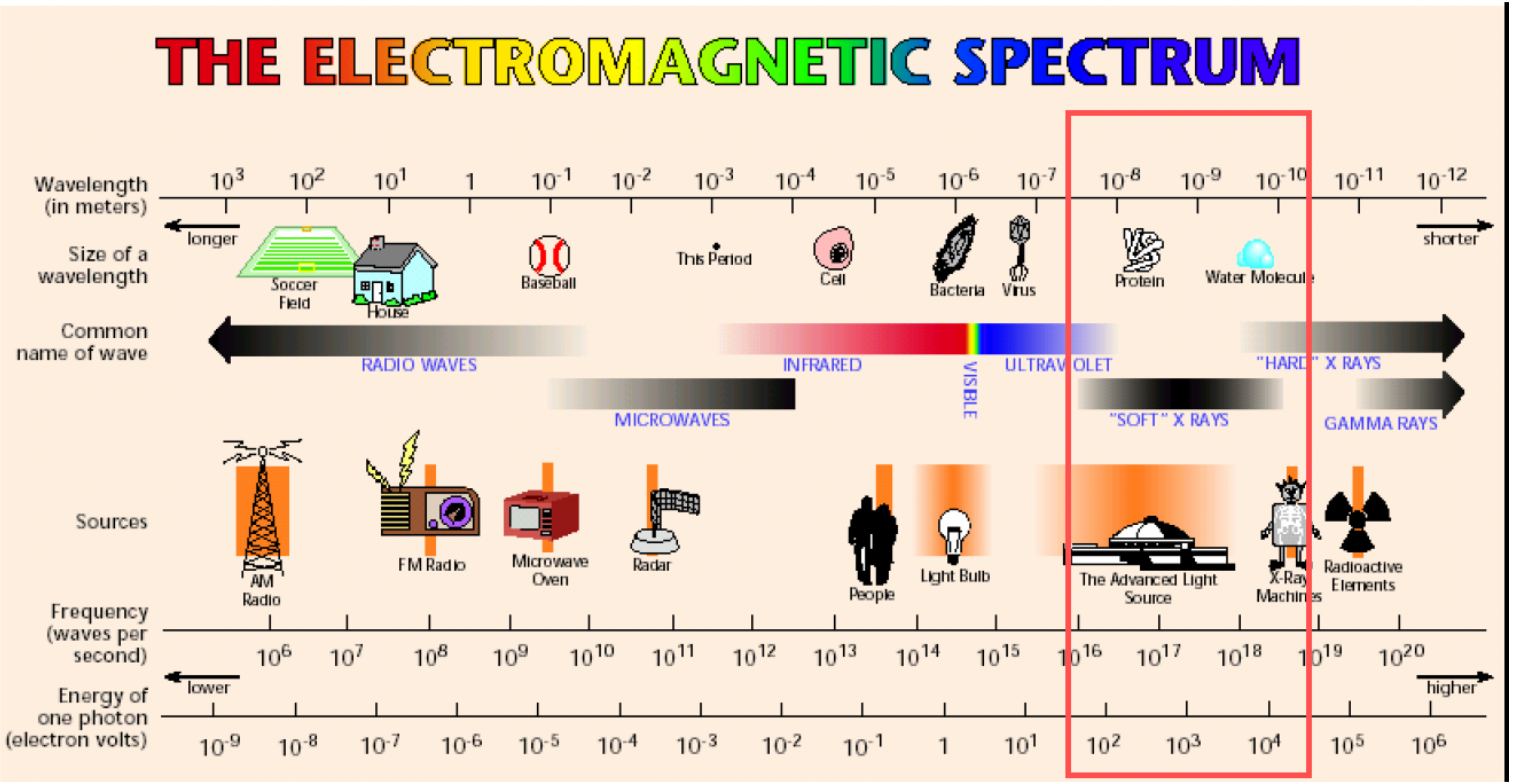

What Does Synchrotron Radiation (SR) Brightness Buy You?

High Energy Resolution

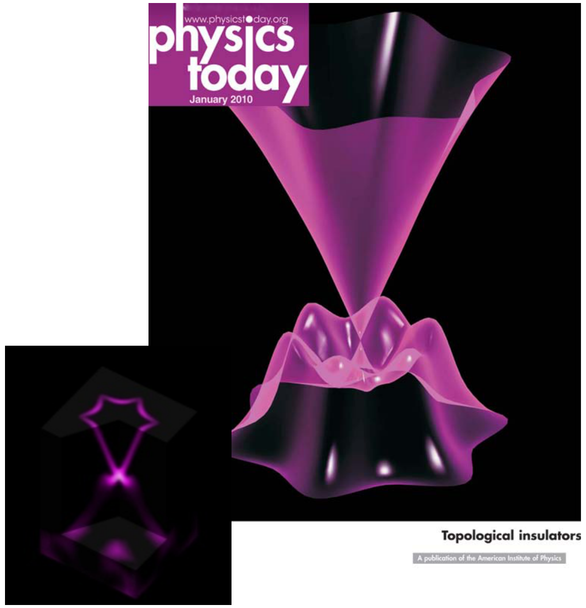

Band Structure of Bi_2Te_3
Y.L Chen… @BL 10.0.1, ALS
(< 10meV resolution)

Nano-meter Spatial Resolution

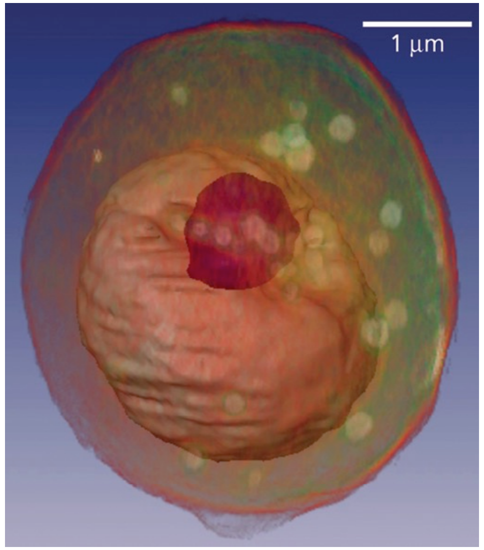

3-D reconstruction of yeast
C. A. Larabell… @ XM1, ALS
(<30nm resolution)

Ultrafast & Coherence

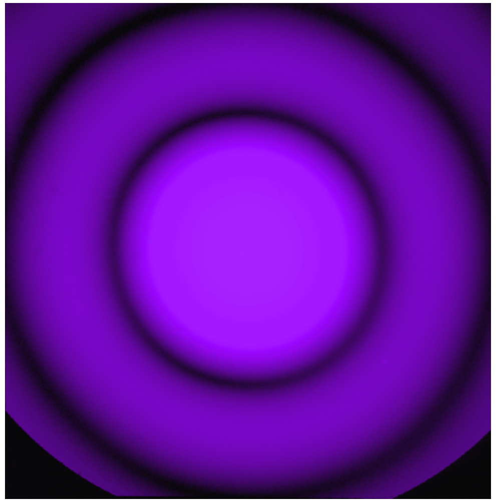

LCLS at Stanford and future
NGLS at LBNL.
(fs x-ray laser)

Outline

A. Brief reviews on
Synchrotron Radiation

B. Various spectroscopic tools with
synchrotron radiation (soft x-ray) : XPS, XAS,XES

C. Recent developments

X-ray Photoelectron Spectroscopy (XPS)

With acknowledgments to:

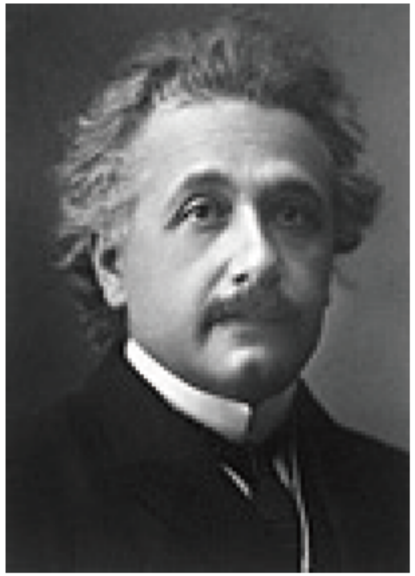

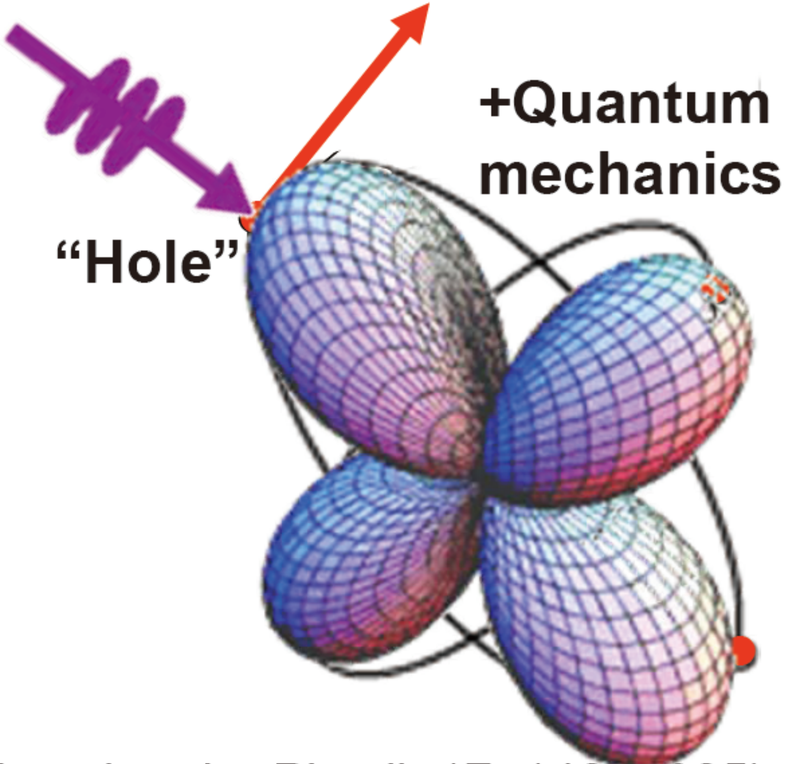

The photoelectric effect: Annalen der Physik 17, 146 (1905)

$$h\nu = E_{initial} - E_{final} = E_{binding} + E_{kinetic}$$

(Nobel Prize for it in1921– But no mention of it in his Nobel lecture)

X-ray Photoelectron Spectroscopy (XPS)

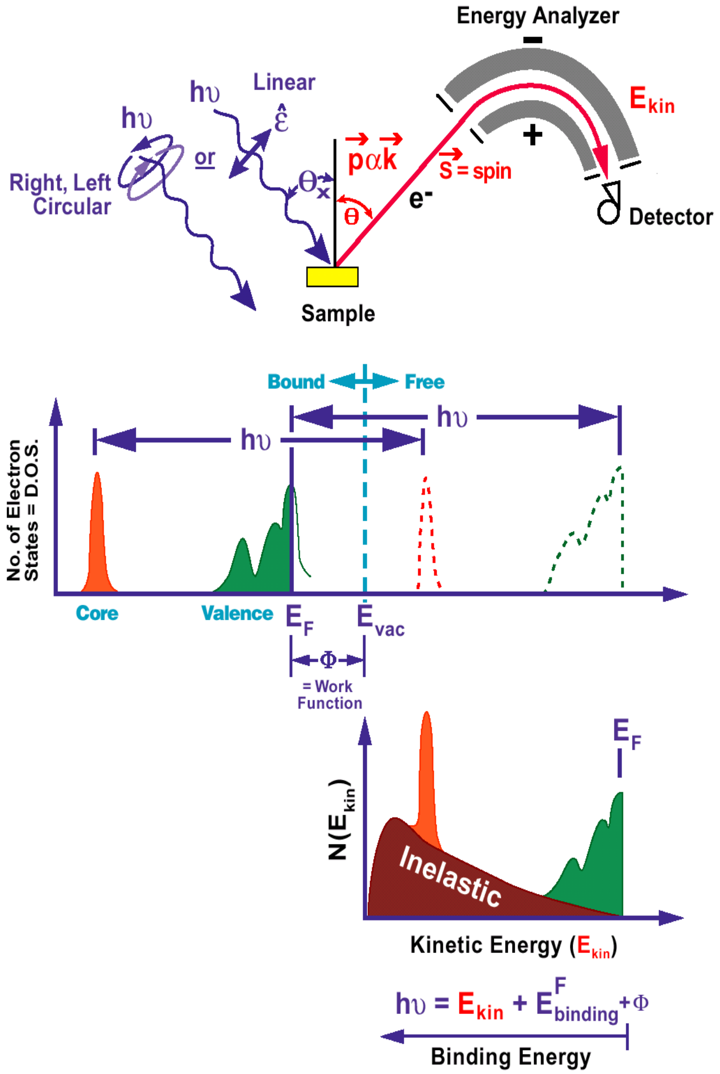

Photoelectric Effect : Einstein (1905)

E(K.E.) = E(hv) – E(B.E.) – Work function

$$I \propto \sum_{f,i} |< f \mid p \cdot A \mid i >|^2 \, \delta(E_k^0 - E_m^0 - \hbar\omega)$$

f = final states
i = initial states
p = momentum of photoelectron
A = vector potential of photon
(Electric fields)

Core level Spectrum

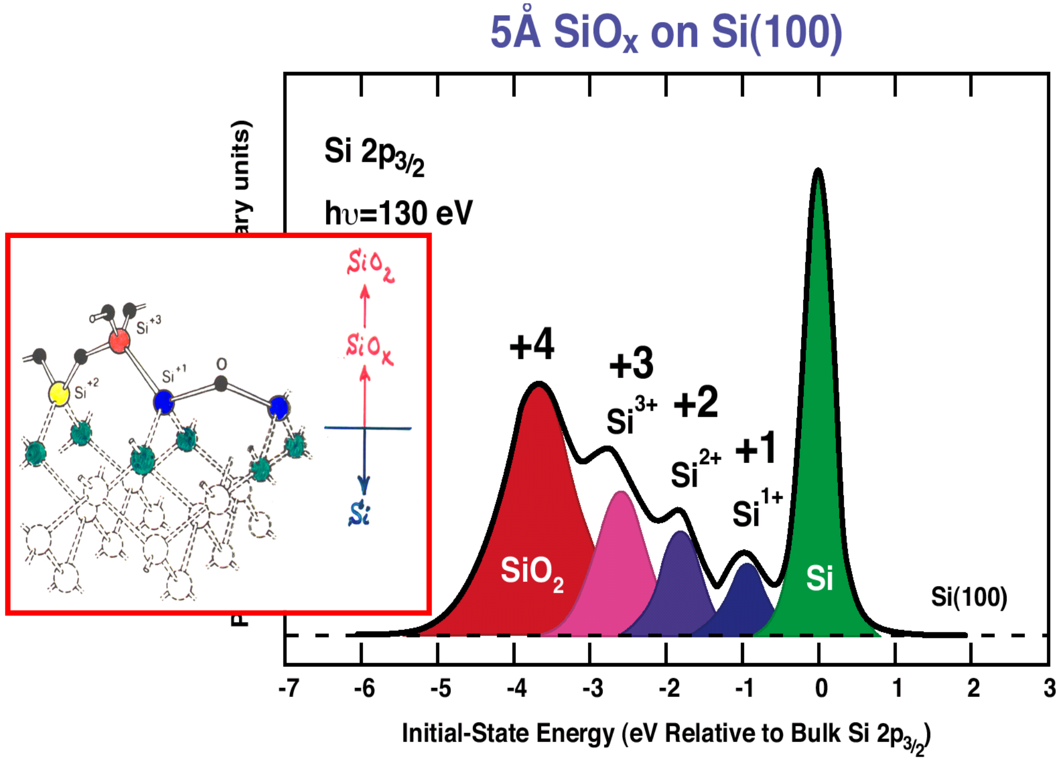

Valence Band Spectrum

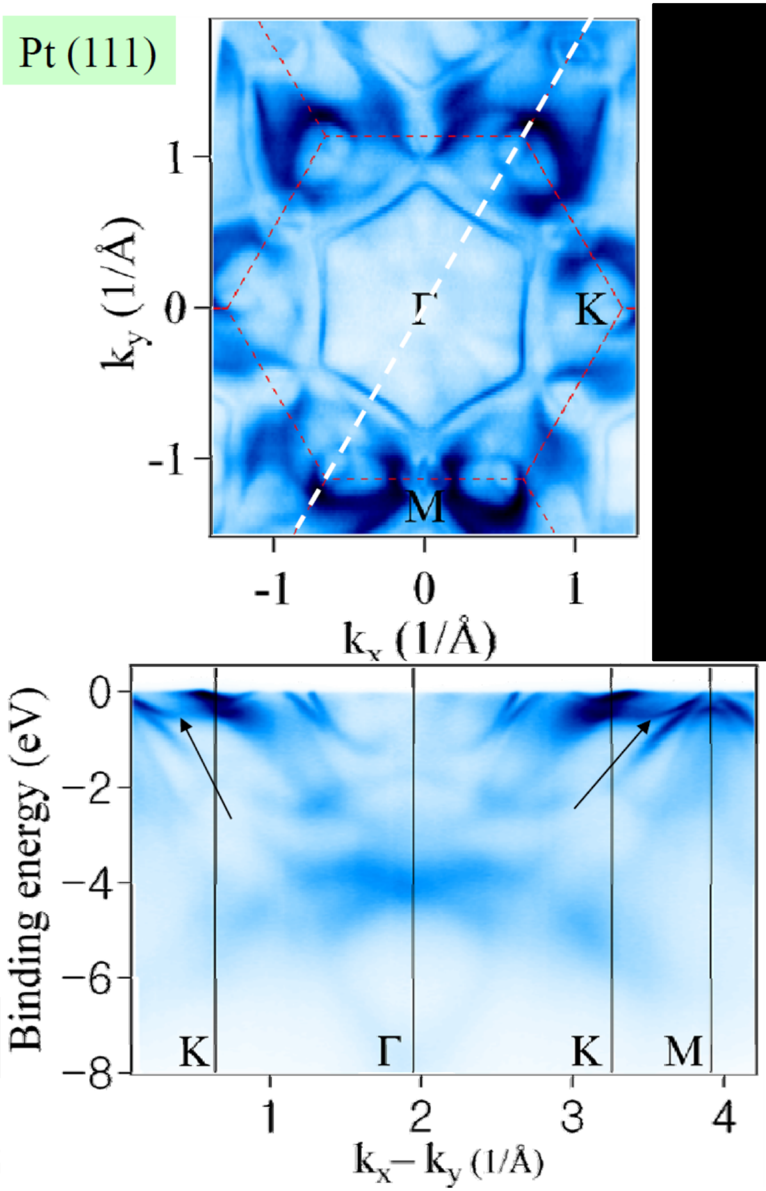

[redacted]

XPS provides "surface sensitive"

- *Element specific,*
- *Chemical environment,*
- *Structural,*
- *Magnetic structure,*
- *Electronic structure,*

Information

Transmission Electron Microscope
: Require careful sample preparation & spectra analysis

Scanning Transmission Electron Microscopy with EELS

Si 2p excitations— like x-ray absorption spectra

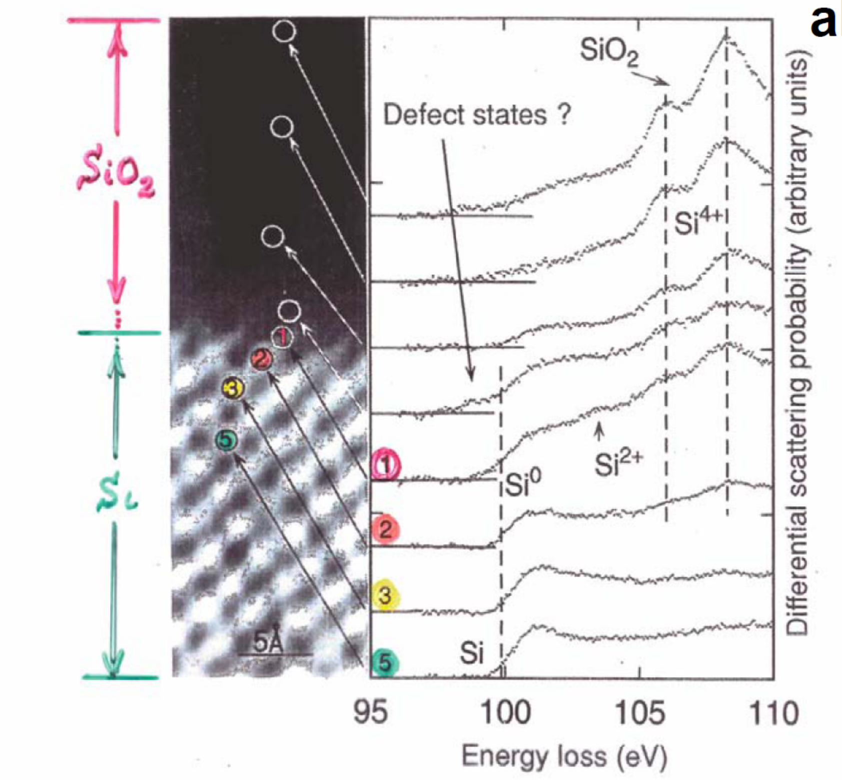

$\Delta E \approx 0.1\,eV$
$\Delta x, \Delta y$
$\approx 0.2\,nm$

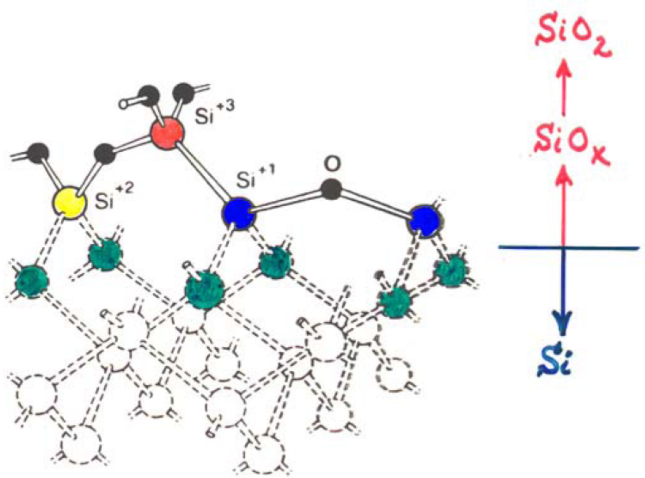

Nature 366, 727 - 728 (30 December 1993)

XPS

A. Non-destructive measurement
B. Superb chemical resolution
(Energy resolution)
C. Structural dependence

Phys. Rev. B 38, 6084 (September 1988)

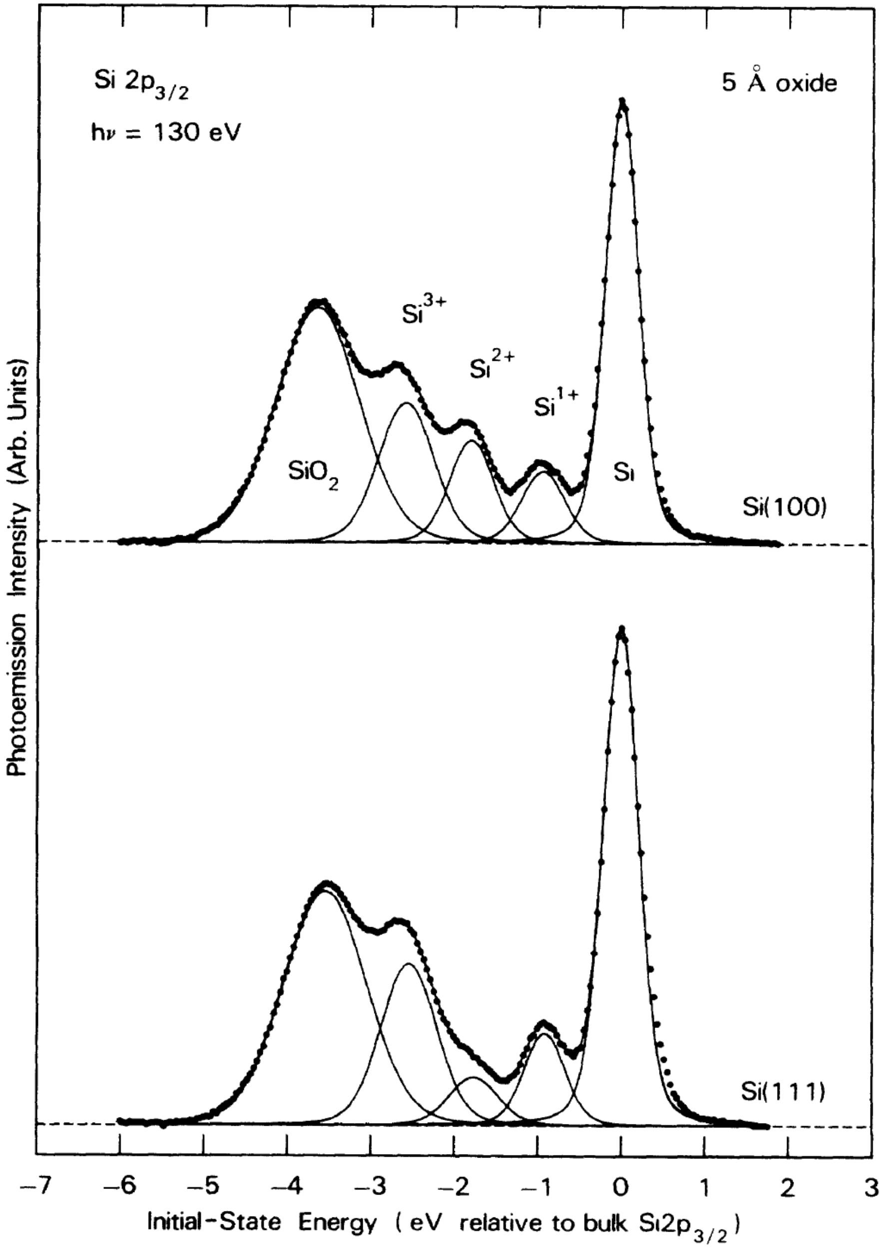

XPS (Core Level Shift)

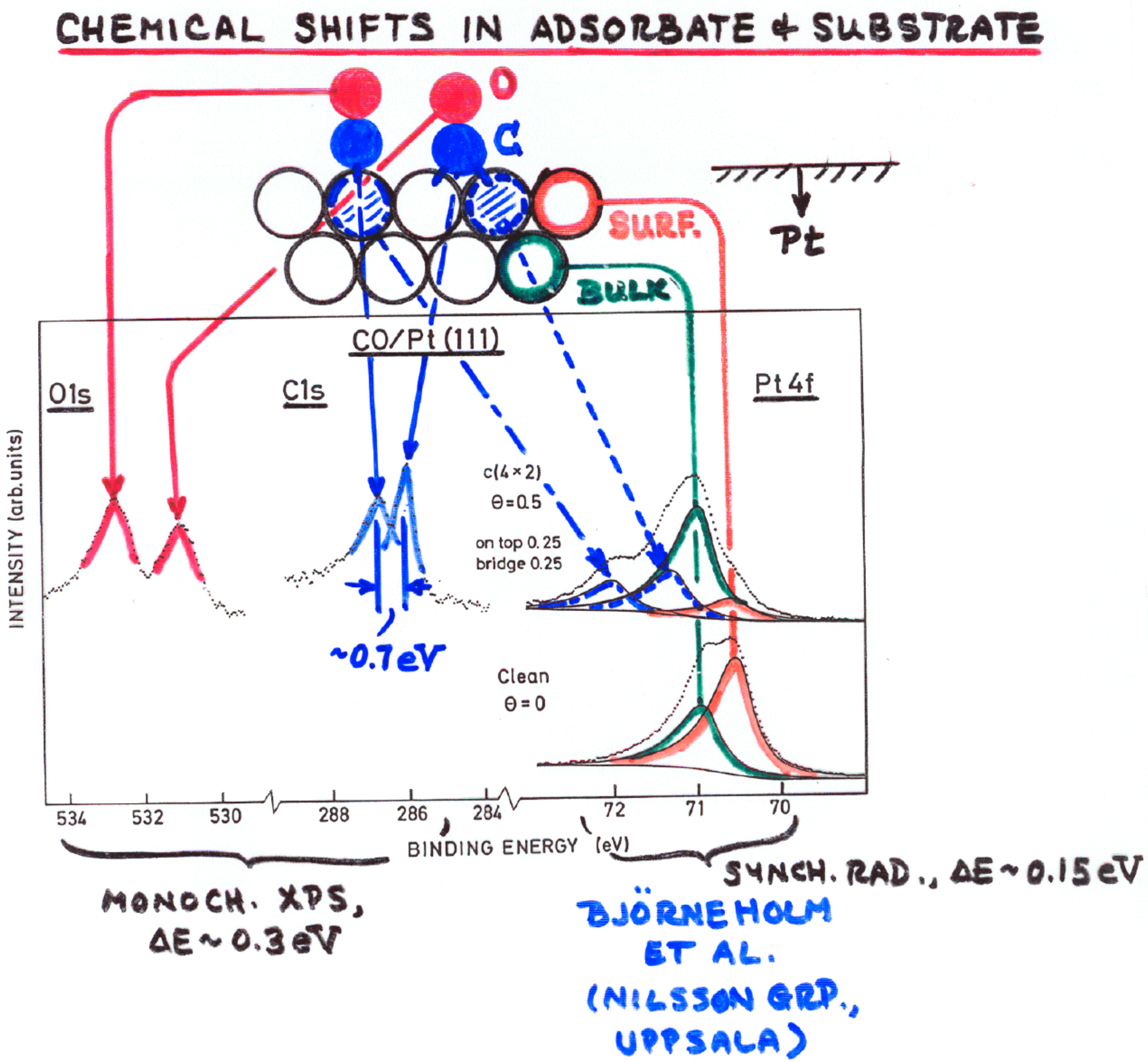

CO Adsorption on Pt(111)

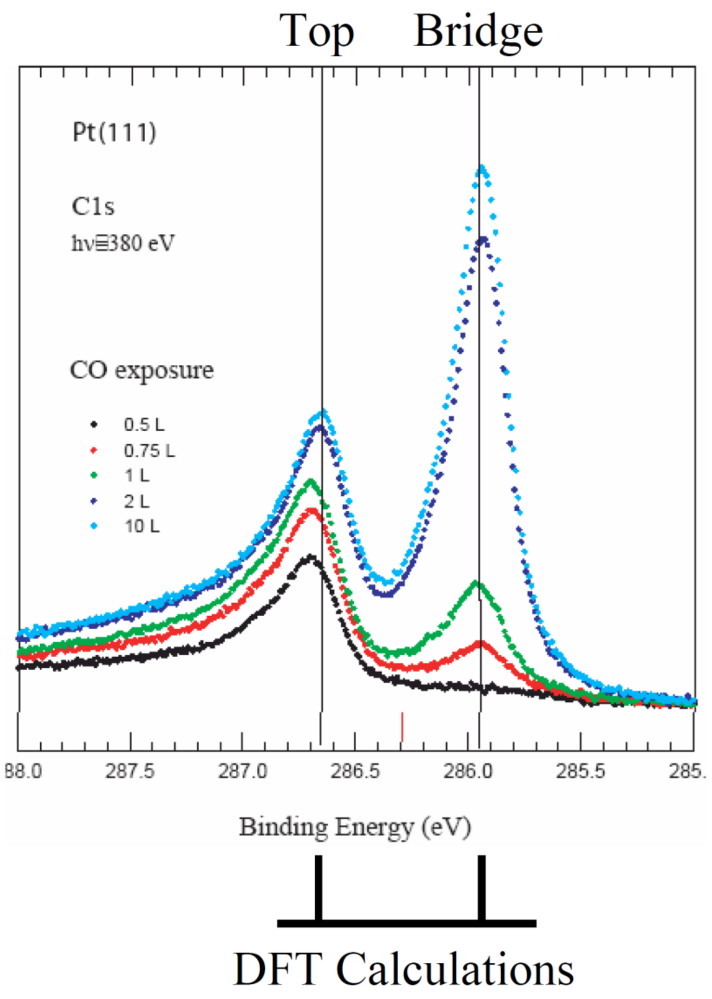

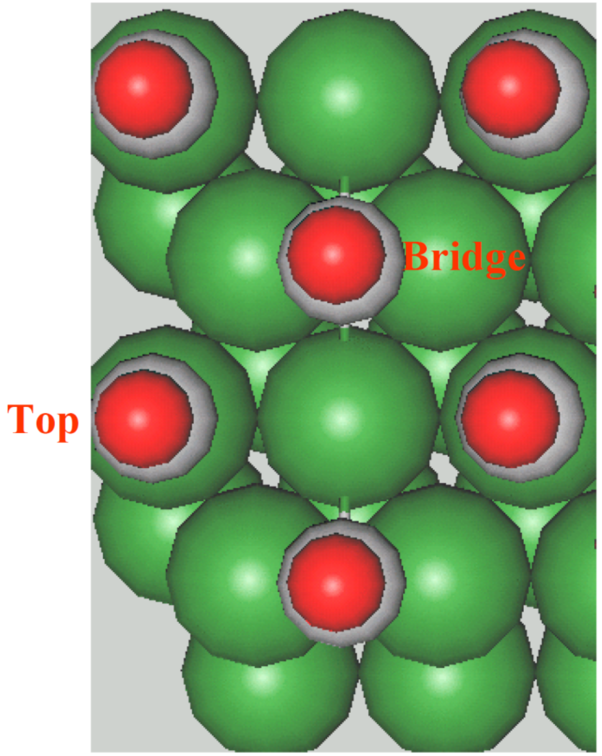

Wang, Li, Borg, Hammer and Andersen et al. Phys. Rev. Lett. 95, 256102 (2005)

The Soft X-Ray Spectroscopies

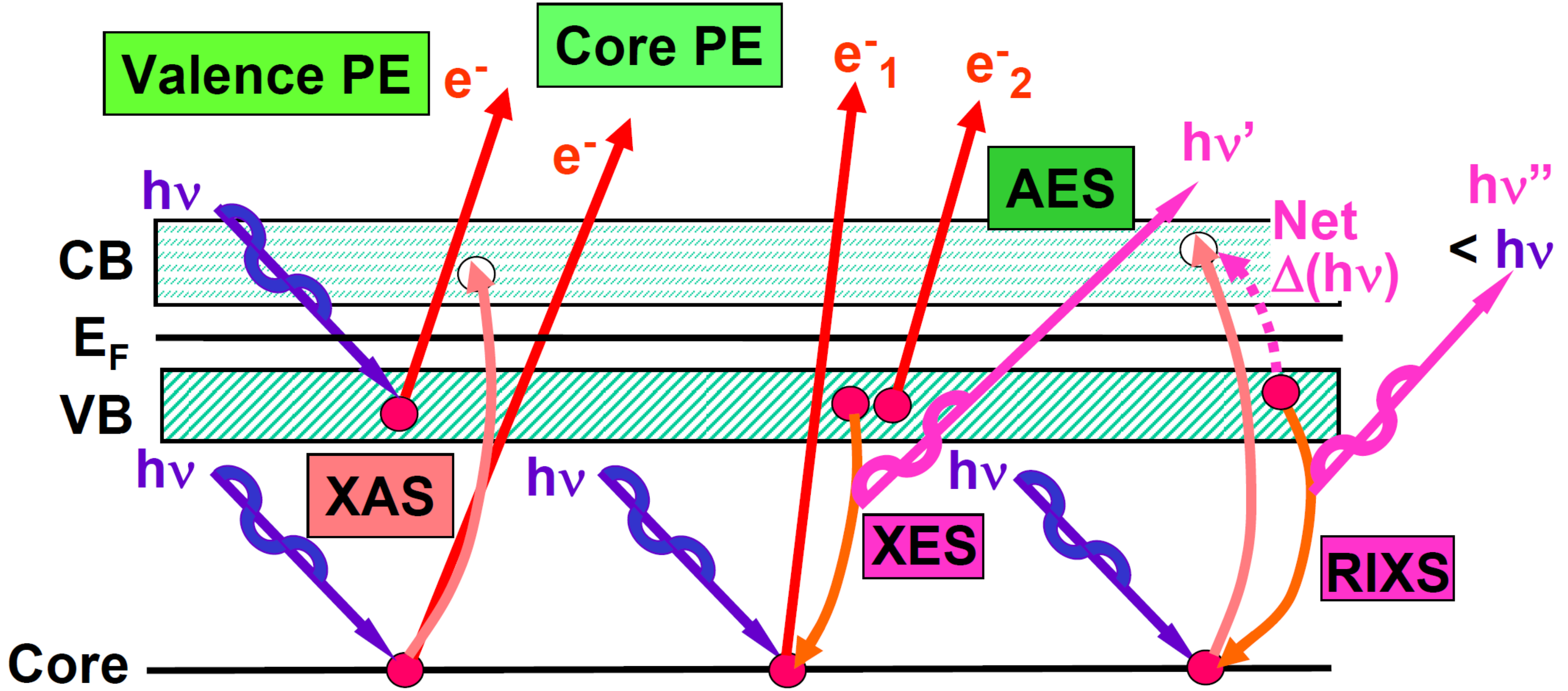

PE = photoemission = photoelectron spectroscopy
XAS = x-ray absorption spectroscopy
AES = Auger electron spectroscopy
XES = x-ray emission spectroscopy
RIXS = resonant inelastic x-ray scattering / x-ray Raman scatt.

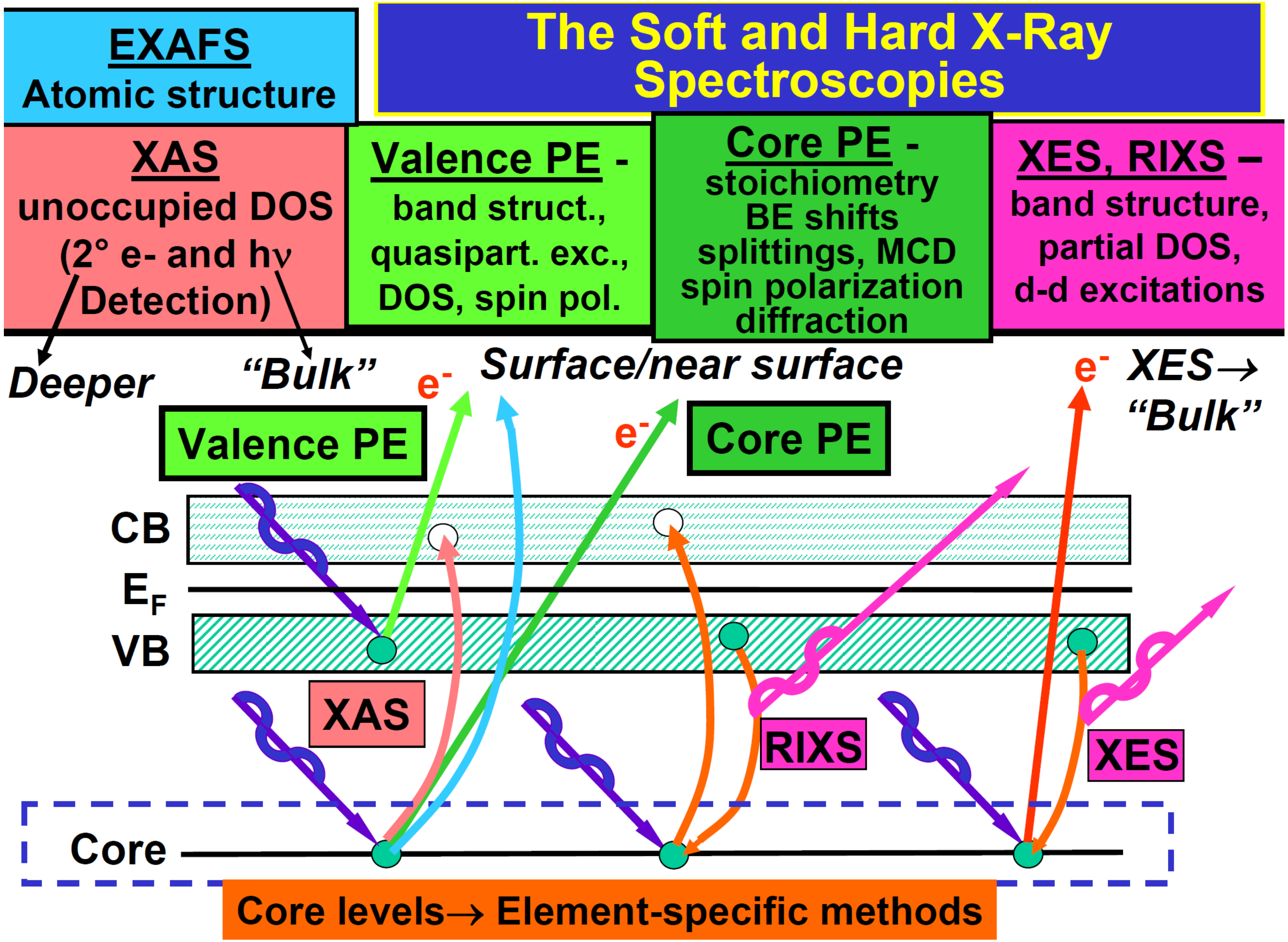

EXAFS
Atomic structure
The Soft and Hard X-Ray Spectroscopies
XAS
unoccupied DOS
(2° e- and hν Detection)
Valence PE -
band struct.,
quasipart. exc.,
DOS, spin pol.
Core PE -
stoichiometry
BE shifts
splittings, MCD
spin polarization
diffraction
XES, RIXS –
band structure,
partial DOS,
d-d excitations
Deeper
"Bulk"
e^-
Surface/near surface
e^-
XES→
"Bulk"
Valence PE
e^-
Core PE
CB
E_F
VB
XAS
RIXS
XES
Core
Core levels→ Element-specific methods

XPS (Core Level Photoelectron Spectroscopy)

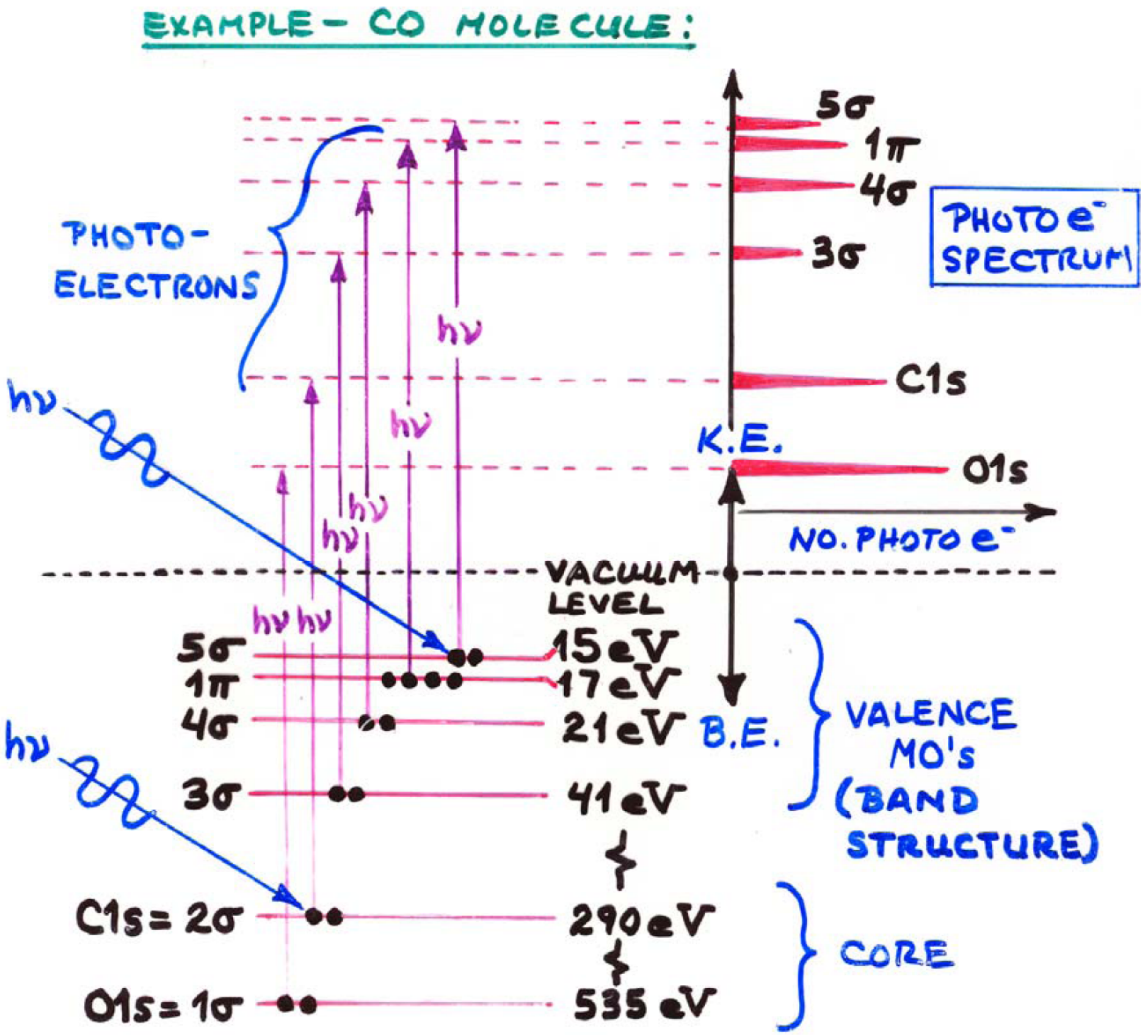

XPS (Instrumentation)

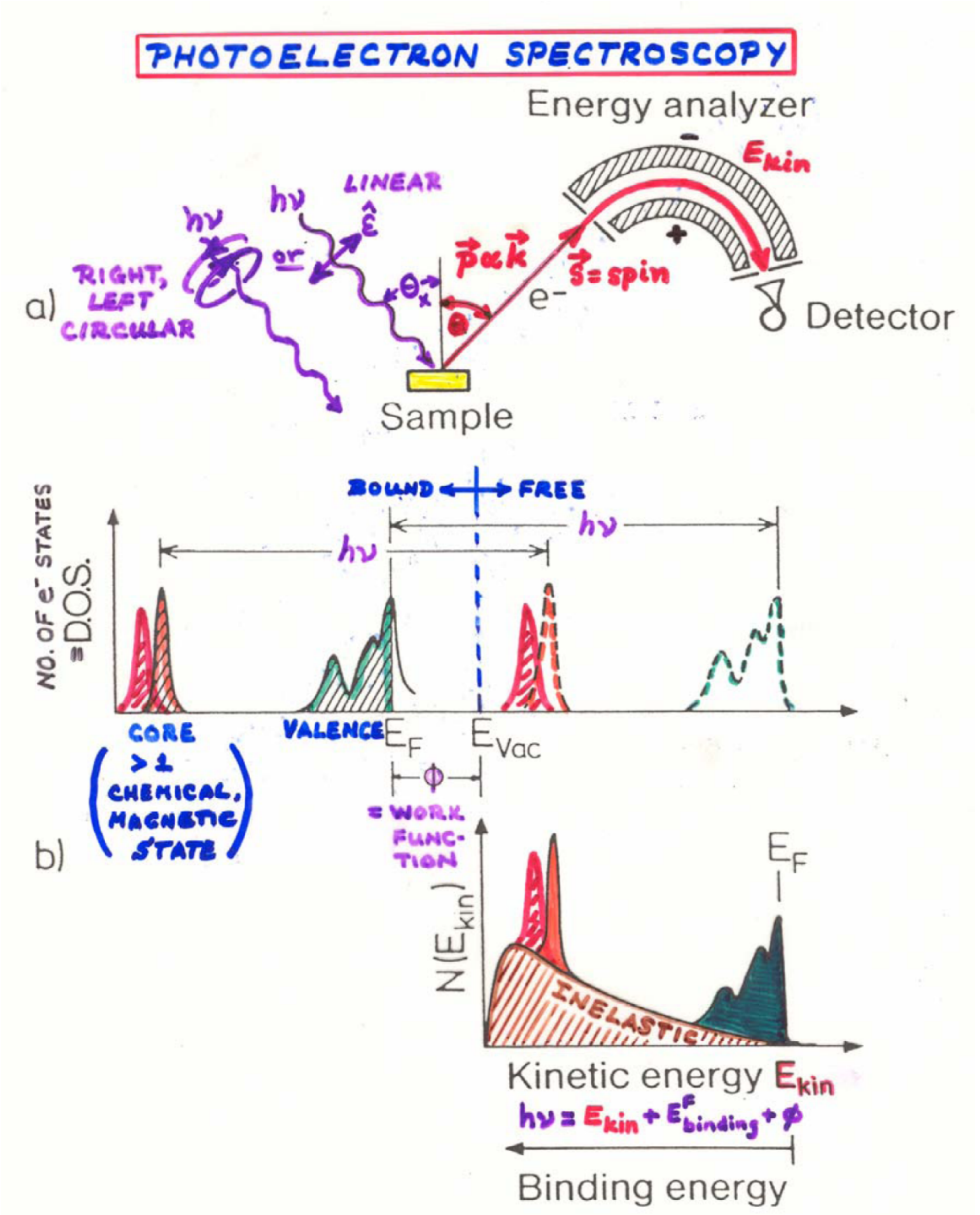

XPS (Core Level Photoelectron Spectroscopy)

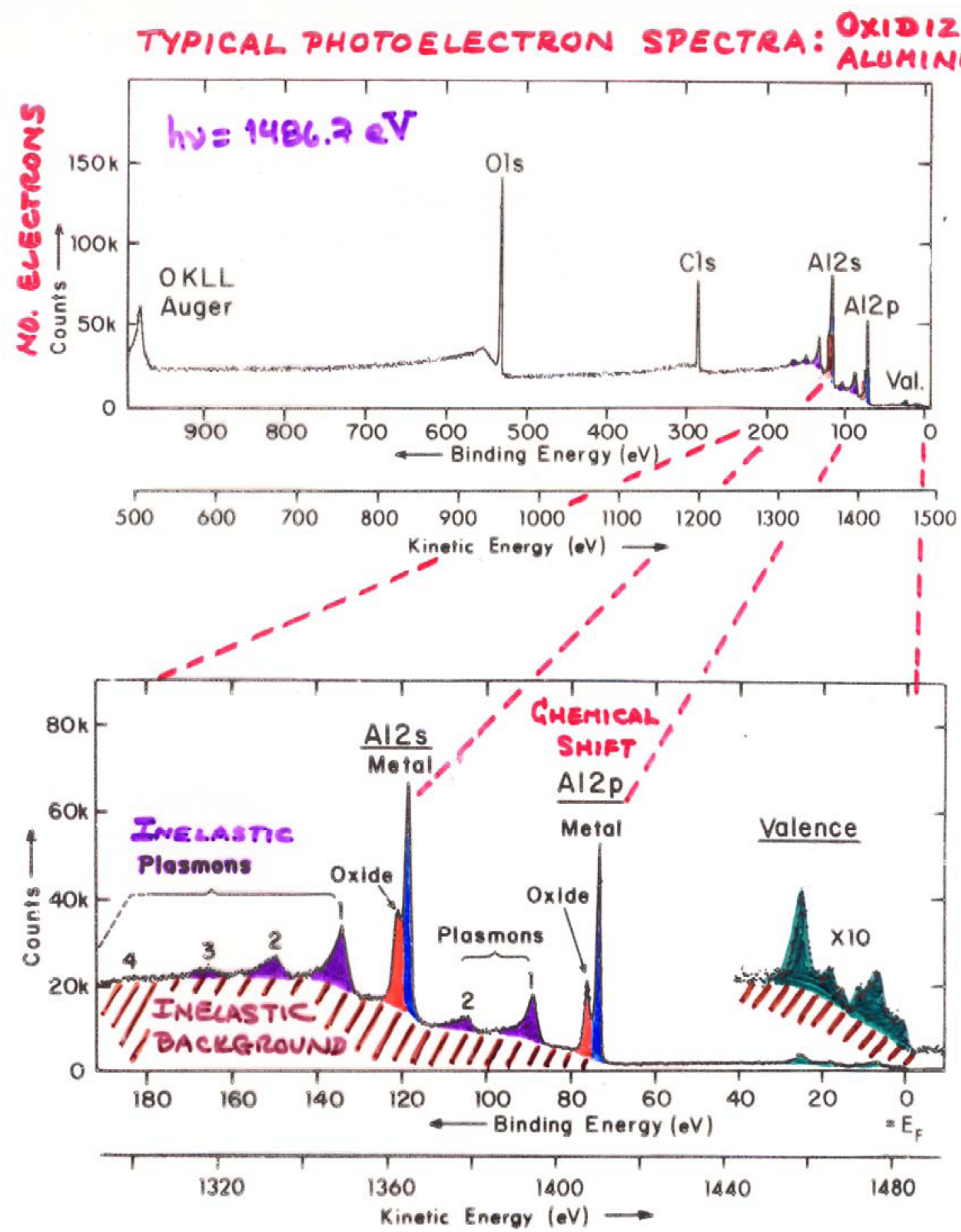

“Basic

Core Level Photoelectron Spectroscopy

BINDING ENERGIES + KOOPMANS' THEOREM:

N-e⁻ SCH. EQN. — $\hat{H}(N)\Psi_j(N) = E_j(N)\Psi_j(N)$, $j = 1, 2 \ldots$

MINIMIZE $E_j(N)$ $\downarrow$ $\Psi_j \approx \Phi_j$ = SLATER DET.

N 1-e⁻ HARTREE-FOCK EQNS. — $\hat{h}(1)\varphi_k(1) = \varepsilon_k(1)\varphi_k(1)$

- COUPLED INTEGRO-DIFF.
- COULOMB + EXCHANGE

$E_b(k)$ = k^{th} BINDING ENERGY = $E_f(N-1, k \text{ hole}) - E_i(N)$
EXACT

(+) OR $E_b(k) = -\varepsilon_k$ IF $\varphi_{ki} = \varphi_{kf}$ (FROZEN ORBITAL)

KOOPMANS' THEOREM

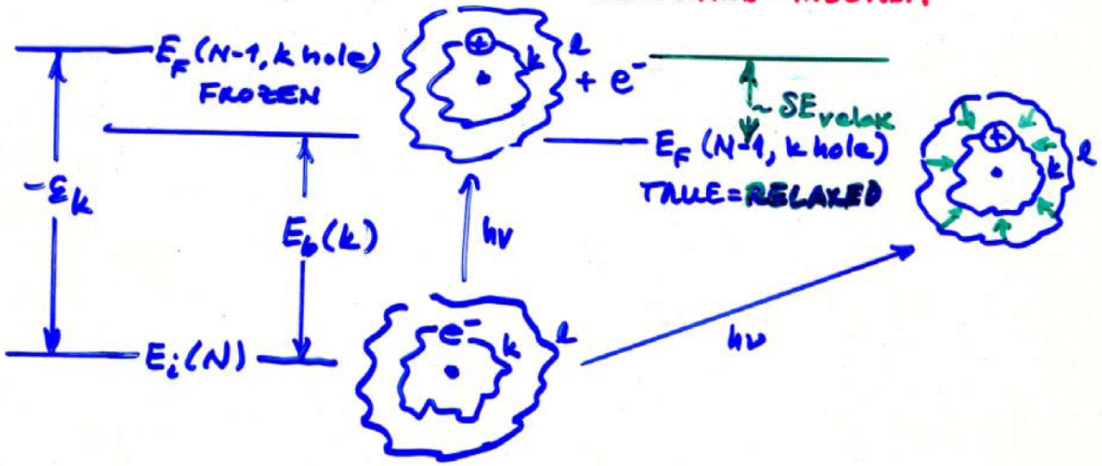

⇒ RELAXATION, SCREENING, CONFIGURATION INTERACTION, SELF-ENERGY EFFECTS ALWAYS PRESENT; ANDERSON IMPURITY MODEL ETC.

Core Level Photoelectron Spectroscopy

MAKING THE ATOMIC ORBITALS REAL (E.G., FOR CHEMICAL BONDING):

$$\underbrace{\Psi_{n\ell m_\ell}}_{\text{COMPLEX}}(r,\theta,\phi) = \underbrace{R_{n\ell}(r)}_{\text{REAL}}\underbrace{\Theta_{\ell m_\ell}(\theta)}_{\text{REAL}}\frac{1}{\sqrt{2\pi}}\underbrace{e^{im_\ell\phi}}_{\text{COMPLEX IF } m_\ell \neq 0}$$

SO JUST TAKE COMB. OF $\pm m_\ell$ AS:

$$\Psi_{n\ell(-)}(r,\theta,\phi) = \begin{cases} \frac{1}{2}\left[\Psi_{n\ell m_\ell} + \Psi_{n\ell -m_\ell}\right] \propto R_{n\ell}\Theta_{\ell m_\ell}\cos m_\ell\phi \\ \frac{1}{2i}\left[\Psi_{n\ell m_\ell} - \Psi_{n\ell -m_\ell}\right] \propto R_{n\ell}\Theta_{\ell m_\ell}\sin m_\ell\phi \end{cases}$$

REAL

EXAMPLE: 2p ORBITALS

$$\Psi_{210} = \Psi_{2p_0} = \Psi_{2p_z} \propto r\cos\theta = z \quad \text{(ALREADY REAL)}$$

$$\Psi_{211} = \Psi_{2p_{+1}} \propto r\sin\theta\, e^{i\phi} = r\sin\theta[\cos\phi + i\sin\phi]$$

$$\Psi_{21-1} = \Psi_{2p_{-1}} \propto r\sin\theta\, e^{-i\phi} = r\sin\theta[\cos\phi - i\sin\phi]$$

$\therefore$

$$\frac{1}{2}[\Psi_{2p_{+1}} + \Psi_{2p_{-1}}] = \Psi_{2p_x} \propto r\sin\theta\cos\phi = x$$

$$\frac{1}{2i}[\Psi_{2p_{+1}} - \Psi_{2p_{-1}}] = \Psi_{2p_y} \propto r\sin\theta\sin\phi = y$$

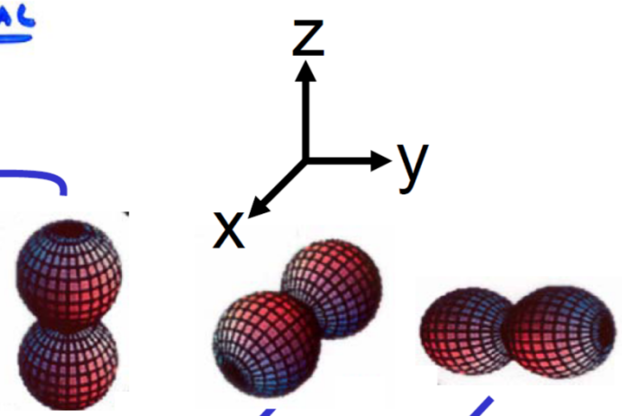

Core Level Photoelectron Spectroscopy

Atomic orbitals:

COMPLEX, IF $m \neq 0$

TABLE 6.1

NORMALIZED WAVE FUNCTIONS OF THE HYDROGEN ATOM FOR n = 1, 2, AND 3* ($Z = 1$ = HYDROGEN)

n	ℓ	m_ℓ		$\Phi_{m_\ell}(\phi)$	$\Theta_{\ell m_\ell}(\theta)$	$R_{n\ell}(r)$	$\psi_{n\ell m_\ell}(r,\theta,\phi) = \Phi_{m_\ell}\Theta_{\ell m_\ell}R_{n\ell}$
1	0	0	1s	$\frac{1}{\sqrt{2\pi}}$	$\frac{1}{\sqrt{2}}$	$\frac{2}{a_0^{3/2}} e^{-r/a_0}$	$\frac{1}{\sqrt{\pi}\, a_0^{3/2}} e^{-r/a_0}$
2	0	0	2s	$\frac{1}{\sqrt{2\pi}}$	$\frac{1}{\sqrt{2}}$	$\frac{1}{2\sqrt{2}\, a_0^{3/2}} \left(2 - \frac{r}{a_0}\right) e^{-r/2a_0}$	$\frac{1}{4\sqrt{2\pi}\, a_0^{3/2}} \left(2 - \frac{r}{a_0}\right) e^{-r/2a_0}$
2	1	0	$2p_0$	$\frac{1}{\sqrt{2\pi}}$	$\frac{\sqrt{6}}{2} \cos\theta$	$\frac{1}{2\sqrt{6}\, a_0^{3/2}} \frac{r}{a_0} e^{-r/2a_0}$	$\frac{1}{4\sqrt{2\pi}\, a_0^{3/2}} \frac{r}{a_0} e^{-r/2a_0} \cos\theta$
2	1	±1	$2p_{\pm1}$	$\frac{1}{\sqrt{2\pi}} e^{\pm i\phi}$	$\frac{\sqrt{3}}{2} \sin\theta$	$\frac{1}{2\sqrt{6}\, a_0^{3/2}} \frac{r}{a_0} e^{-r/2a_0}$	$\frac{1}{8\sqrt{\pi}\, a_0^{3/2}} \frac{r}{a_0} e^{-r/2a_0} \sin\theta\, e^{\pm i\phi}$
3	0	0	3s	$\frac{1}{\sqrt{2\pi}}$	$\frac{1}{\sqrt{2}}$	$\frac{2}{81\sqrt{3}\, a_0^{3/2}} \left(27 - 18\frac{r}{a_0} + 2\frac{r^2}{a_0^2}\right) e^{-r/3a_0}$	$\frac{1}{81\sqrt{3\pi}\, a_0^{3/2}} \left(27 - 18\frac{r}{a_0} + 2\frac{r^2}{a_0^2}\right) e^{-r/3a_0}$
3	1	0	$3p_0$	$\frac{1}{\sqrt{2\pi}}$	$\frac{\sqrt{6}}{2} \cos\theta$	$\frac{4}{81\sqrt{6}\, a_0^{3/2}} \left(6 - \frac{r}{a_0}\right) \frac{r}{a_0} e^{-r/3a_0}$	$\frac{\sqrt{2}}{81\sqrt{\pi}\, a_0^{3/2}} \left(6 - \frac{r}{a_0}\right) \frac{r}{a_0} e^{-r/3a_0} \cos\theta$
3	1	±1	$3p_{\pm1}$	$\frac{1}{\sqrt{2\pi}} e^{\pm i\phi}$	$\frac{\sqrt{3}}{2} \sin\theta$	$\frac{4}{81\sqrt{6}\, a_0^{3/2}} \left(6 - \frac{r}{a_0}\right) \frac{r}{a_0} e^{-r/3a_0}$	$\frac{1}{81\sqrt{\pi}\, a_0^{3/2}} \left(6 - \frac{r}{a_0}\right) \frac{r}{a_0} e^{-r/3a_0} \sin\theta\, e^{\pm i\phi}$
3	2	0	$3d_0$	$\frac{1}{\sqrt{2\pi}}$	$\frac{\sqrt{10}}{4} (3\cos^2\theta - 1)$	$\frac{4}{81\sqrt{30}\, a_0^{3/2}} \frac{r^2}{a_0^2} e^{-r/3a_0}$	$\frac{1}{81\sqrt{6\pi}\, a_0^{3/2}} \frac{r^2}{a_0^2} e^{-r/3a_0} (3\cos^2\theta - 1)$
3	2	±1	$3d_{\pm1}$	$\frac{1}{\sqrt{2\pi}} e^{\pm i\phi}$	$\frac{\sqrt{15}}{2} \sin\theta\cos\theta$	$\frac{4}{81\sqrt{30}\, a_0^{3/2}} \frac{r^2}{a_0^2} e^{-r/3a_0}$	$\frac{1}{81\sqrt{\pi}\, a_0^{3/2}} \frac{r^2}{a_0^2} e^{-r/3a_0} \sin\theta\cos\theta\, e^{\pm i\phi}$
3	2	±2	$3d_{\pm2}$	$\frac{1}{\sqrt{2\pi}} e^{\pm 2i\phi}$	$\frac{\sqrt{15}}{4} \sin^2\theta$	$\frac{4}{81\sqrt{30}\, a_0^{3/2}} \frac{r^2}{a_0^2} e^{-r/3a_0}$	$\frac{1}{162\sqrt{\pi}\, a_0^{3/2}} \frac{r^2}{a_0^2} e^{-r/3a_0} \sin^2\theta\, e^{\pm 2i\phi}$

*The quantity $a_0 = 4\pi\epsilon_0\hbar^2/me^2 = 5.3 \times 10^{-11}$ m is equal to the radius of the innermost Bohr orbit.

IS SAME FOR MANY e^- ATOMS

CHANGES FOR MANY e^- ATOMS

Core Level Photoelectron Spectroscopy

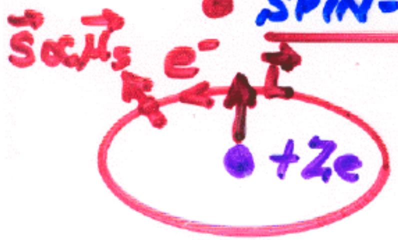

- SPIN-ORBIT SPLITTING OF LEVELS:

$\Rightarrow$ EFFECTIVE $\vec{B}$ (NUCLEUS AROUND e^-) $\propto \vec{L}$

$$\hat{H}_{s\text{-}o} = \xi(r)\,\vec{\ell}\cdot\vec{s}$$

- SPLITS ALL $n\ell$ LEVELS $2(2\ell+1)$ → $n\ell_j = \ell + 1/2$ — $2\ell+2$; → $n\ell_j = \ell - 1/2$ — 2ℓ

- MIXES SPIN + ORBITAL ANGULAR MOM.:

$$\psi_{n\ell j m_j} = C_1 \psi_{n\ell, m_j - 1/2} \underbrace{\begin{pmatrix}1\\0\end{pmatrix}}_{m_s = +1/2 \,=\, \uparrow} + C_2 \psi_{n\ell, m_j + 1/2} \underbrace{\begin{pmatrix}0\\1\end{pmatrix}}_{m_s = -1/2 \,=\, \downarrow}$$

WITH C1 AND C2 TABULATED CLEBSCH-GORDAN OR WIGNER 3j SYMBOLS

Core Level Photoelectron Spectroscopy

Some spin-orbit splittings: (in eV)

Level			
$2p^6 \rightarrow 2p_{1/2}^2,\ 2p_{3/2}^4$	Z = 13 (Al)	28 (Ni)	46 (Pd)
	0.4	17.8	157.0
$3d^{10} \rightarrow 3d_{3/2}^4,\ 3d_{5/2}^6$	Z = 30 (Zn)	48 (Cd)	64 (Gd)
	0.1	6.7	32.3
$4f^{14} \rightarrow 4f_{5/2}^6,\ 4f_{7/2}^8$	Z = 74 (W)	84 (Pb)	92 (U)
	2.2	7.0	64

Increase with Z for a given level.

In general:

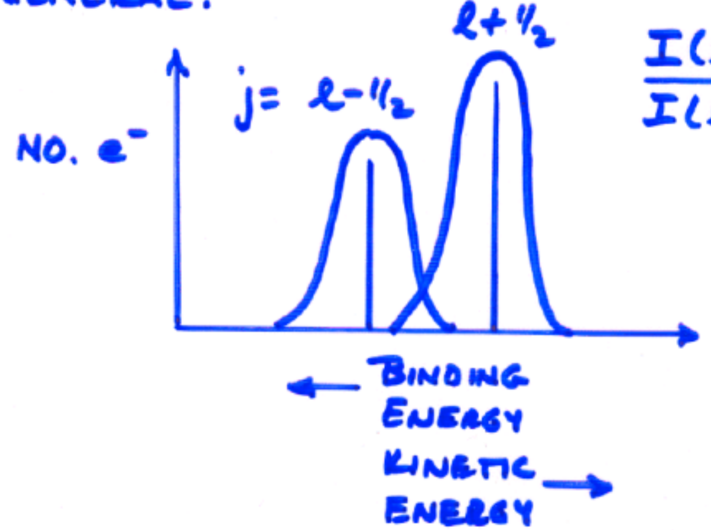

$$\frac{I(\ell + 1/2)}{I(\ell - 1/2)} = \frac{2\ell + 2}{2\ell}$$

Core Level Photoelectron Spectroscopy

PHOTOELECTRON EMISSION –
BASIC MATRIX ELEMENTS + SELECTION RULES:

- **ATOMIC-LIKE (LOCALIZED) STATES ⇒ CORE:**

$$\varphi_i(\vec{r}) = \varphi_{n_i \ell_i m_i}(r,\theta,\phi) = R_{n_i \ell_i}(r) Y_{\ell_i m_i}(\theta,\phi)$$

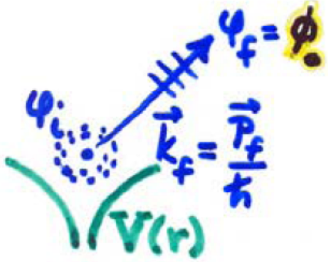

$$\varphi_f(\vec{r},\vec{k}_f) = \varphi_{E_f}(\vec{r},\vec{k}_f)$$

PHASE SHIFT OF ℓ_f WAVE IN V(r)

$$= 4\pi \sum_{\ell_f, m_f} i^{\ell_f} e^{-i\delta_{\ell_f}} Y^*_{\ell_f m_f}(\theta_{k_f}, \phi_{k_f}) Y_{\ell_f m_f}(\theta,\phi) R_{E_f,\ell_f}(r)$$

DIPOLE APPROX.: $\mathrm{INT.} \propto |\langle \varphi_f | \hat{\varepsilon}\cdot\vec{r} | \varphi_i \rangle|^2 = |\hat{\varepsilon}\langle \varphi_f | \vec{r} | \varphi_i \rangle|^2 \Rightarrow$

- $\Delta \ell = \ell_f - \ell_i = \pm 1$ TWO CHANNELS
- $\Delta m = m_f - m_i = 0, \pm 1$ LINEAR POLARIZ.
- $\Delta m = \pm 1$, CIRCULAR POLARIZATION

$\vec{r} \updownarrow \vec{p} \updownarrow \vec{\nabla} V(r)$ — EQUIVALENT WITHIN CONSTANT FACTOR

What are the advantages of using SR over Conventional X-ray source?

Energy Tunability

a. Varying the kinetic energy of electron

b. Tuning Cross section

Electron escape depth vs. Electron kinetic energy
: so-called "Universal curve"

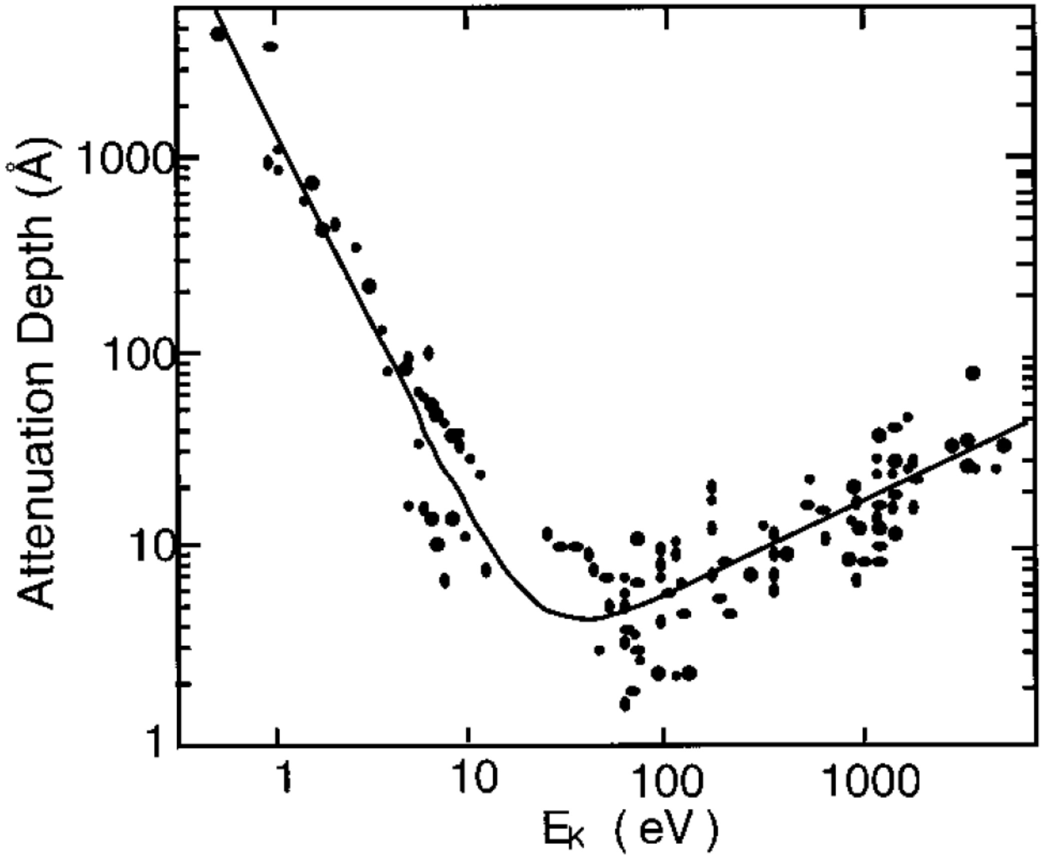

XPS (Electron Mean Free Path)

Inelastic mean free paths in solids

Database of experimental and theoretically estimated mean free paths at http://www.nist.gov/srd/webguide/nist71/71imfp.htm#elements

Plus estimation with the TPP-2M (TPP-2) formula of Tanuma, Powell, Penn:

Web calculation for elements from: http://www.ss.teen.setsunan.ac.jp/e-imfp2.html

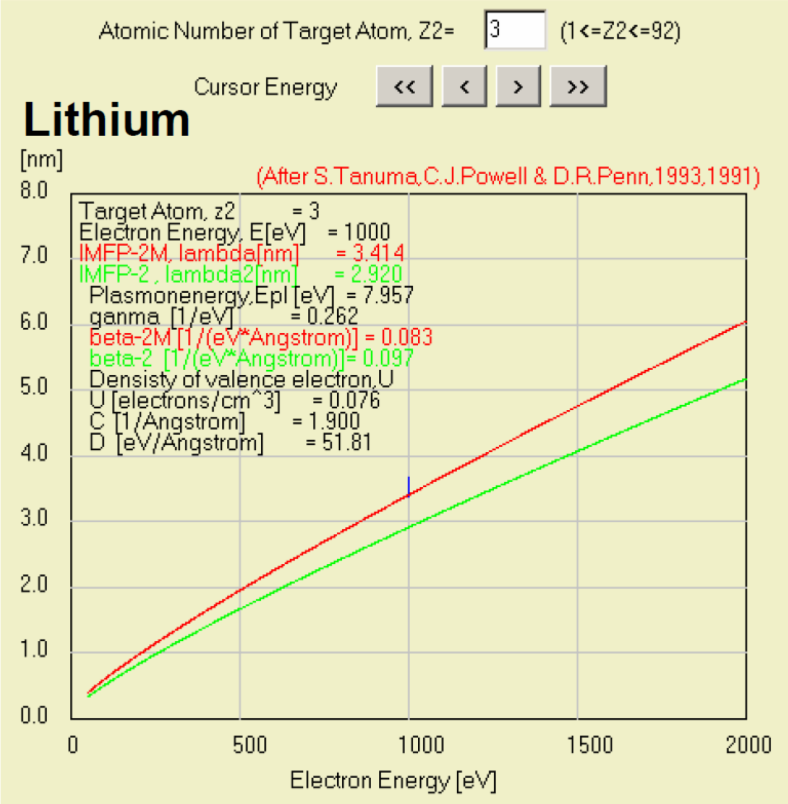

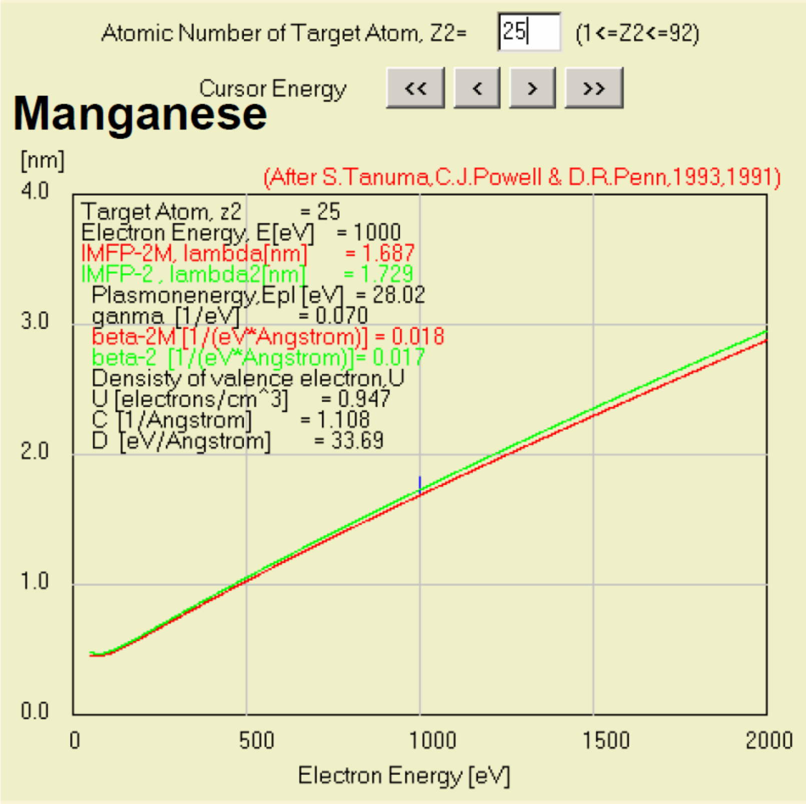

XPS (Electron Mean Free Path)

Inelastic mean free paths in solids

Estimation from the TPP-2M formula: any compound

$$\Lambda_e \approx \lambda = \frac{E}{E_p^2[\beta \ln(\gamma E) - (C/E) + (D/E^2)]}$$

where

$$\beta = -0.10 + 0.944/(E_p^2 + E_g^2)^{1/2} + 0.069\rho^{0.1}$$

$$\gamma = 0.191\rho^{-0.50}$$

$$C = 1.97 - 0.91U$$

$$D = 53.4 - 20.8U$$

$$U = N_v\rho/M = E_p^2/829.4$$

and $E_p = 28.8\,(N_v\rho/M)^{1/2}$ is the free-electron plasmon energy (in eV), ρ is the density (in g cm^{-3}), N_v is the number of valence electrons per atom (for an element) or molecule (for a compound), M is the atomic or molecular weight, and E_g is the bandgap energy (in eV). These equations are collectively known as the TPP-2M equation.

Tanuma, Powell, Penn, Surf. Interface Anal. 21, 165 (1994)

Depth Profiling Information

With synchrotron radiation, kinetic energy of electron can be easily tuned by varying incoming photon energy.

E(K.E.) = E(P.E.) - E(B.E.)
Binding energy (Si 2p) : ~100eV
Photon energy (130~400 eV)
Kinetic energy (30~300 eV)

•Depth profiling can be done with different take-off angle measurement in the case of flat solid sample.

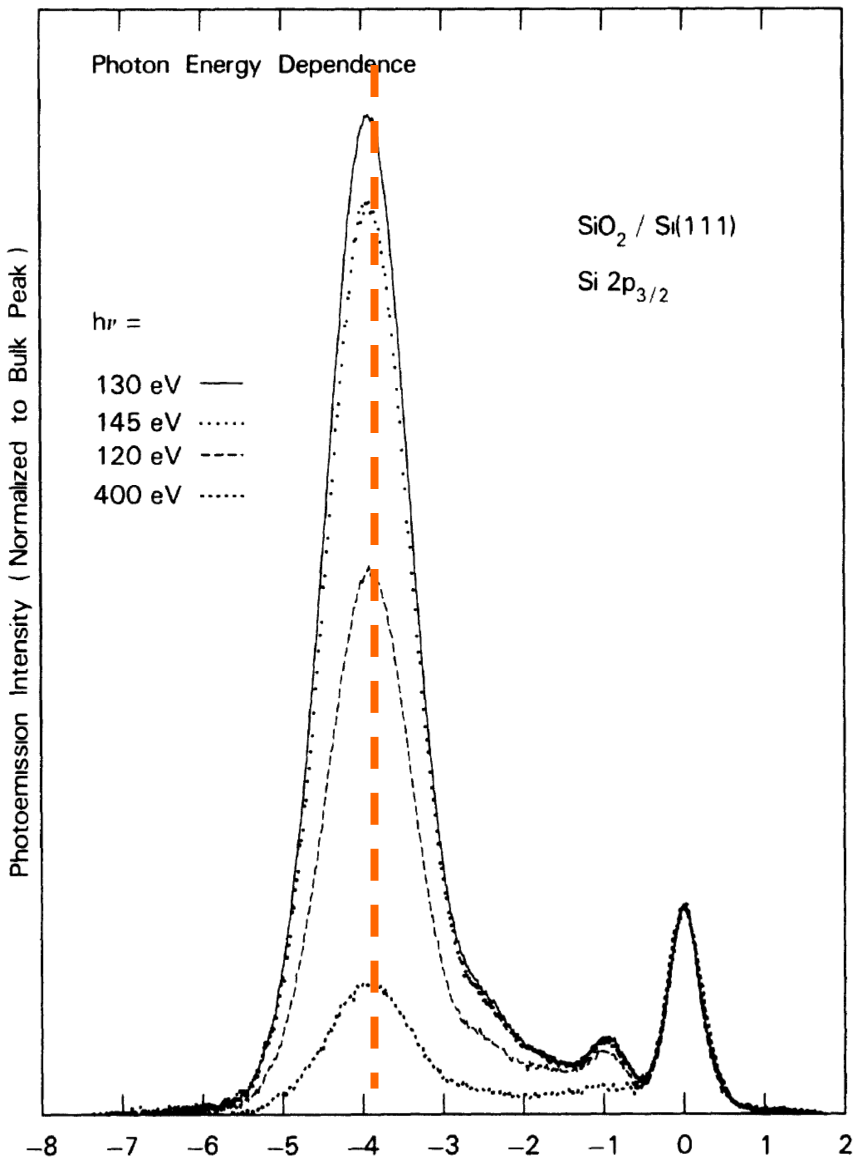

Phys. Rev. B 38, 6084 (September 1988)

Depth Profiling Information

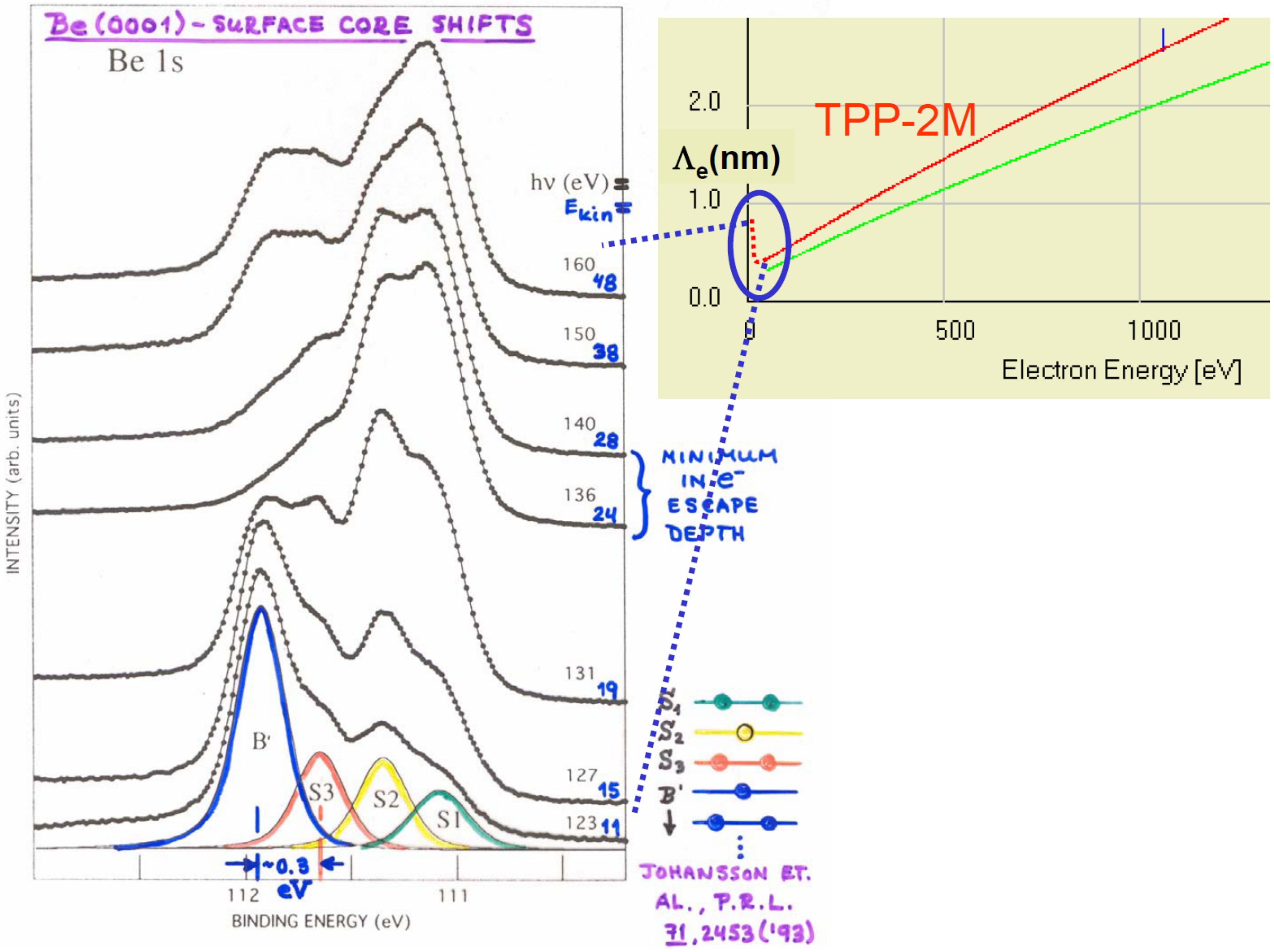

XPS (Depth Profile)

Surface sensitivity enhancement for grazing exit angles

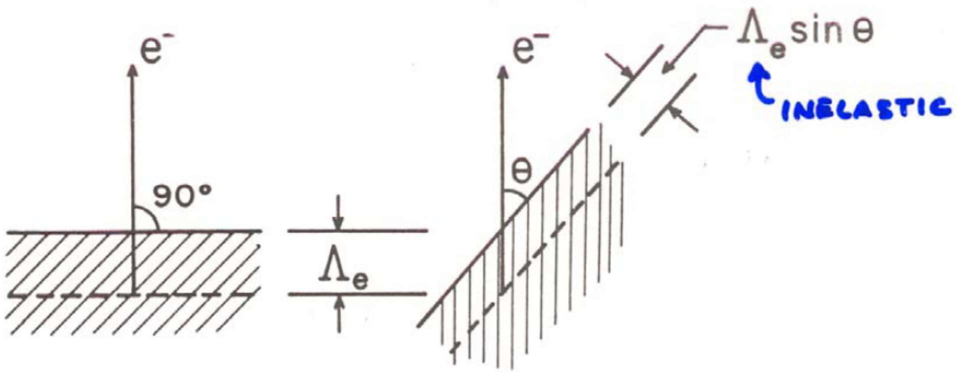

$5\,\text{Å} \lesssim \Lambda_e \lesssim 80\,\text{Å}$

Fig. 5. Illustration of the basic mechanism producing surface sensitivity enhancement for low electron exit angles θ. The average depth for no-loss emission as measured perpendicular to the surface is $\Lambda_e \sin\theta$.

E.g.- Λ_e = 28Å in Au(s) at 1400 eV

	θ	Mean Depth	No. layers
"BULK" →	90°	28Å	~9
"SURFACE" →	10°	~4.4Å	~1.5

... BUT REFRACTION AT SURFACE AND ELASTIC SCATTERING CAN REDUCE SURFACE ENHANCEMENT, ESP. AT LOW $\theta \lesssim 30°$

XPS (Depth Profile)

Surface sensitivity enhancement for grazing exit angles

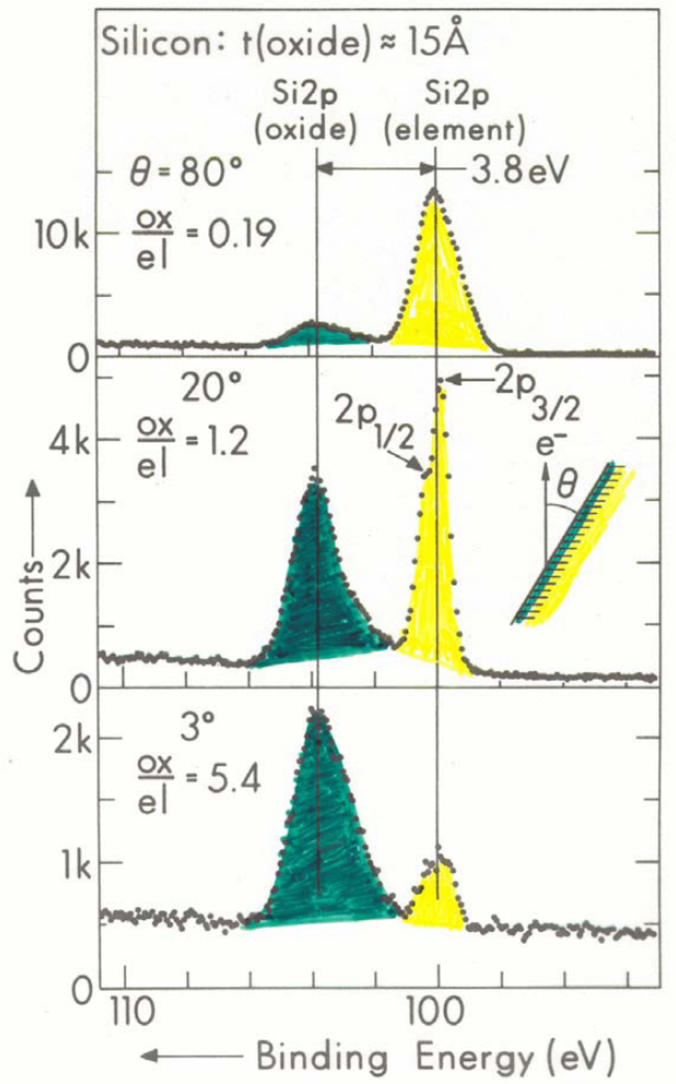

Fadley, Progress in Surface Science, 16, 275 ('84)

Fig. 7. Si2p spectra at three electron exit angles for a Si specimen with a 15-Å thick oxide overlayer. Note the complete reversal of the relative intensities of oxide and element between high and low θ. (From Hill et al., ref. (19).)

Nanoparticle Alloys :

Surface Composition is varied by
The

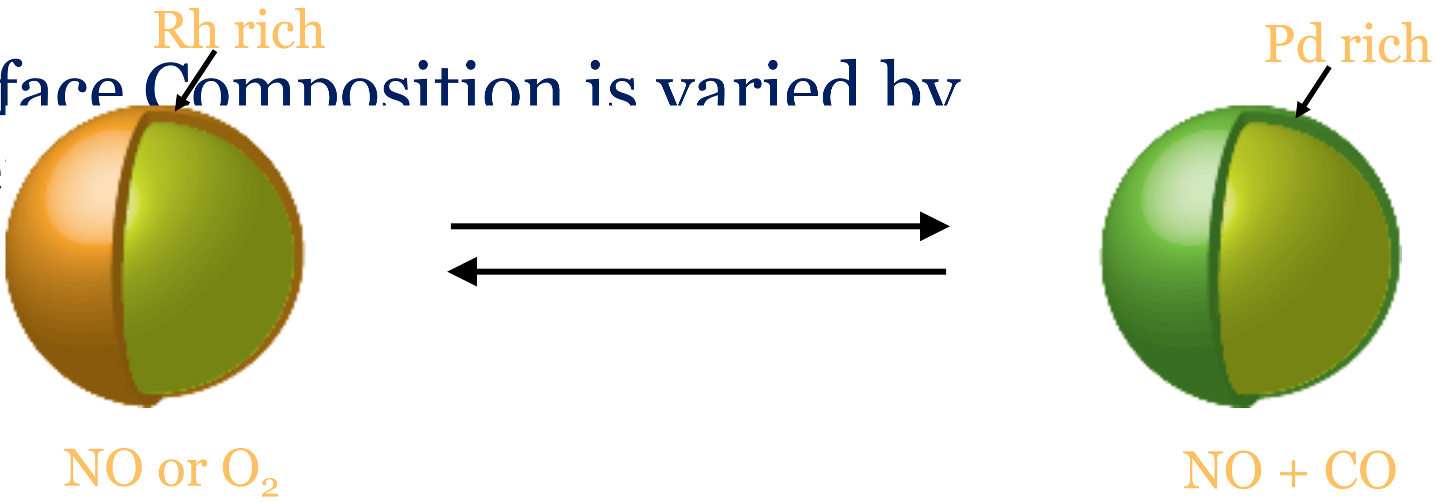

Rh_2O_3 more stable than PdO

Pd has a lower surface free energy (1.87 J m^{-2} at 1173 K) than Rh (2.52 J m^{-2})

Maillet, et al. *J. Catal.* 202 (2001) 367

$Rh_{0.5}Pd_{0.5}$ Nanoparticle
: Surface Segregation and Restructuring

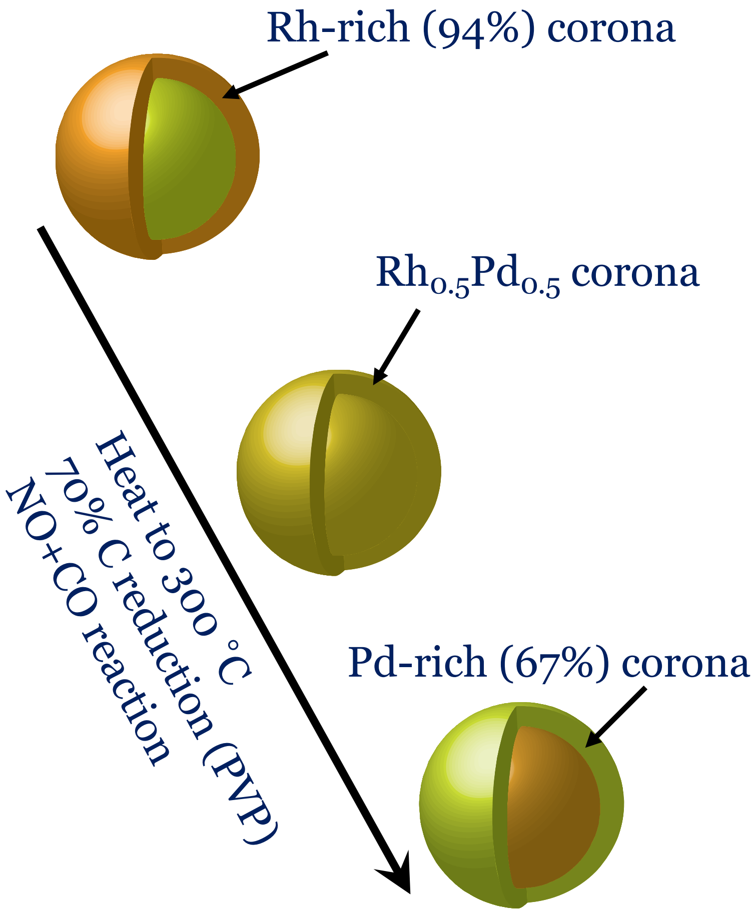

Depth Profile : XPS Atomic Concentrations (E_{photon} = 645 eV or 850 eV)

- Pd pulled to surface at 250 °C in CO + NO
- Pd_{surf} increases from 6% to 67%
- $Pd_{near\ surf}$ increases from 10% to 55%

Surface Segregation and Restructuring under Ambient Pressure Condition (CO + NO at T = 300C) :

Not only the temperature, Chemistry drives the segregation

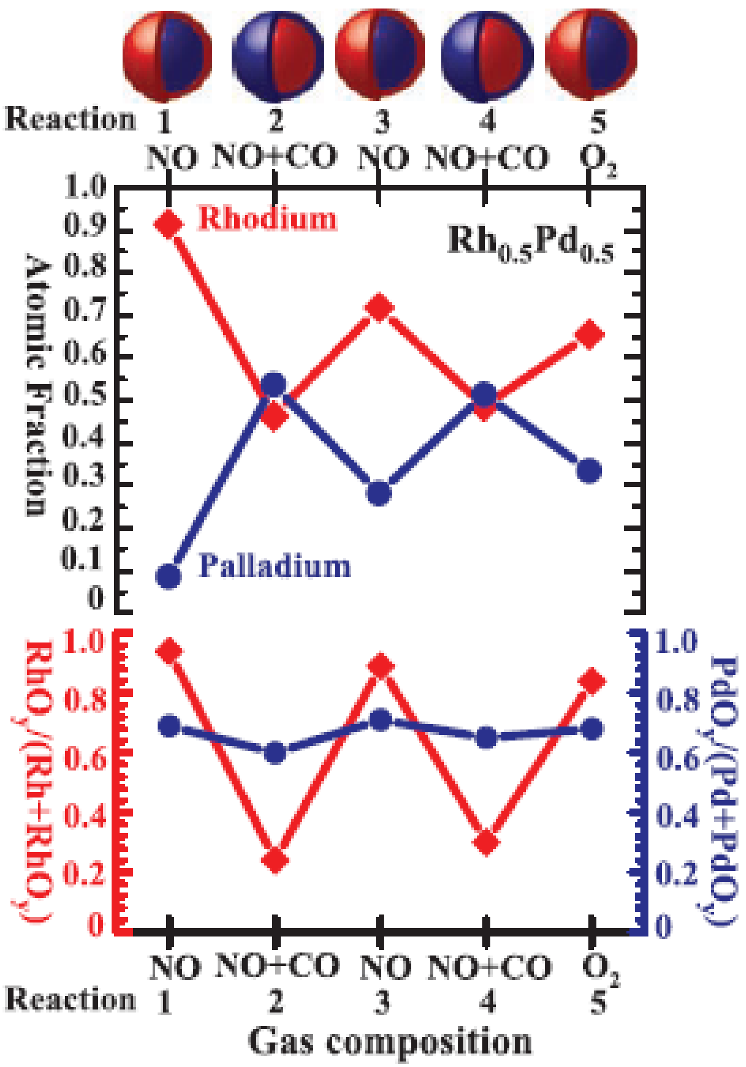

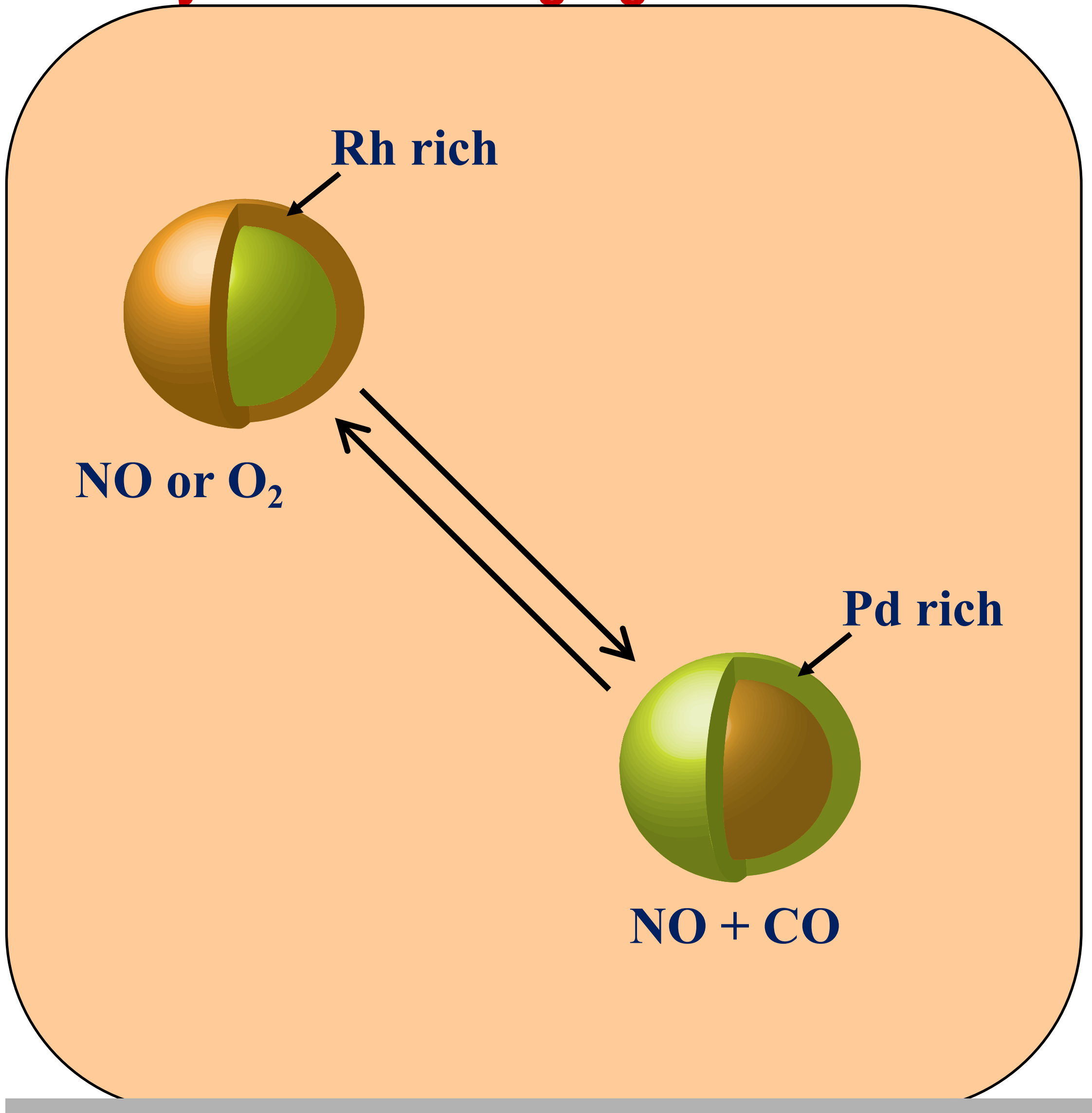

Feng Tao, M. Salmeron, G. Somorjai, Science. 2008

What are the advantages of using SR over Conventional X-ray source?

Energy Tunability

a. Varying the kinetic energy of electron

b. Tuning Cross section

$$\overset{\text{Initial state}}{\Psi_{tot}^{i}(N),\ E_{tot}^{i}(N)} \xrightarrow{h\nu} \overset{\text{Final state ion}}{\Psi_{tot}^{f}(N-1,\ K),\ E_{tot}^{f}(N-1,\ K)} + \overset{\text{Photoelectron}}{\phi^{f}(1)\chi^{f}(1),\ E_{kin}}$$

Photoelectric Cross-Section : Transition probability per unit time for exciting element from a initial state to final state

$$|M_{if}|^2 = \left| \langle \Psi^f(N) | \sum_{i=1}^{N} \mathbf{A}(\mathbf{r}_i) \cdot \hat{p}_i | \Psi^i(N) \rangle \right|^2$$

$$= \hbar^2 A_0^2 \left| \langle \Psi^f(N) | \sum_{i=1}^{N} \exp(i\mathbf{k}_{h\nu} \cdot \mathbf{r}_i) \mathbf{e} \cdot \nabla_i | \Psi^i(N) \rangle \right|^2$$

$$\frac{d\sigma}{d\Omega} = C \left(\frac{1}{h\nu} \right) \left| \langle \Psi^f(N) | \sum_{i=1}^{N} \exp(i\mathbf{k}_{h\nu} \cdot \mathbf{r}_i) \mathbf{e} \cdot \nabla_i | \Psi^i(N) \rangle \right|^2$$

Yeh & Lindau, Atomic Data and Nuclear Data Tables, 32, 1-155 (1985).

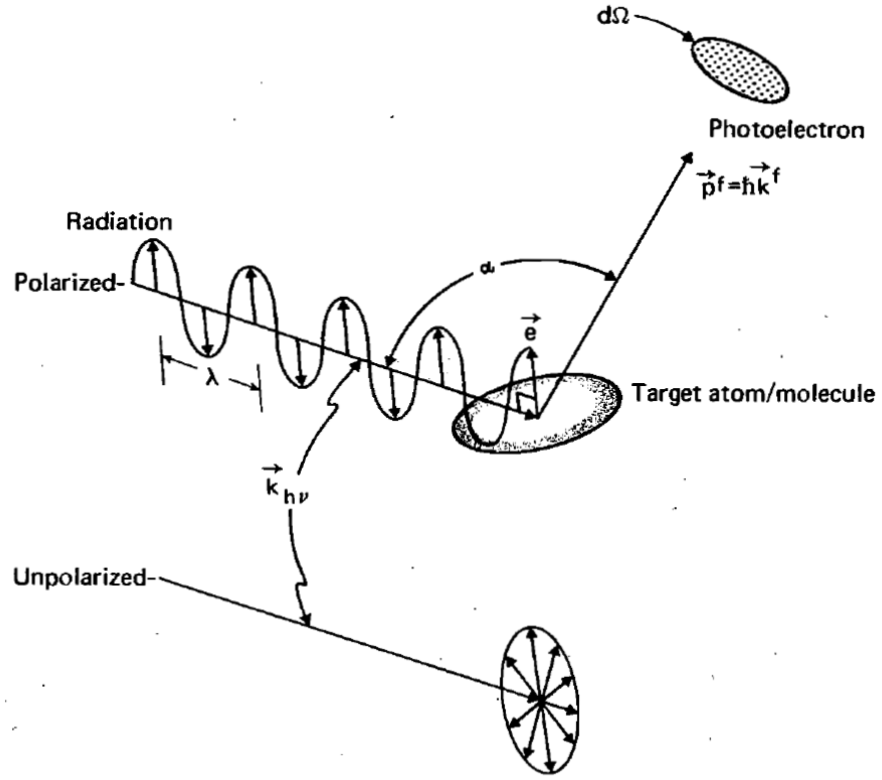

$$\frac{d\sigma_{nl}}{d\Omega}(E^f) = \frac{\sigma_{nl}}{4\pi}\left[1 - \tfrac{1}{2}\beta_{nl}(E^f)P_2(\cos\alpha)\right]$$

$$= \frac{\sigma_{nl}}{4\pi}\left[1 + \tfrac{1}{2}\beta_{nl}(E^f)\left(\tfrac{3}{2}\sin^2\alpha - 1\right)\right]$$

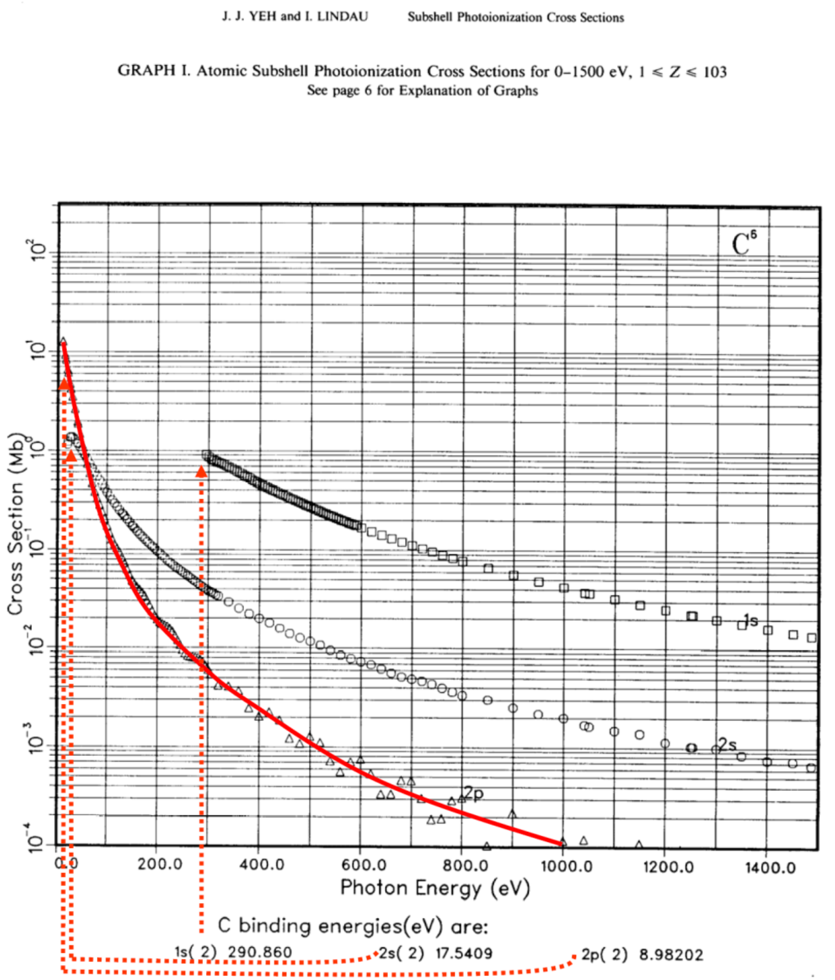

Yeh & Lindau, Atomic Data and Nuclear Data Tables, 32, 1-155 (1985).

By adjusting the photon energy, the cross-section can be easily tuned. Also, using the polarization of light, the molecular geometry on surface can be determined.

COOPER MINIMUM IN In 4d (Z = 49)
CROSS SECTION—Radial Matrix Element Variation

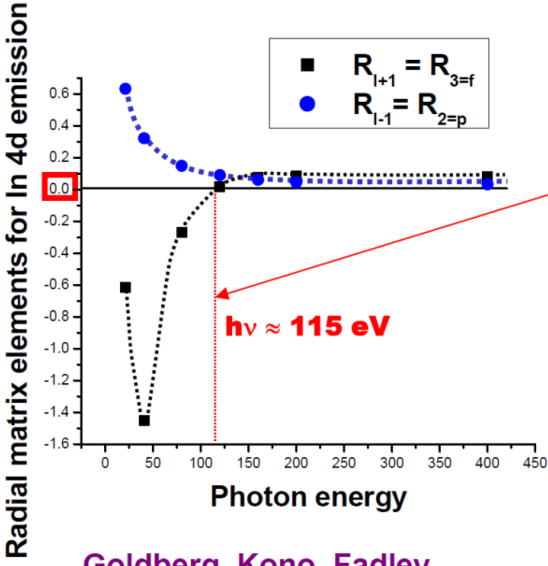

Goldberg, Kono, Fadley
J. Elect. Spect. 21, 285 (‘81)

J. J. YEH and I. LINDAU Subshell Photoionization Cross Sections

GRAPH I. Atomic Subshell Photoionization Cross Sections for 0–1500 eV, 1 ≤ Z ≤ 103
See page 6 for Explanation of Graphs

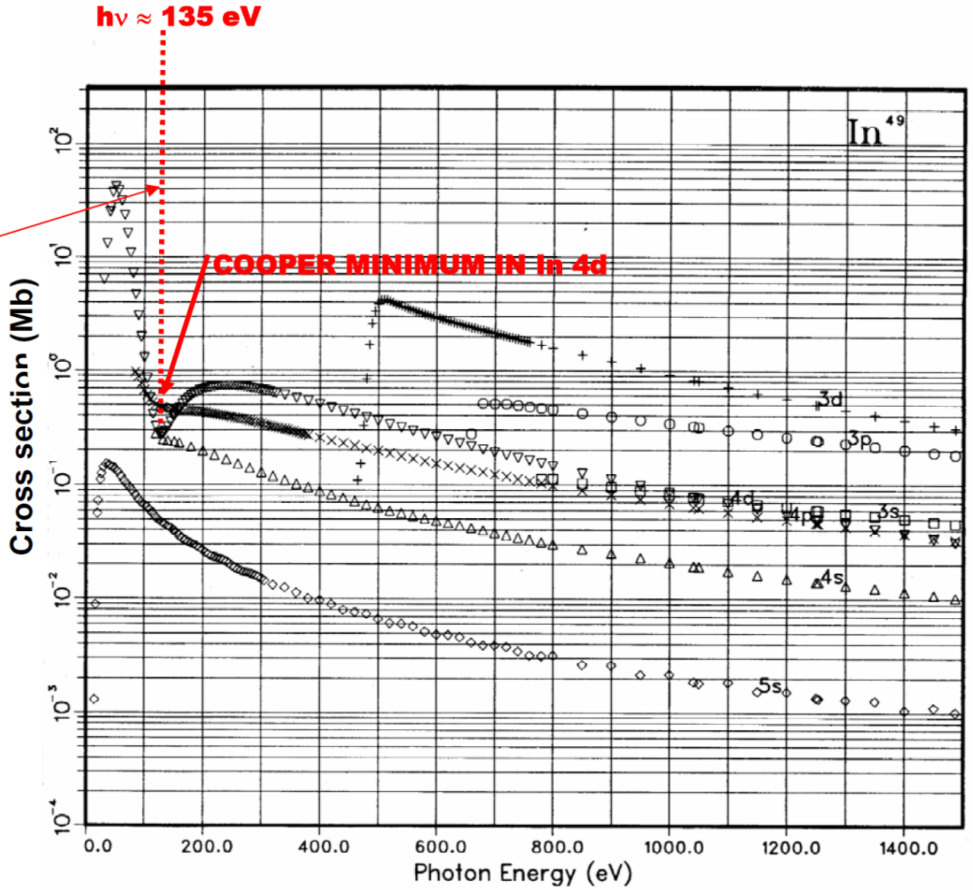

In binding energies(eV) are:

1s(2) 26971.5	2s(2) 3983.01	2p(6) 3731.41
3s(2) 764.232	3p(6) 659.286	4s(2) 118.953
3d(10) 462.909	4p(6) 84.0558	5s(2) 10.1384
4d(10) 26.2168	5p(1) 4.69781	

“ Copper-minimum effect arises from *the presence of a node on the radial portion of the initial-state wave function* of several subshells (e.g. 4d and 5d) and the consequent cancellation of the matrix elements for transition”

Rossi et al. Phys. Rev. B. 28,3031 (1993)

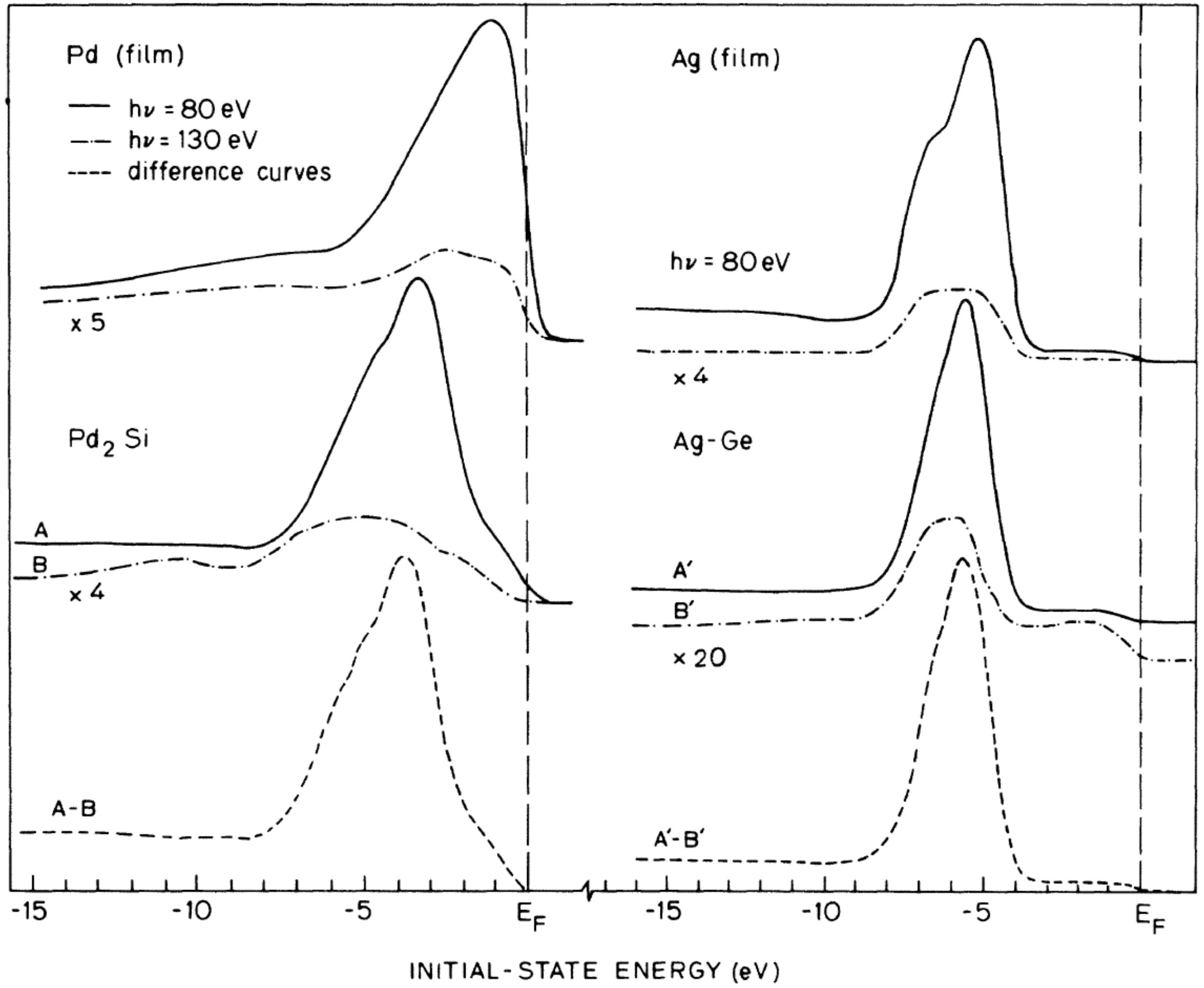

From the difference curve out of Cooper minimum & non-Cooper minimum spectra, redistribution of valence band state can be studied in the bimetallic-alloy system

Rossi et al. Phys. Rev. B. 28,3031 (1993)

XPS (Cross Section)

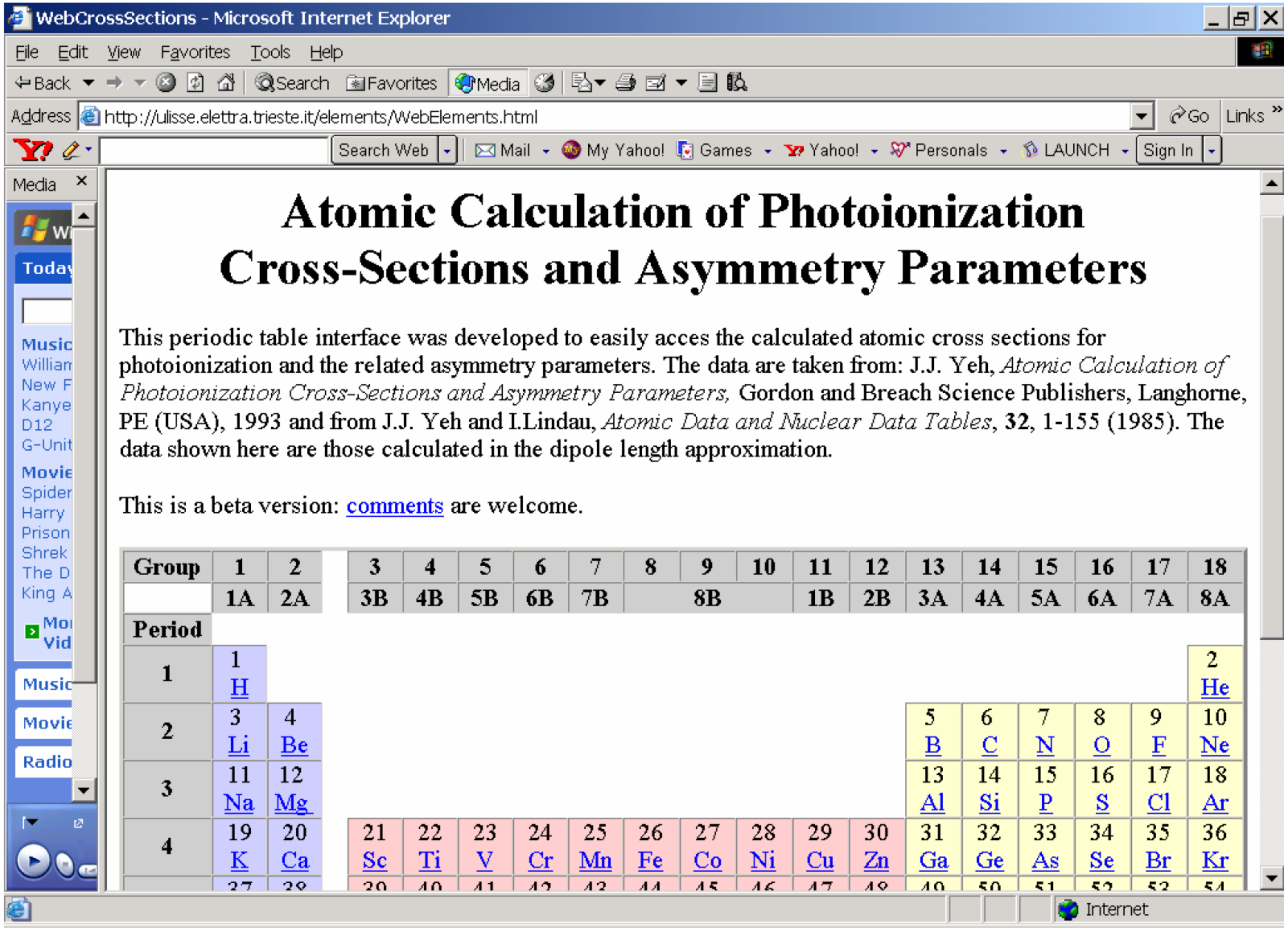

Atomic Calculation of Photoionization Cross-Sections and Asymmetry Parameters

This periodic table interface was developed to easily acces the calculated atomic cross sections for photoionization and the related asymmetry parameters. The data are taken from: J.J. Yeh, *Atomic Calculation of Photoionization Cross-Sections and Asymmetry Parameters,* Gordon and Breach Science Publishers, Langhorne, PE (USA), 1993 and from J.J. Yeh and I.Lindau, *Atomic Data and Nuclear Data Tables*, **32**, 1-155 (1985). The data shown here are those calculated in the dipole length approximation.

This is a beta version: comments are welcome.

Group	1	2	3	4	5	6	7	8	9	10	11	12	13	14	15	16	17	18
	1A	2A	3B	4B	5B	6B	7B		8B		1B	2B	3A	4A	5A	6A	7A	8A
Period																		
1	1 H																	2 He
2	3 Li	4 Be											5 B	6 C	7 N	8 O	9 F	10 Ne
3	11 Na	12 Mg											13 Al	14 Si	15 P	16 S	17 Cl	18 Ar
4	19 K	20 Ca	21 Sc	22 Ti	23 V	24 Cr	25 Mn	26 Fe	27 Co	28 Ni	29 Cu	30 Zn	31 Ga	32 Ge	33 As	34 Se	35 Br	36 Kr

XPS (Cross Section)

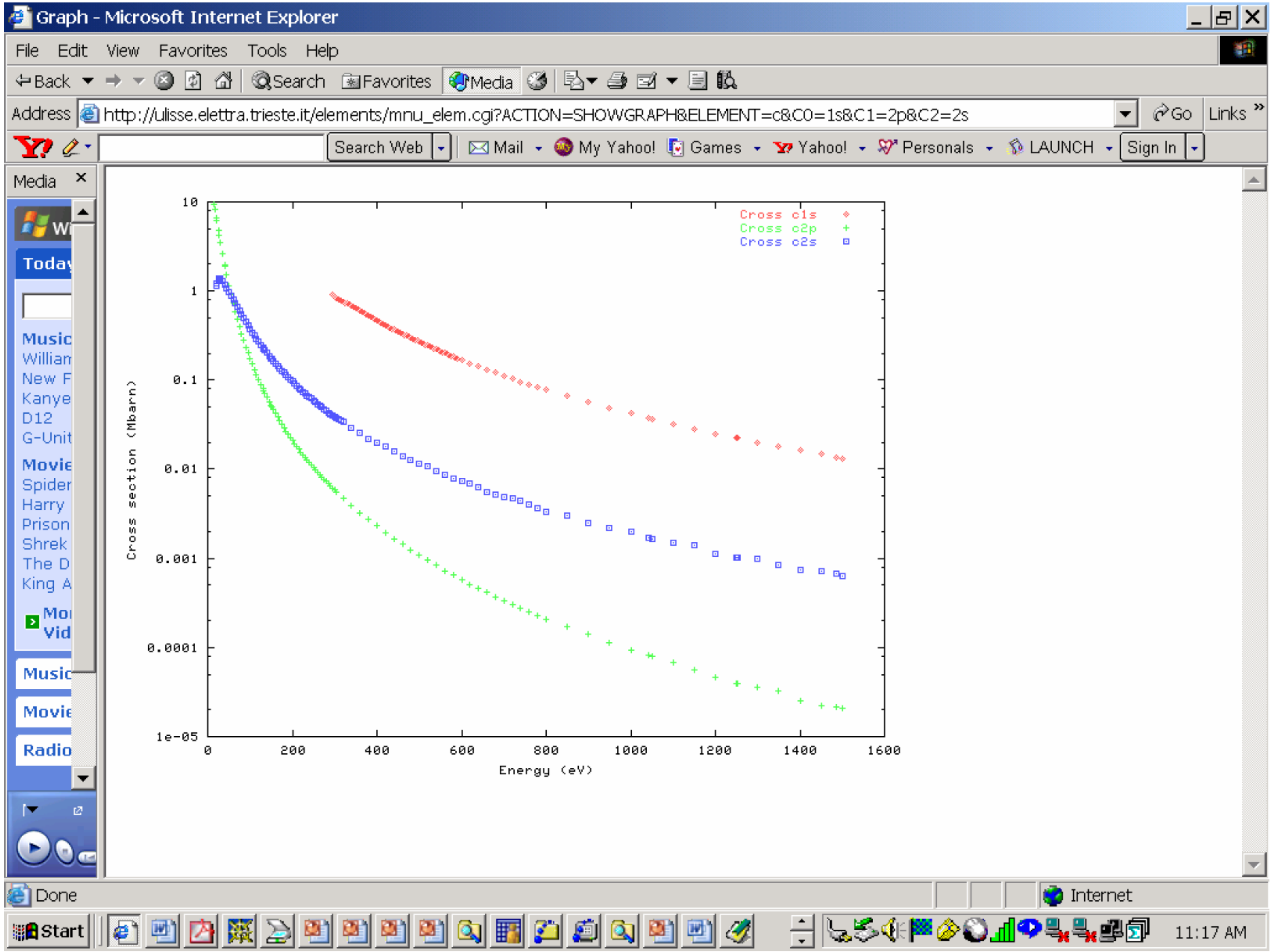

Valence Band
:Electronic Structure

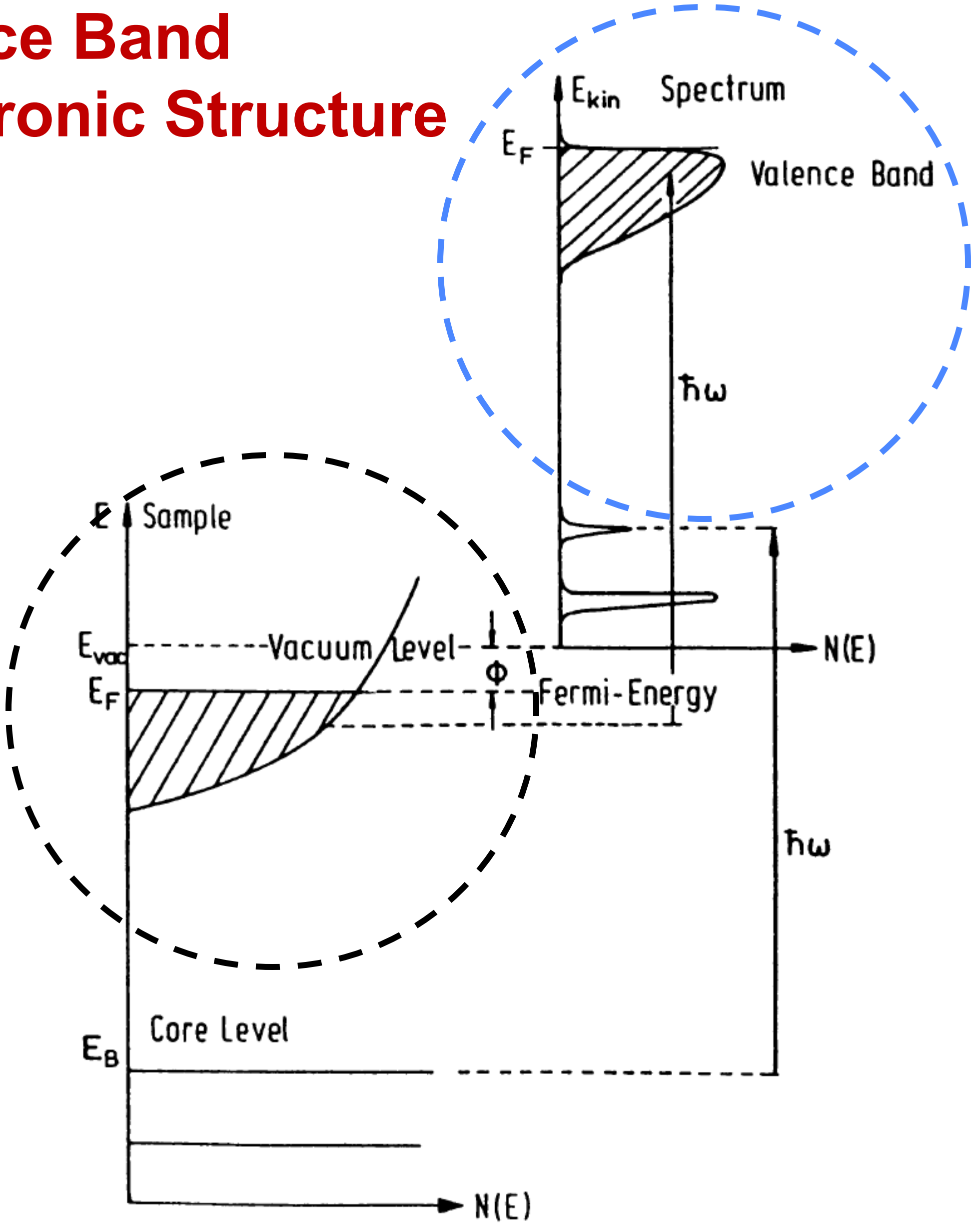

Valence Band Photoelectron Spectroscopy

- BLOCH-FUNCTION (DELOCALIZED) STATES ⇒ VALENCE:

$$\varphi_i(\vec{r}) = u_{\vec{k}_i}(\vec{r})e^{i\vec{k}_i\cdot\vec{r}}$$

$$\varphi_f(\vec{r}) = u_{\vec{k}_f}(\vec{r})e^{i\vec{k}_f\cdot\vec{r}} \; ; \; E_f = \frac{p_f^2}{2m} = \frac{\hbar^2 k_f^2}{2m}$$

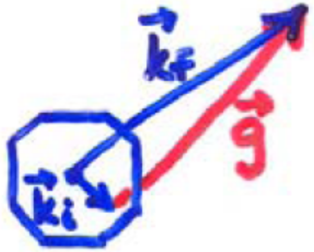

BRILLOUIN ZONE

USUALLY NEGLIG.

$$|\langle\varphi_f|\hat{\varepsilon}\cdot\vec{p}|\varphi_i\rangle|^2 = |\hat{\varepsilon}\cdot\langle\varphi_f|\vec{p}|\varphi_i\rangle|^2 \Rightarrow \Delta\vec{k} = \vec{k}_f - \vec{k}_i - \vec{k}_{h\nu} + \vec{k}_{\text{PHONON}}$$

$$= \vec{g}_{\text{BULK}} \; (\text{OR } \vec{g}_{\text{SURF}})$$

"DIRECT" TRANSITIONS

BUT LATTICE VIBRATIONS ⇒ SUM OVER $\vec{k}_{\text{PHONON}}$

⇒ FRACTION DIRECT ≈ DEBYE-WALLER FACTOR

$$\approx \exp[-g^2\overline{u^2}]$$

Valence Band Photoelectron Spectroscopy

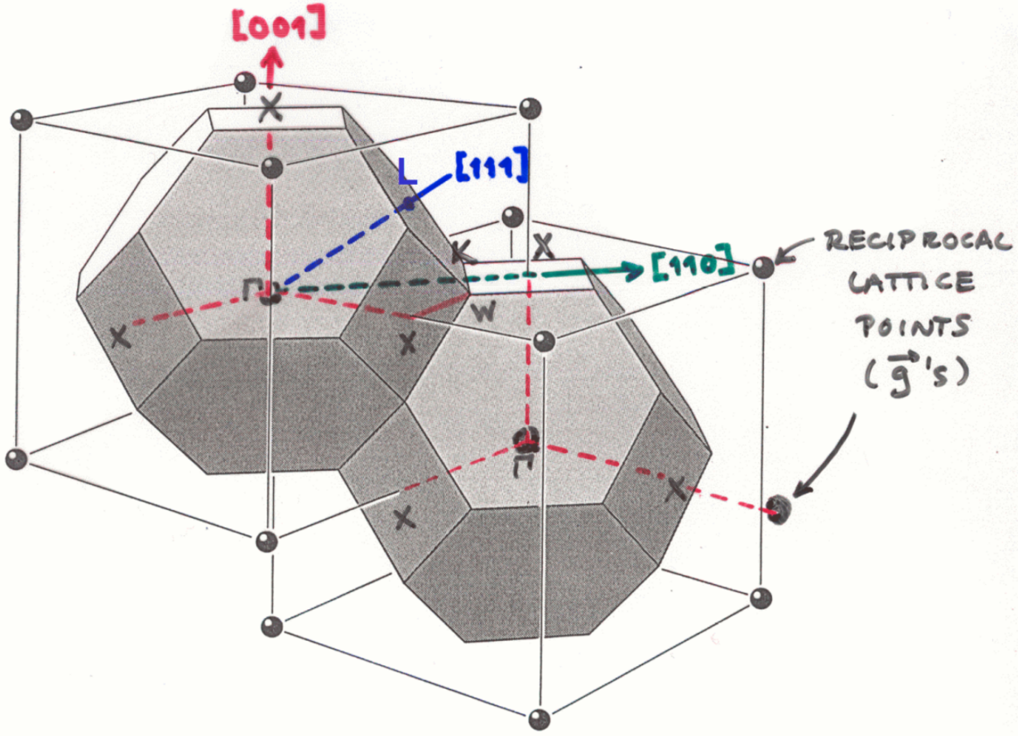

Figure 28 Brillouin zones of the face-centered cubic lattice. The cells are in reciprocal space, and the reciprocal lattice is body-centered, as drawn.

— STACKING OF fcc BRILLOUIN ZONES —

Valence Band Photoelectron Spectroscopy

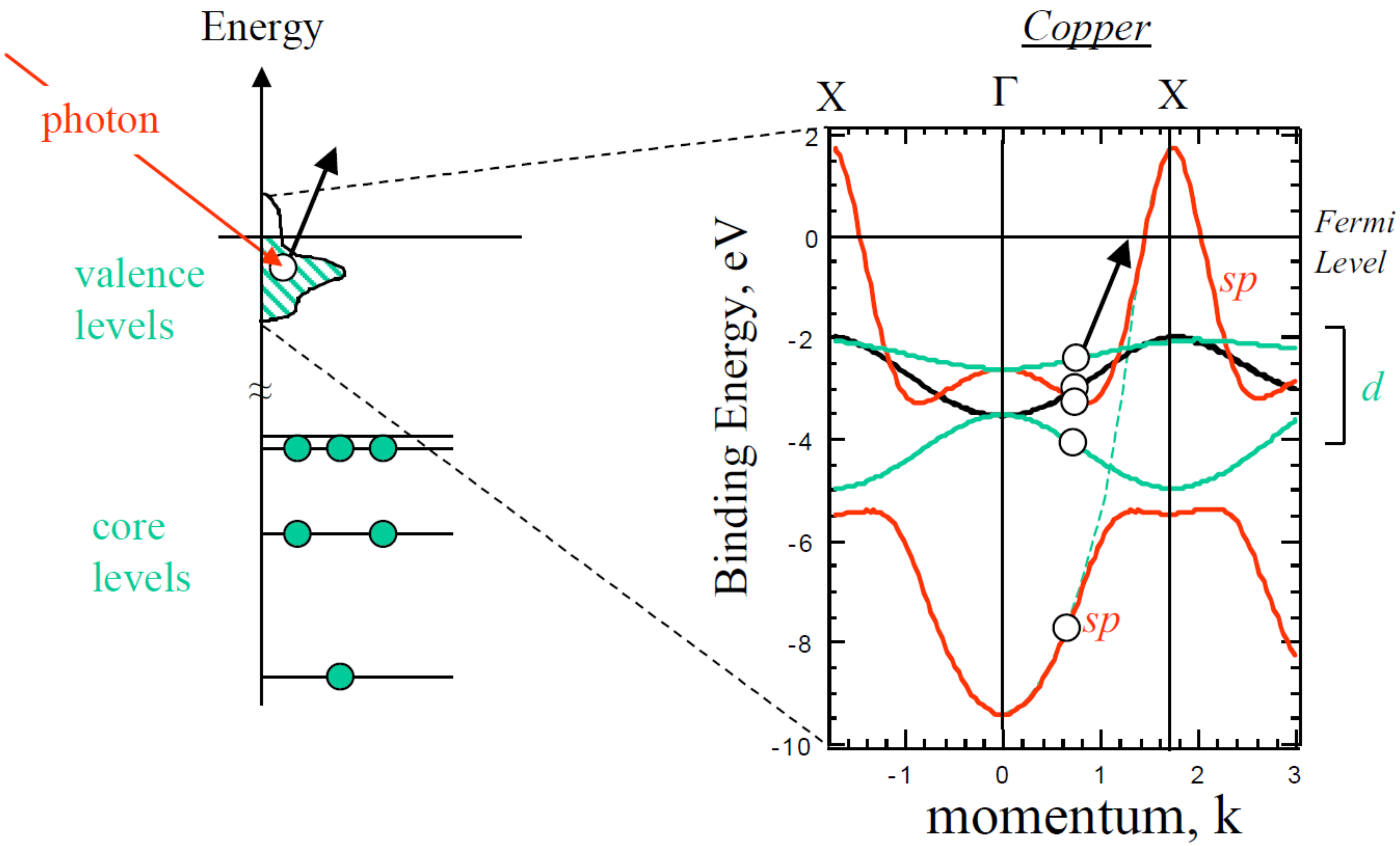

Valence Band Photoelectron Spectroscopy

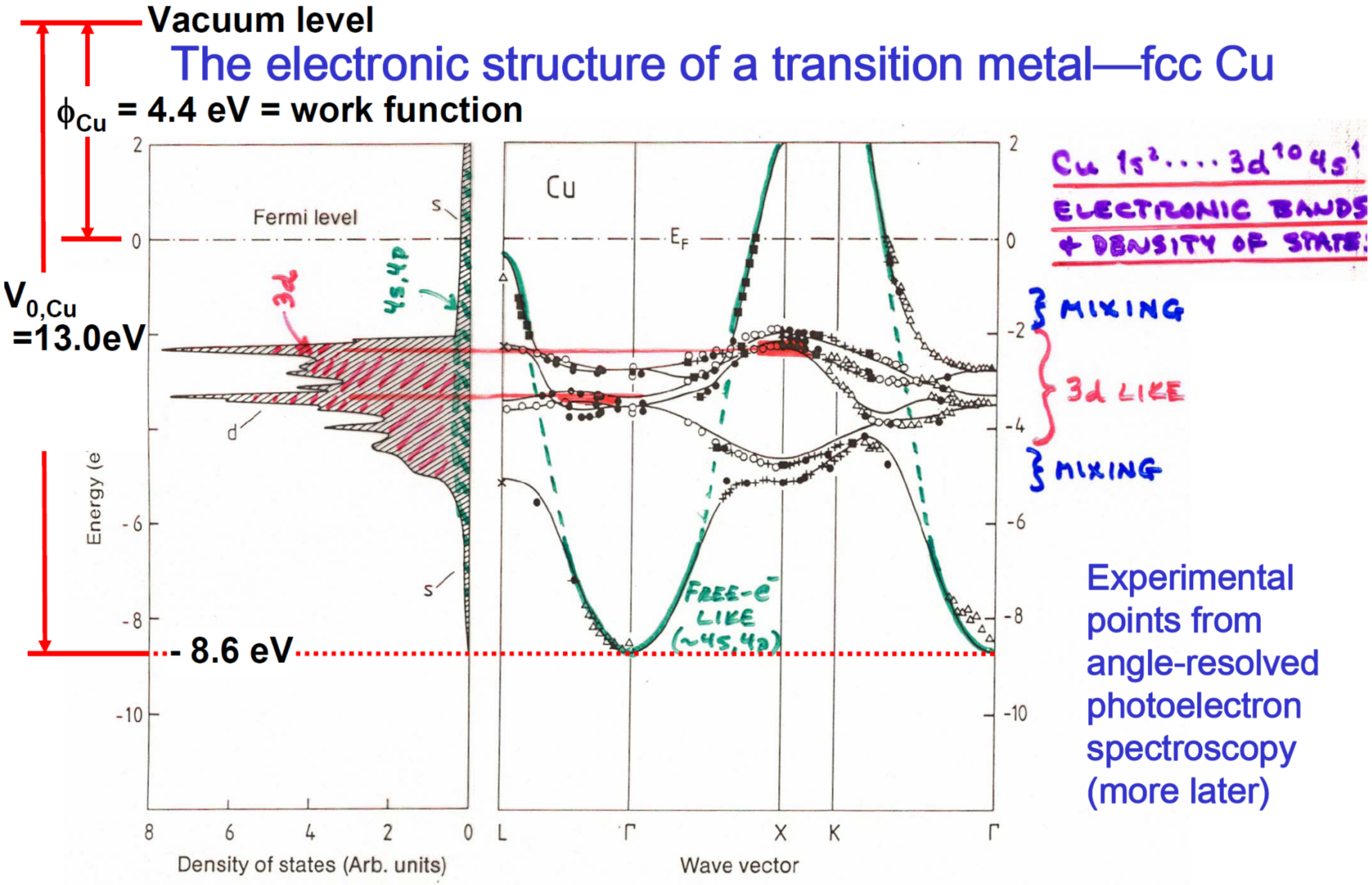

Fig. 7.12. Bandstructure $E(k)$ for copper along directions of high crystal symmetry (*right*). The experimental data were measured by various authors and were presented collectively by Courths and Hüfner [7.4]. The full lines showing the calculated energy bands and the density of states (*left*) are from [7.5]. The experimental data agree very well, not only among themselves, but also with the calculation

Experimental points from angle-resolved photoelectron spectroscopy (more later)

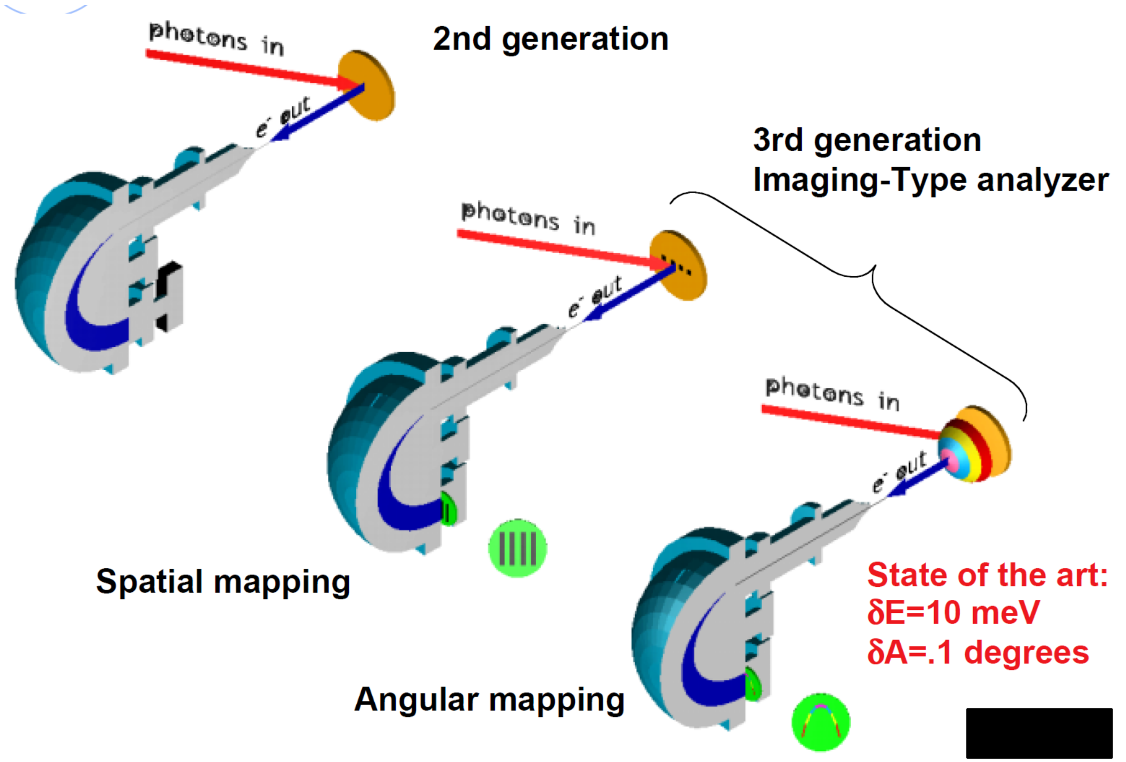

State of the art:
δE=10 meV
δA=.1 degrees

[redacted]

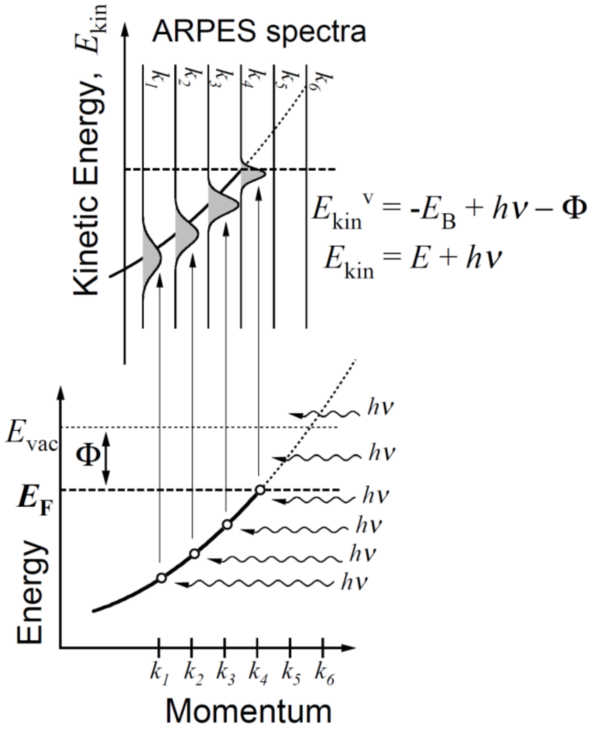

Angle Resolved Photoemission Spectroscopy (ARPES)

- **Electronic band structure measurement**
  (dispersion relation E vs k)
  - **Angle resolved photoemission**
- **hν = 80-1200 eV, Energy resolution = 25-30 meV at hν =95 eV**
- **Angular resolution 0.1° (0.01Å^{-1})**

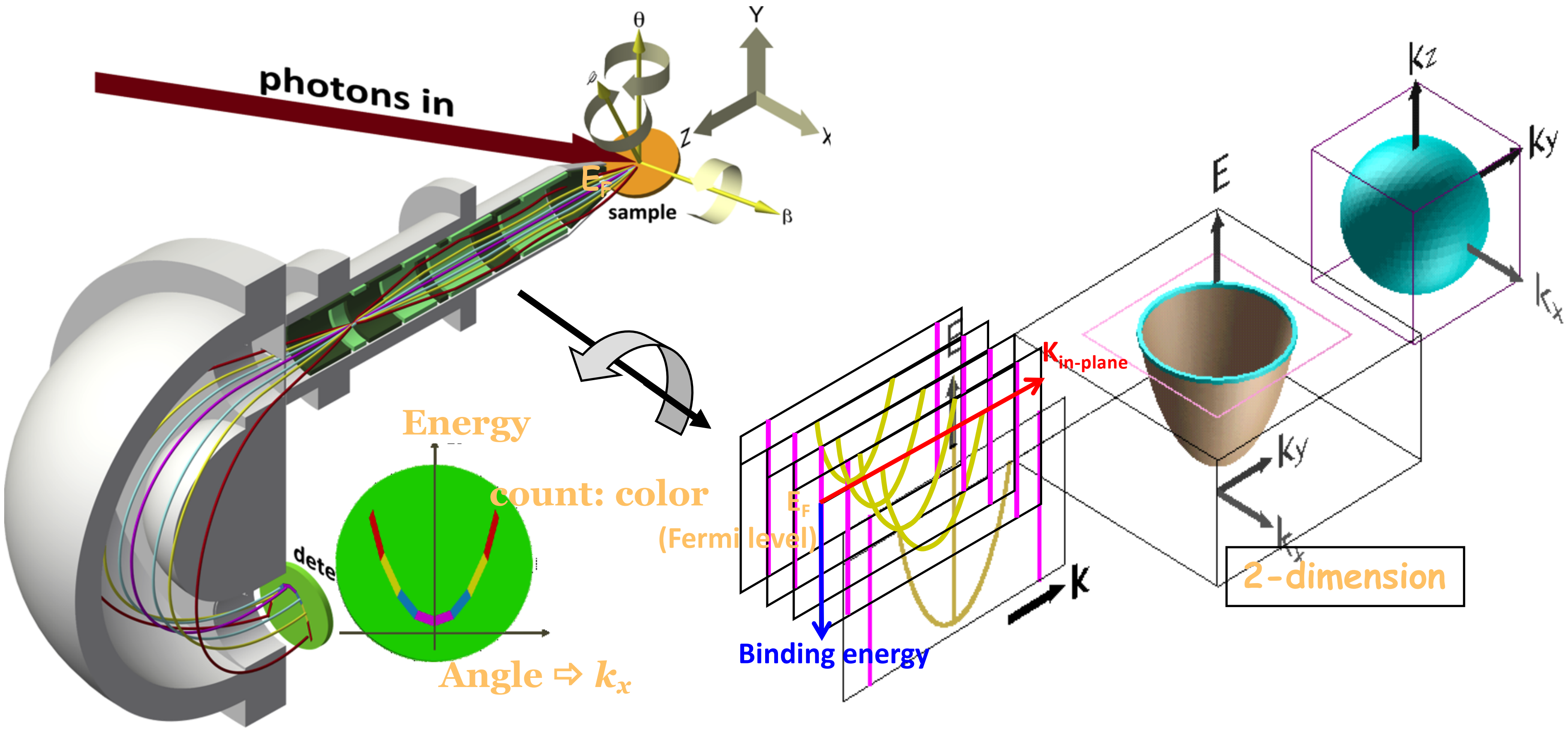

Bonding interaction between chemisorbed atomic oxygen Pt surface state

Band Structure

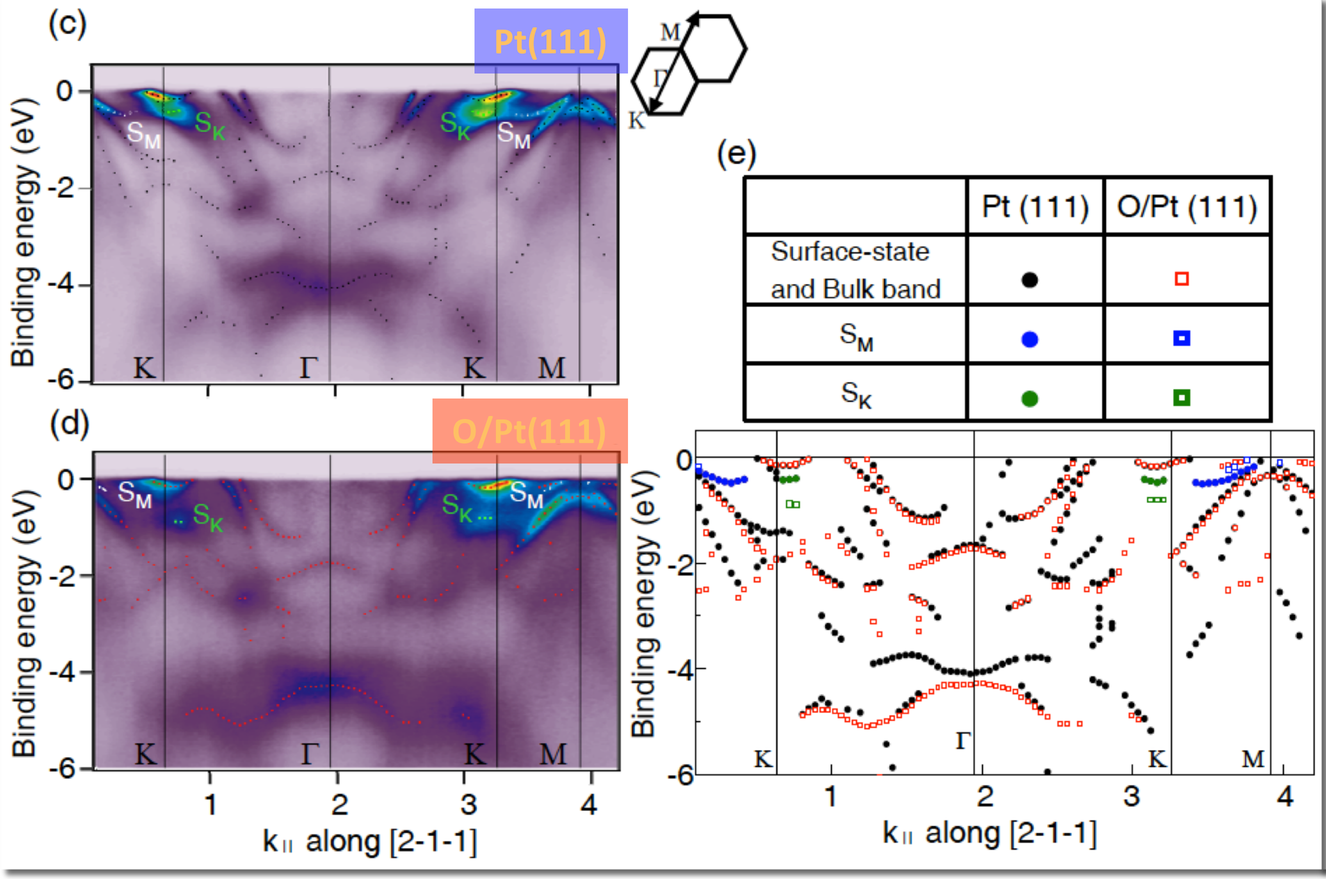

Surface-states & Bulk band

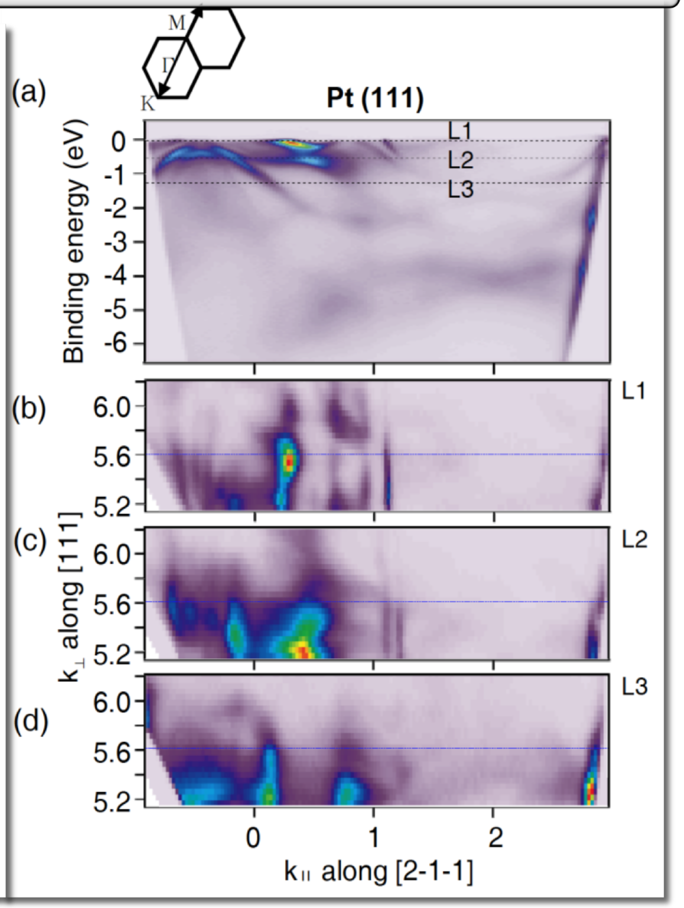

Karl Manne Georg Siegbahn
The Nobel Prize in Physics 1924.
"for his discoveries and research in the field of X-ray spectroscopy"

Kai Manne Börje Siegbahn
The Nobel Prize in Physics 1981.
"for his contribution to the development of high-resolution electron spectroscopy".

XAS (X-ray Absorption Spectroscopy)

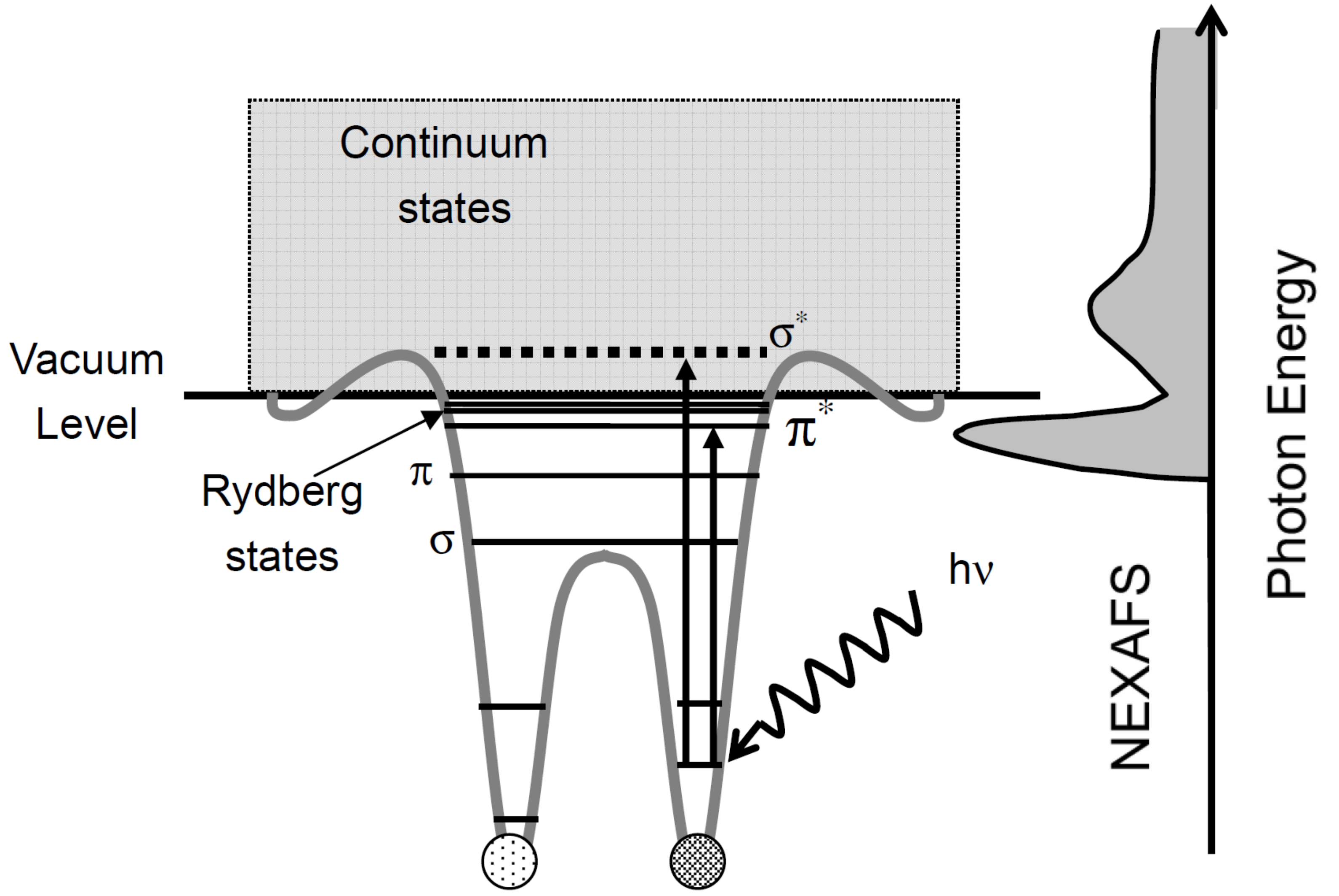

Courtesy of Dr. I. Nakai

XAS (X-ray Absorption Spectroscopy)

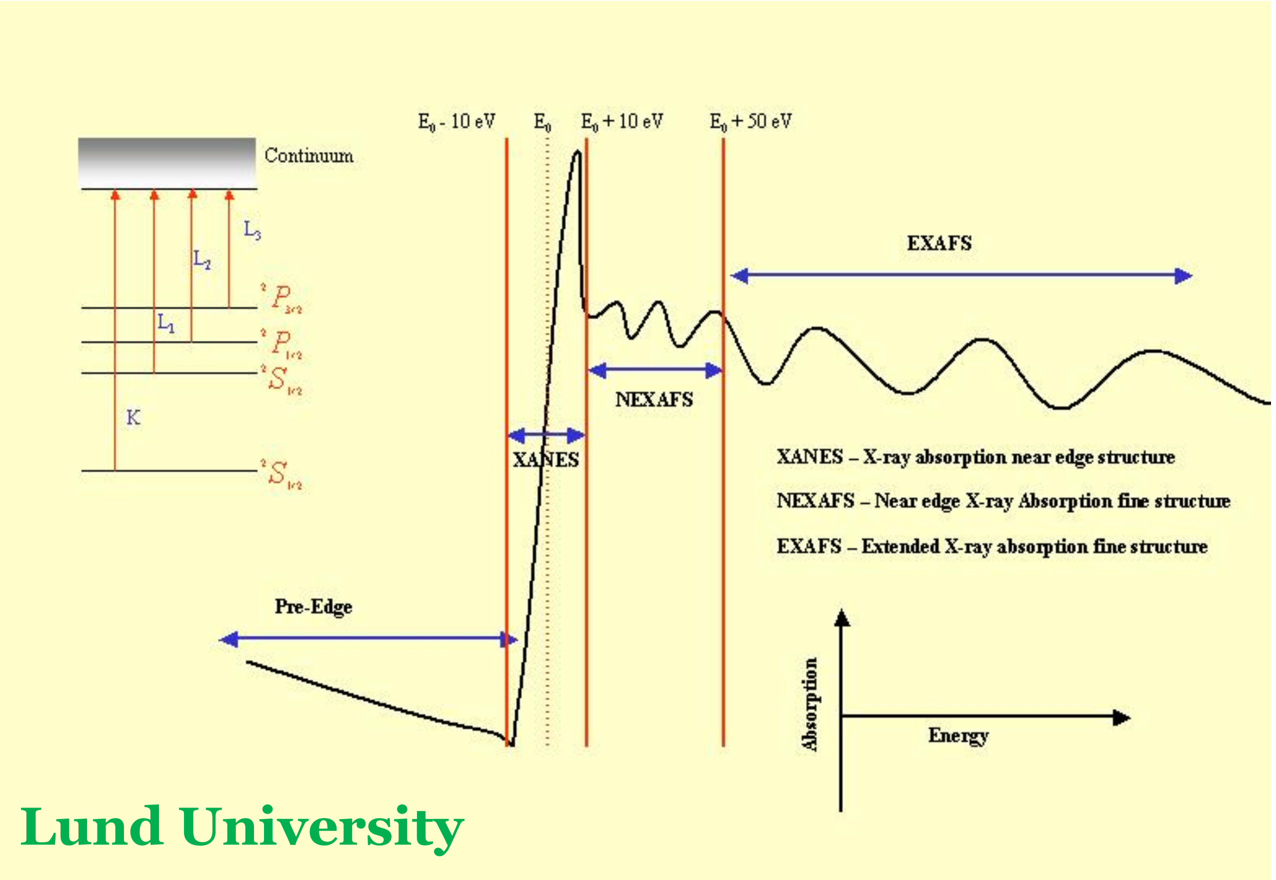

A. Total electrons yield : Sample Current = Bulk sensitive information

B. Partial electrons yields : channeltron = Surface sensitive information

C. X-ray fluorescent yields : photo-diode = Bulk sensitive information

XANES: X-ray Absorption Near Edge Structure : Information concerning the oxidation state of the absorbing atom and its site symmetry.

NEXAFS: Near Edge X-ray Absorption Fine Structure : sensitive to the number, kind and symmetry of atoms adjacent to the absorber atom.

EXAFS: Extended X-ray Absorption Fine Structure : The energy of the photoelectron is high enough that its de Broglie wavelength becomes comparable to the distance to neighbouring atoms.
Information regarding the number, kind and distances of neighbouring atoms from each other and the absorber.

XAS(X-ray Absorption Spectroscopy)

Variation of Near-Edge X-Ray Absorption Fine Structure (NEXAFS) with Atomic No. for Some 3d Transition Metals

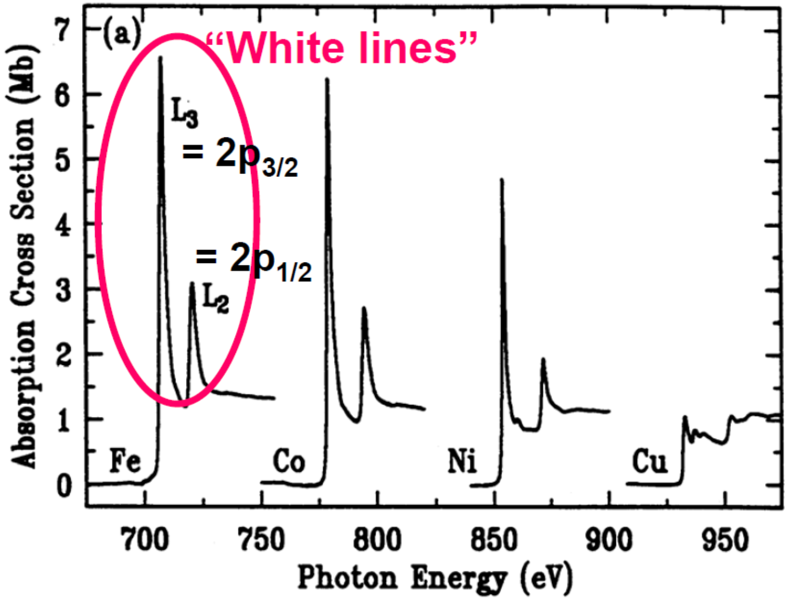

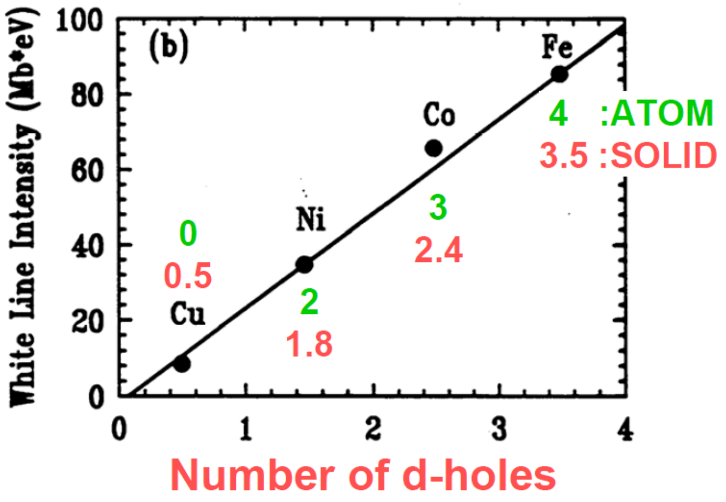

J. Stohr, "NEXAFS Spectroscopy"

XAS(X-ray Absorption Spectroscopy)

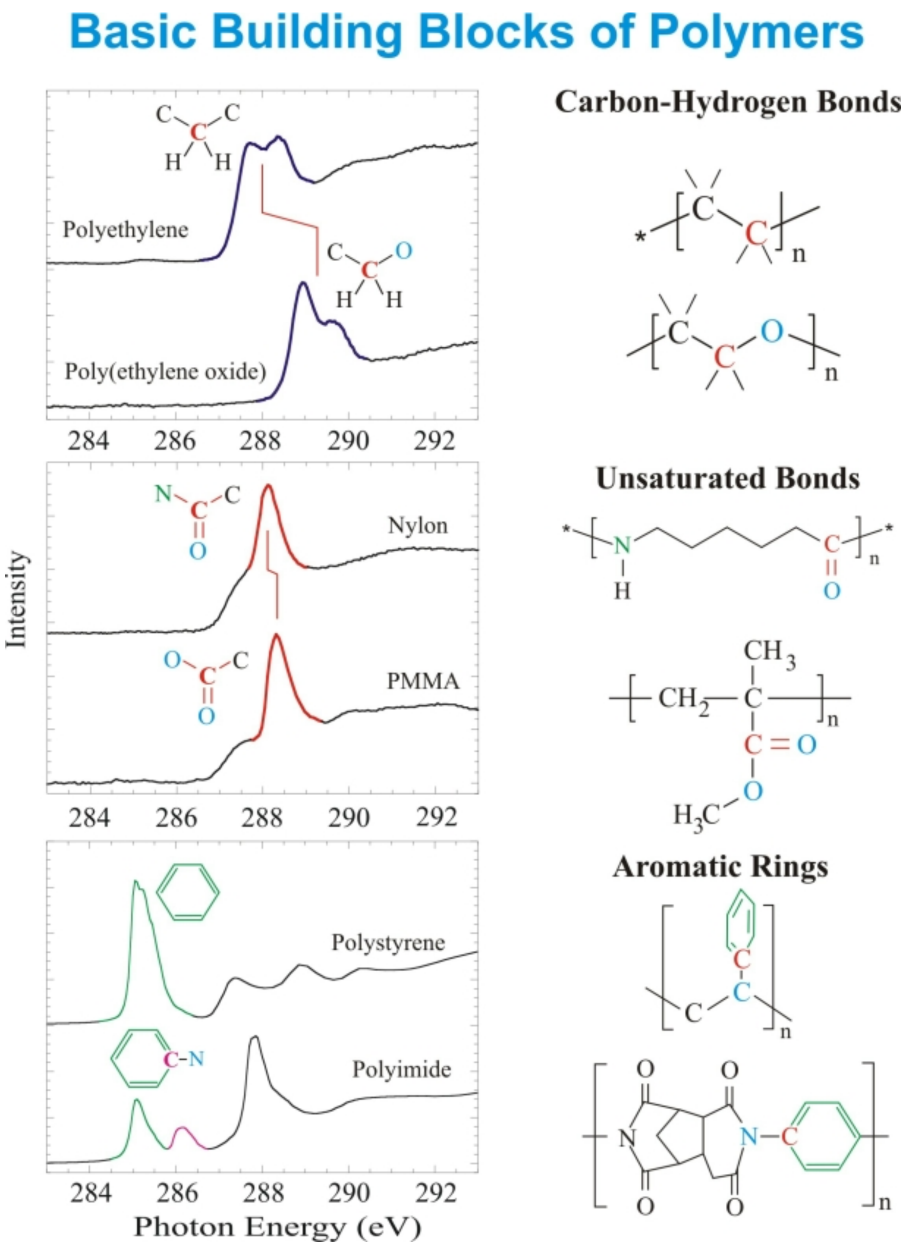

http://ssrl.slac.stanford.edu/stohr/nexafs.htm

- Sensitivity to molecular functional groups.
- Ability to determine molecular orientations.
- Study of charge and spin phenomena in materials.

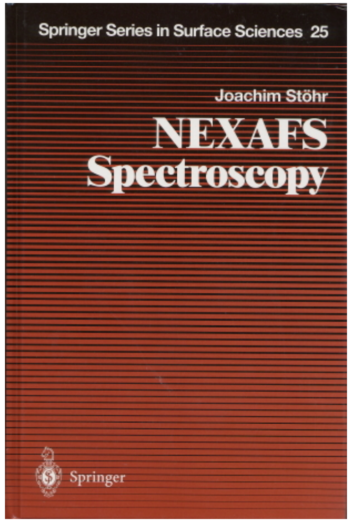

XAS : Magnetic Circular Dichroism

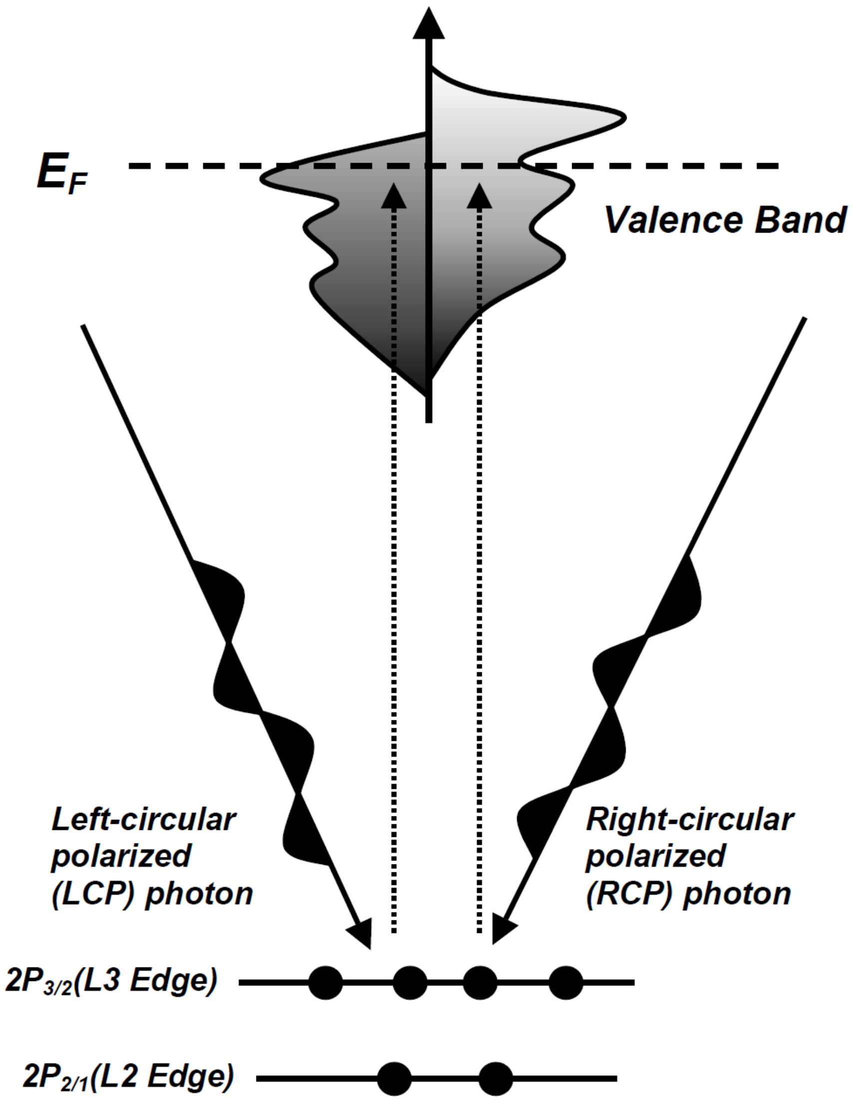

XAS : Magnetic Circular Dichroism

Magnetic Circular Dichroism in X-Ray Absorption (XMCD)

Ferromagnetic cobalt with magnetization along incident light direction

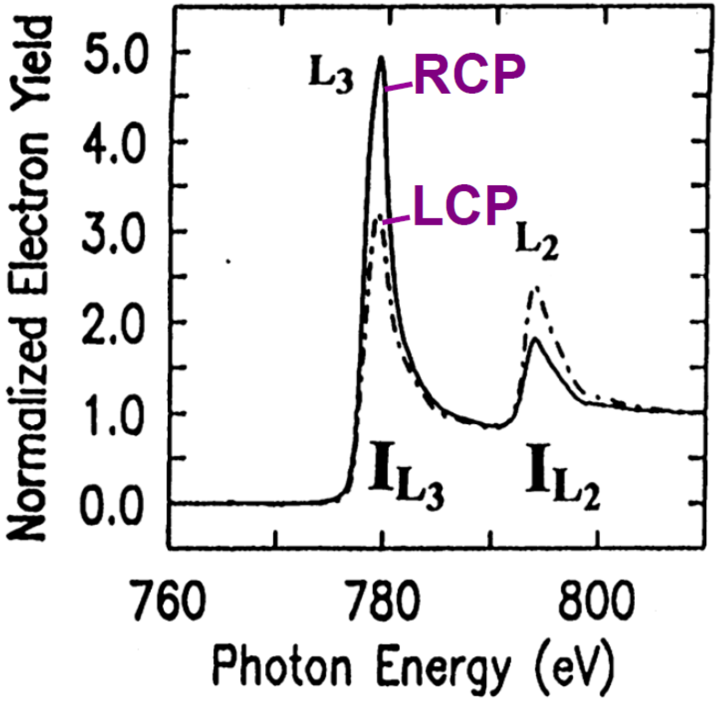

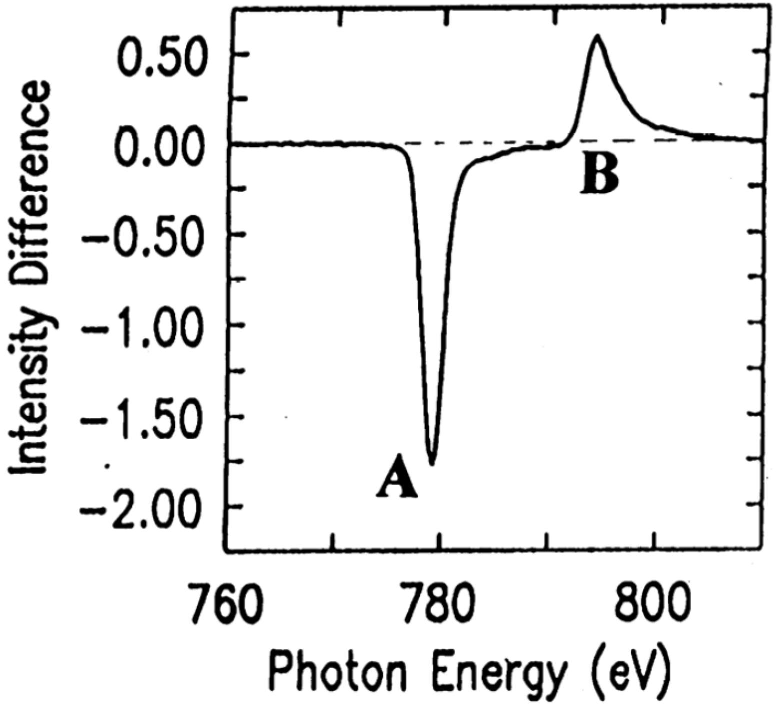

XAS (X-ray Absorption Spectroscopy)

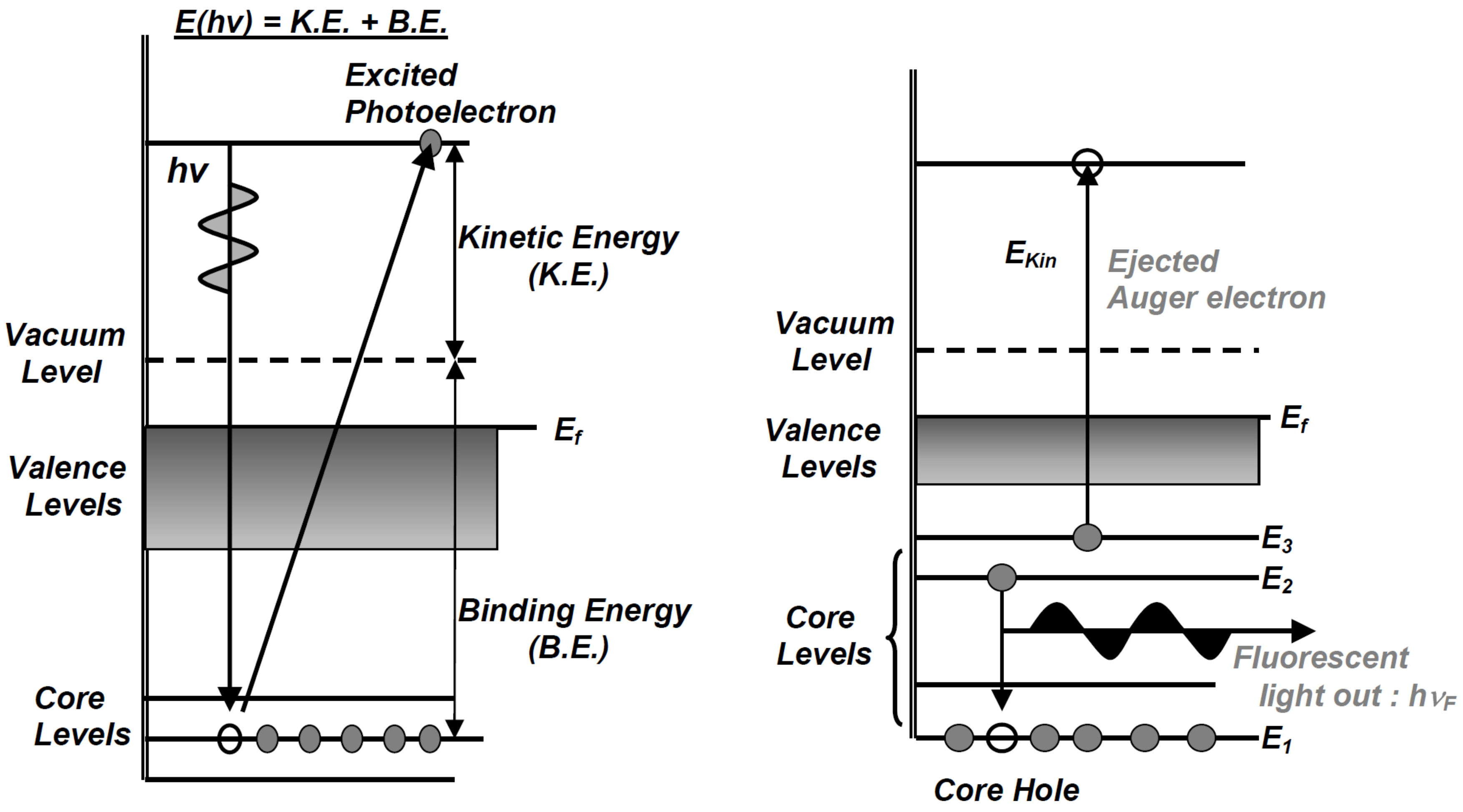

XAS & XES are coherence process !

XAS (X-ray Absorption Spectroscopy)

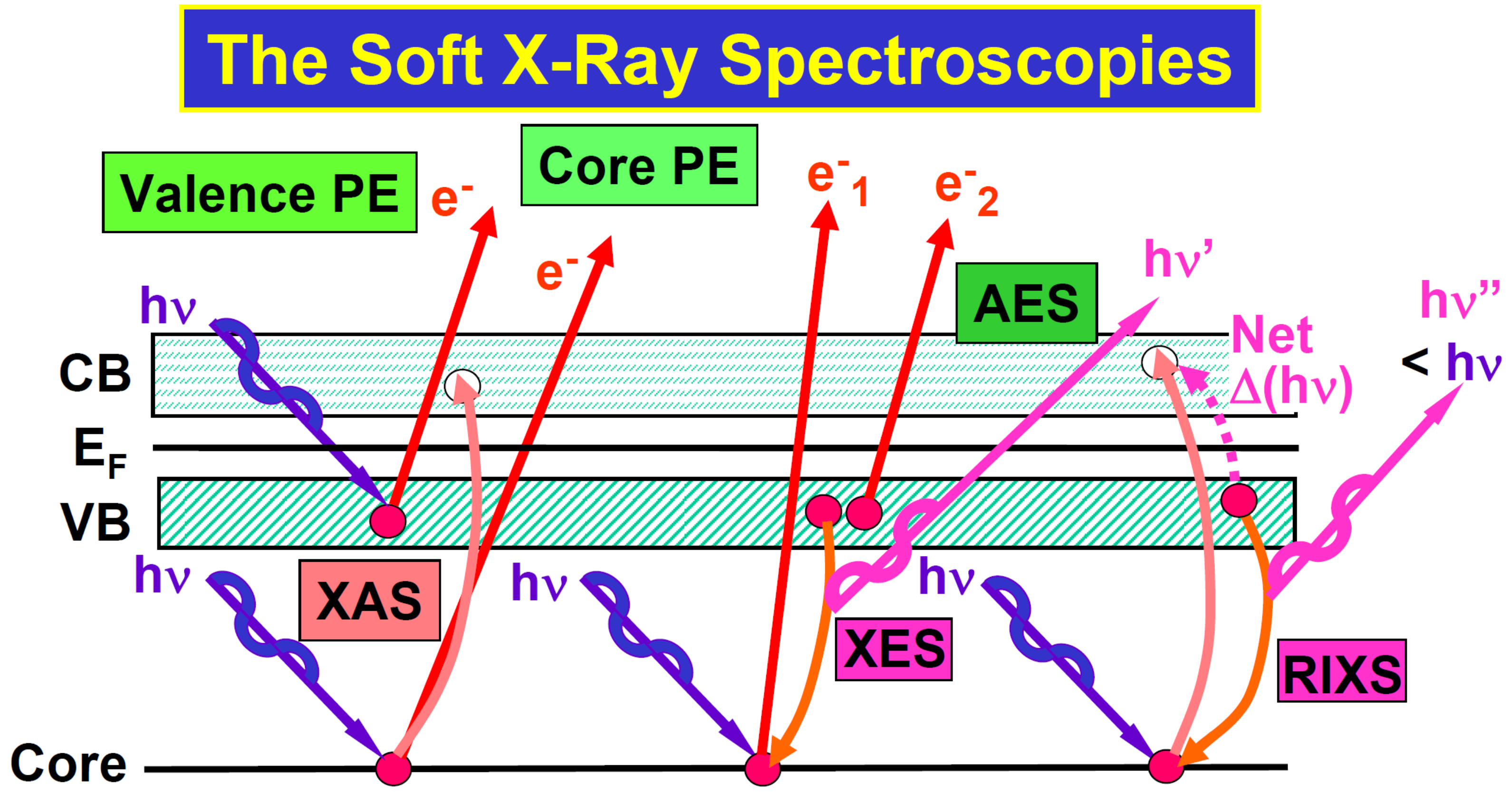

PE = photoemission = photoelectron spectroscopy
XAS = x-ray absorption spectroscopy
AES = Auger electron spectroscopy
XES = x-ray emission spectroscopy
RIXS = resonant inelastic x-ray scattering / x-ray Raman scatt.

Soft-x-ray spectroscopy

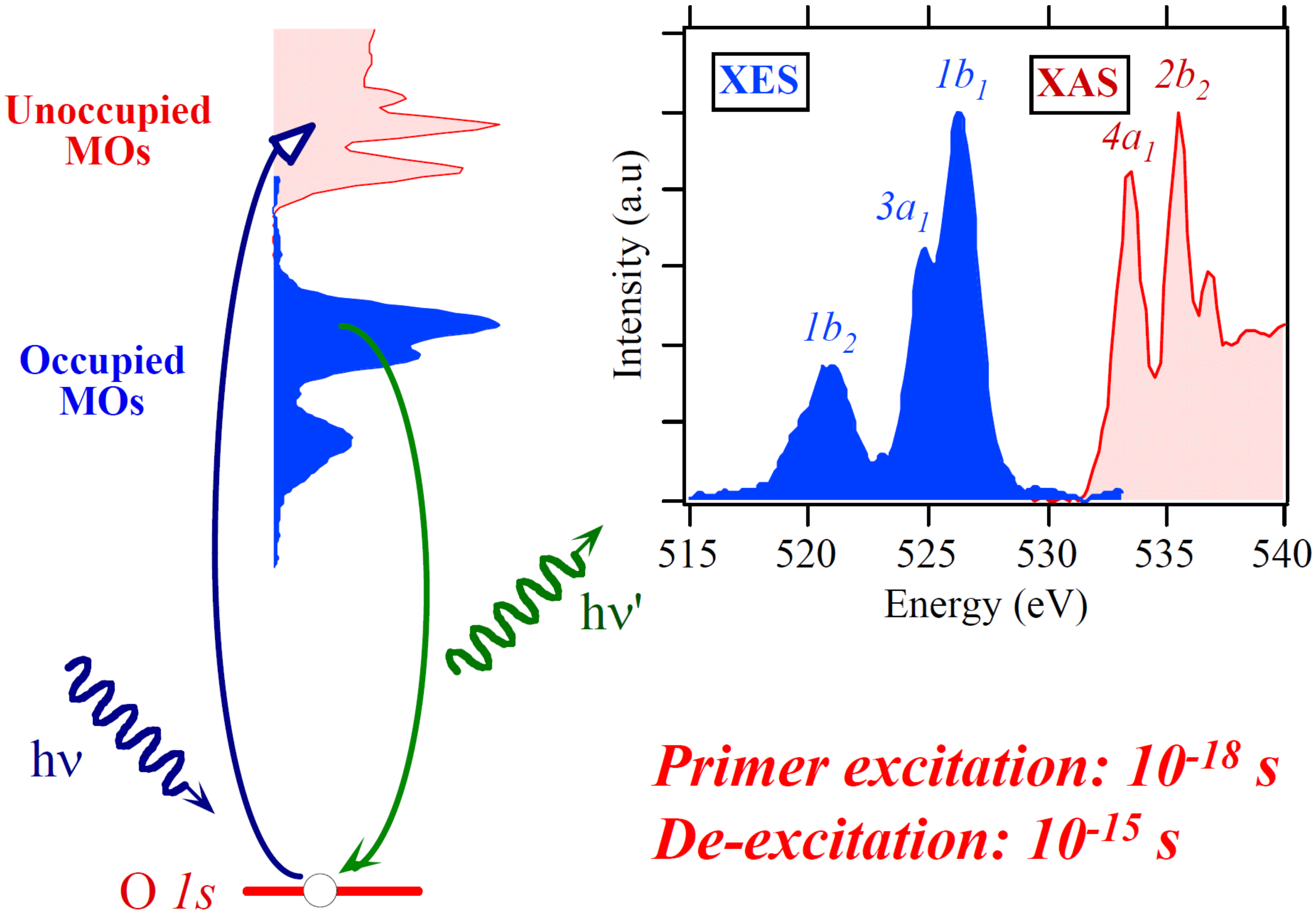

Primer excitation: 10^{-18} s

De-excitation: 10^{-15} s

Courtesy of Dr. J.Guo

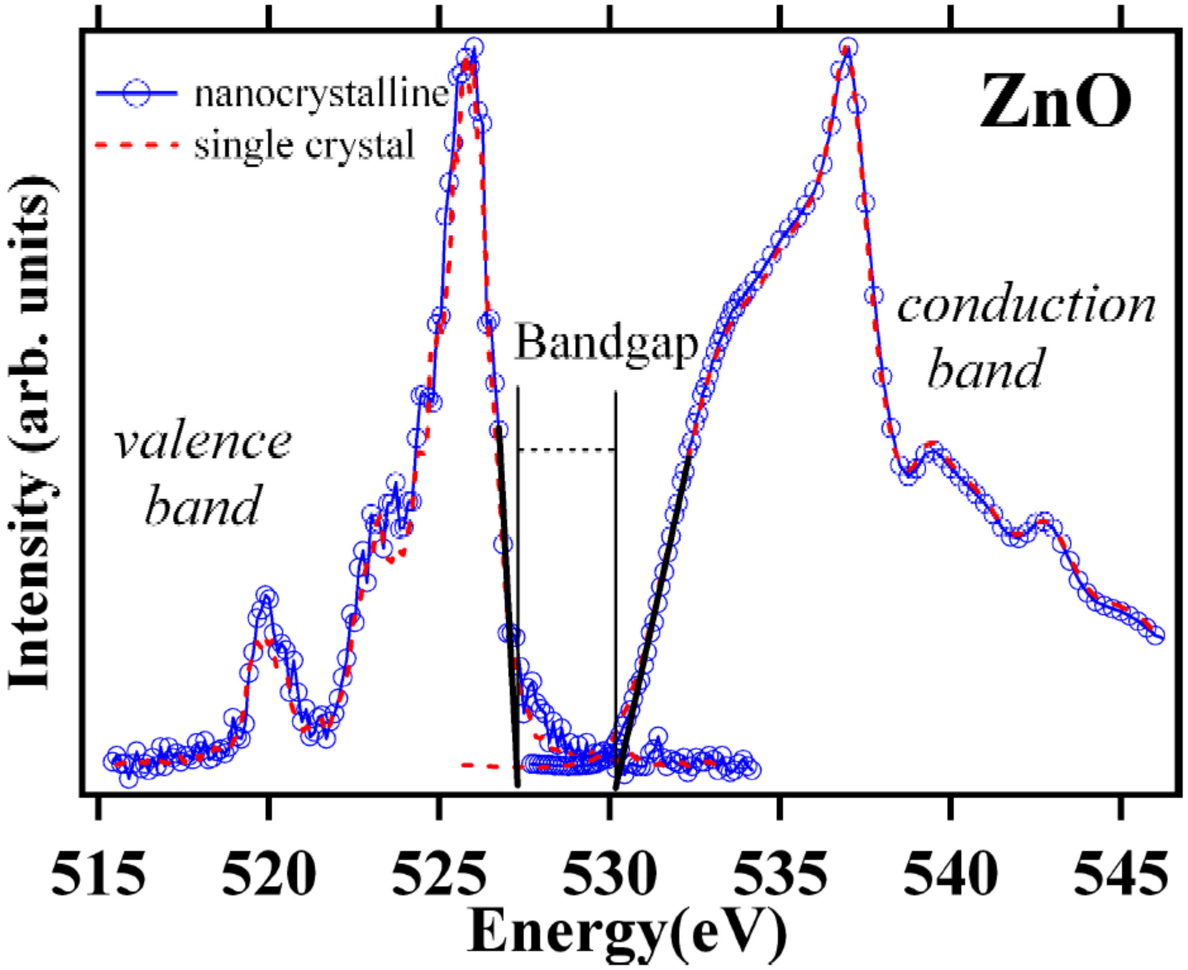

nanocrystalline
single crystal
ZnO
Intensity (arb. units)
valence band
Bandgap
conduction band
515
520
525
530
535
540
545
Energy(eV)

XRES (X-ray Resonant Emission Spectroscopy)

X-ray fluorescence spectroscopy =X-ray emission spectroscopy (XES)

Resonant inelastic x-ray scattering (RIXS) and Resonant elastic x-ray scattering (REXS)

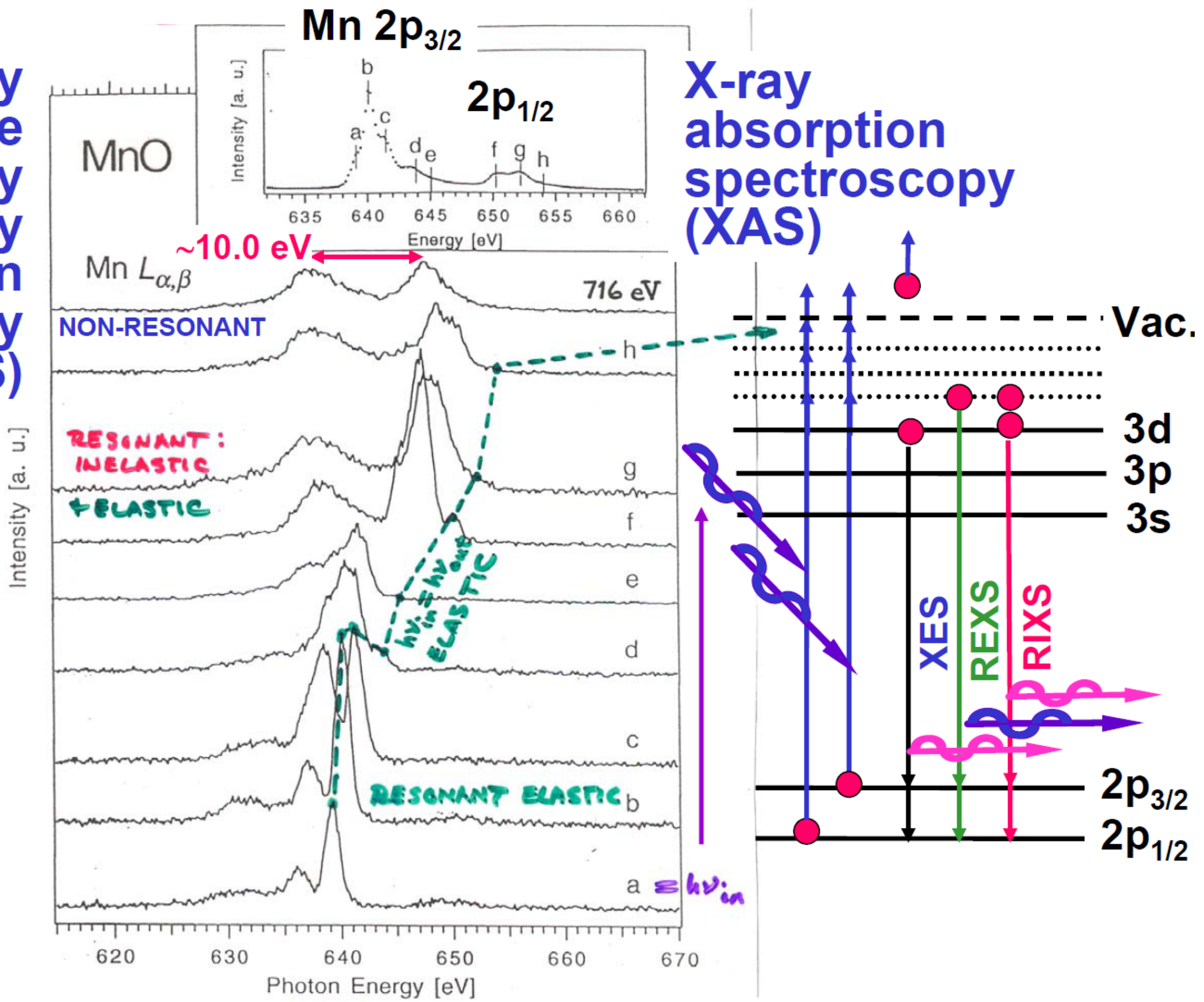

Butorin et al., Phys. Rev. B 54, 4405 ('96)

XES (X-ray Emission Spectroscopy)

MATRIX ELEMENTS IN THE SOFT X-RAY SPECTROSCOPIES: DIPOLE LIMIT

- ***Photoelectron spectroscopy/photoemission:***

$$I \propto \left|\hat{e}\bullet\langle\varphi_f(1)|\vec{r}\,|\varphi_i(1)\rangle\right|^2$$

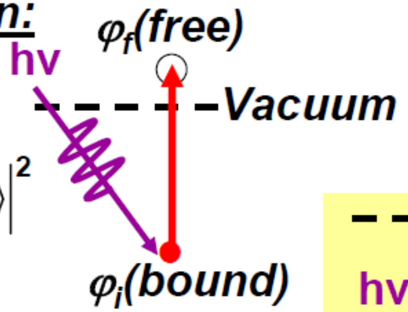

- ***Near-edge x-ray absorption:***

$$I \propto \left|\hat{e}\bullet\langle\varphi_f(1)|\vec{r}\,|\varphi_i(1)\rangle\right|^2$$

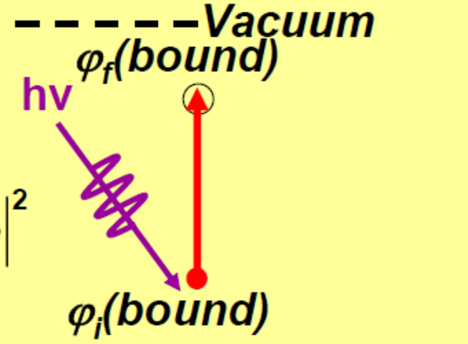

- ***Auger electron emission:***

$$I \propto \left|\overset{\text{Direct}}{\langle\varphi_f(1)\varphi_1(2)|\frac{e^2}{r_{12}}|\varphi_3(1)\varphi_2(2)\rangle} - \overset{\text{Exchange}}{\langle\varphi_1(1)\varphi_f(2)|\frac{e^2}{r_{12}}|\varphi_3(1)\varphi_2(2)\rangle}\right|^2$$

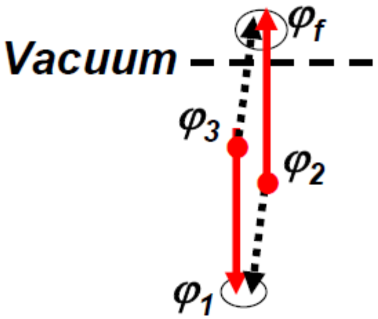

XES (X-ray Emission Spectroscopy)

MATRIX ELEMENTS IN THE SOFT X-RAY SPECTROSCOPIES: RESONANT EFFECTS

- ***X-ray emission:***

$$I \propto \left| \hat{\mathbf{e}} \bullet \langle \varphi_f(1) | \vec{r} | \varphi_i(1) \rangle \right|^2$$

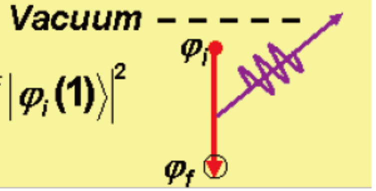

- ***Resonant inelastic x-ray scattering:***

$$I \propto \sum_f \left| \sum_m \frac{\langle \Psi_f(N) | \hat{e}_{emi} \bullet \vec{r} | \Psi_m(N) \rangle \langle \Psi_m(N) | \hat{e}_{inc} \bullet \vec{r} | \Psi_i(N) \rangle}{h\nu + E_i(N) - E_m(N) - i\Gamma} \right|^2 \times \delta(h\nu - (E_m(N) - E_i(N)))$$

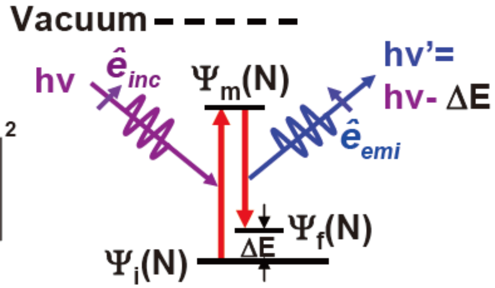

The five ways in which x-rays Interact with Matter:

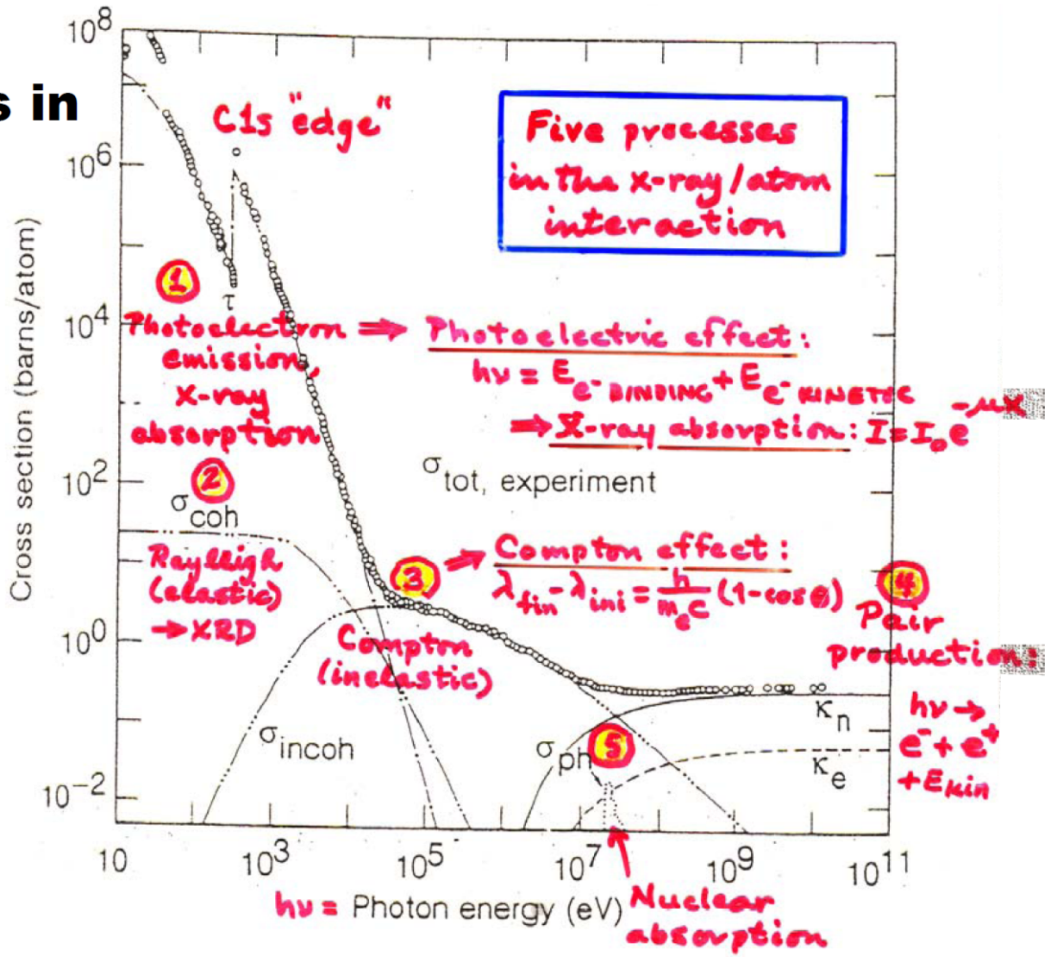

Fig. 3-1. *Total photon cross section σ_{tot} in carbon, as a function of energy, showing the contributions of different processes: τ, atomic photo-effect (electron ejection, photon absorption); σ_{coh}, coherent scattering (Rayleigh scattering—atom neither ionized nor excited); σ_{incoh}, incoherent scattering (Compton scattering off an electron) κ_n, pair production, nuclear field; κ_e, pair production, electron field; σ_{ph}, photonuclear absorption (nuclear absorption, usually followed by emission of a neutron or other particle). (From Ref. 3; figure courtesy of J. H. Hubbell.)*

"X-Ray Data Booklet"
Section 3.1

SR-based XPS & X-ray Optics

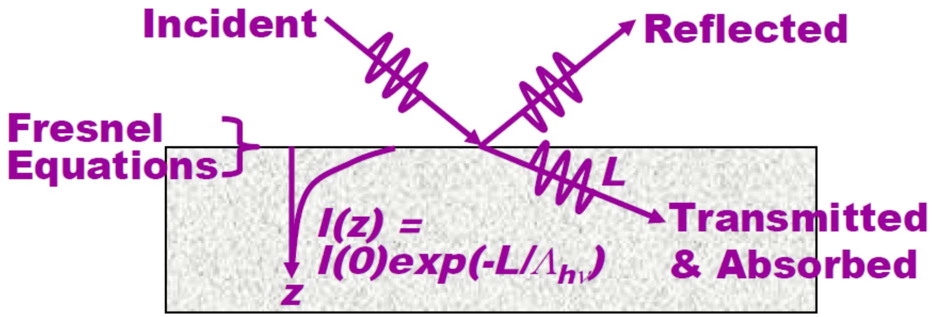

A LITTLE X-RAY OPTICS

(E.G. See pp. 1-38, 1-44, 5-18-5-19 in X-Ray Data Booklet)

Index of refraction = $n = 1 - \delta - i\beta$

δ = + no. = refractive decrement << 1 **(Sometimes negative through absorption resonances)**

β = + no. = absorptive decrement << 1

δ and β linked by Kramers-Kronig transform

n also = $1 - (r_e/2\pi)\lambda_{h\nu}^2\Sigma n_i f_i$(0=fwd. scatt.)

r_e = classical electron radius
= $e^2/4\pi\varepsilon_0 m_e e^2$ = 2.817 x 10^{-15} m
$\lambda_{h\nu}$ = x-ray wavelength

n_i = no. i atoms per unit volume

f_i = x-ray scattering factor for ith type of atom, in forward direction

Exponential absorption length = $l_{abs} = \lambda_{h\nu}/(4\pi\beta) = \Lambda_{h\nu}$

θ_{CRIT} = critical grazing angle at which reflectivity begins (R ≈ 0.20) = $[2\delta]^{0.5}$

Online data and calculations at:
http://www-cxro.lbl.gov/optical_constants/

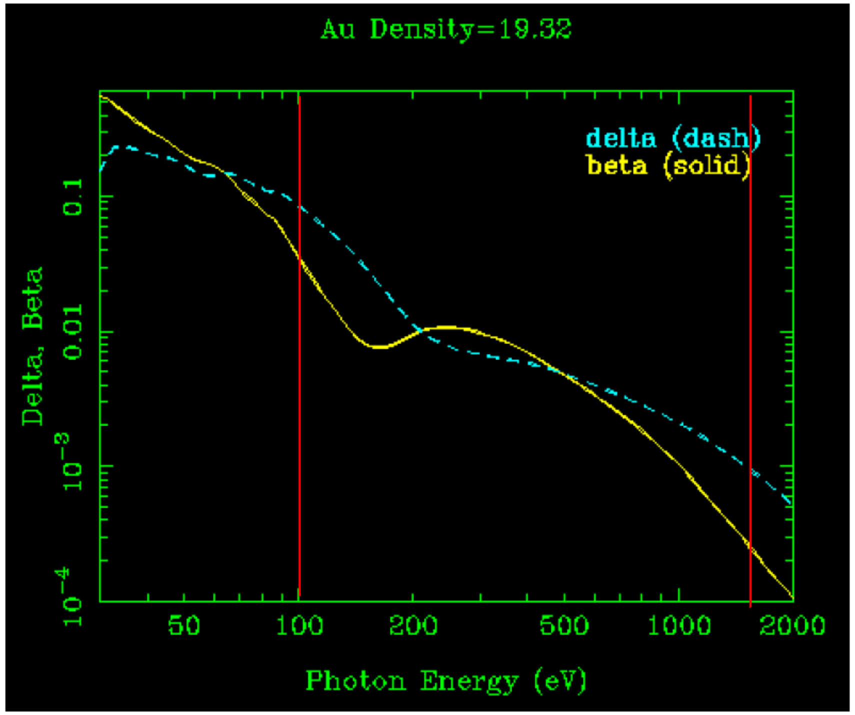

SR-based XPS & X-ray Optics

http://www-cxro.lbl.gov/optical_cor

Website

Atomic Scattering Factors

X-Ray Interactions with Matter

Contents

- Introduction
- Access the atomic scattering factor files.
- Look up x-ray properties of the elements.
- The index of refraction for a compound material.
- The x-ray attenuation length of a solid.
- X-ray transmission
  - Of a solid.
  - Of a gas.
- X-ray reflectivity
  - Of a thick mirror.
  - Of a single layer.
  - Of a bilayer.
  - Of a multilayer.
- The diffraction efficiency of a transmission grating.
- Related calculations:
  - Synchrotron bend magnet radiation.

NEW! What's New?

Other x-ray web resources.

These pages utilize *JavaScript*, but the decaffeinated versions are still available.

Reference

B.L. Henke, E.M. Gullikson, and J.C. Davis. *X-ray interactions: photoabsorption, scattering, transmission, and reflection at E=50-30000 eV, Z=1-92*, Atomic Data and Nuclear Data Tables Vol. **54** (no.2), 181-342 (July 1993).

By Eric Gullikson. Please direct any comments to EMGullikson@lbl.gov

Server Statistics © 1995-2001

SR-based XPS & X-ray Optics

Optical constants through Mn 2p edges of MnO—
Web data <u>without absorption peaks</u>

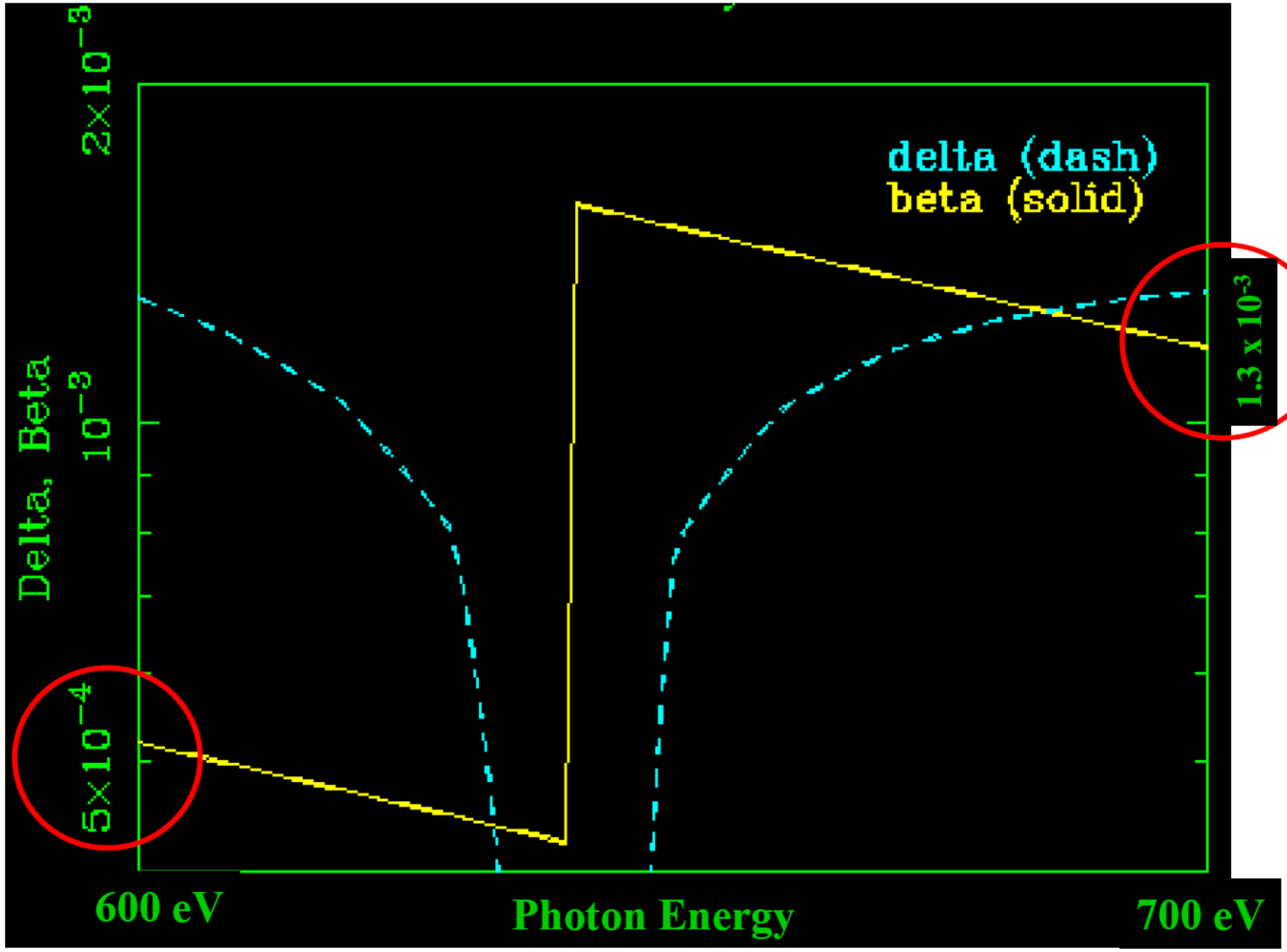

Dr. Neville Smith, a former ALS scientific director, coined the term “Ambient Pressure “ XPS for the first time.

A leading authority in the field of momentum-resolved photoemission spectroscopy.

Inverse photoemission

Neville V Smith

AT&T Bell Laboratories, Murray Hill, NJ 07974, USA

Bremsstrahlung isochromat spectroscopy (BIS) is a vintage technique which is now being marketed under the new appellation of inverse photoemission spectroscopy (IPES). The aim of this report is to savour the present condition of this technique and to assess how it will mature. The procedure of the report will be to sample interesting cases, to distil the essence, and to extract the ferment of this effervescent new spectroscopy.

Rep. Prog. Phys. 51 (1988) 1227-1294. Printed in the UK